

Alma Mater Studiorum – Università di Bologna

**DOTTORATO DI RICERCA IN**

**Ingegneria Elettrotecnica**

**Ciclo XXIII**

**Settore/i scientifico-disciplinare/i di afferenza:**

ing-inf/07 Misure Elettriche e Elettroniche

**Development of Human Visual System  
Analysis Methods for the Implementation of a  
New Instrument for Flicker Measurements**

**Presentata da: Ing. Maria Gabriella Masi**

**Coordinatore Dottorato**

**Prof. Domenico Casadei**

**Relatore**

**Prof. Lorenzo Peretto**

**Esame finale anno 2011**

# 1. Introduction

Flicker is a Power Quality phenomenon defined as the impression of unsteadiness of visual sensation induced by a light source whose luminance or spectral distribution fluctuates with time. Usually, it applies to cycle instability of light intensity resulting from supply voltage fluctuation, which, in turn, can be caused by disturbances introduced during power generation, transmission or distribution.

The Standards EN 61000-4-15 [1] which has been adopted by the IEEE as IEEE std 1453 [2], gives functional and design specification about the actual Flickermeter based on the analysis of the voltage supplying the considered light source. Such instrument implements an analytical model of the lamp-human eye-brain chain which is graphically plotted by the so-called flicker curve. Such a curve was obtained several years ago by statistically analyzing the results of tests where people were subjected to flicker produced by a specific incandescent filament lamp, the most commonly source used in Europe when the Flickermeter has been designed. In this way, the measurement results provided by that instrument are correct only if a 60 W- 230 V incandescent-filament lamp is considered; moreover, the implemented response to flicker is “subjective” given that it relies on the people answer about their feelings.

In this context, it’s opportune to highlight that a recent directive of the European Commission has scheduled the banning of all the incandescent-filament lamps for this year. The 60 W one in particular will be removed from the market on September 2011.

For the above reasons, in the last 15 years, researches have tackled these issues by investigating the possibility to develop a novel model of the eye-brain response to flicker and overcome the strict dependence of the standard on the kind of the light source. As a matter of fact, a correct evaluation of the annoyance due to flicker might lead also to review the limits endorsed by international standard EN 50160 [3] on voltage quality given that, as highlighted in the report of the CIGRE Task Force C4.108 “Flicker Objective HV, MV & LV, Systems, the modern lighting technologies are less susceptible to flicker”.

An important contribution for a new Flickermeter may be the development of an improved visual system model using a physiological parameter, thus allowing to get a more “objective” representation of the response to flicker. So, in this thesis, the use of

the mean value of the pupil diameter and the development of a system to measure it under flicker condition have been suggested.

The structure of the thesis is the following:

- *Chapter 2*: this chapter is devoted to an extensive background about the power quality.
- *Chapter 3*: some significant information about the human eye physiology and the eye-brain dynamics are reported in this chapter , to better understand the effects and the eye responses to flickering lights.
- *Chapter 4*: the flicker phenomenon and the characteristics of the current instrument used to measure the flicker severity, with its limitations, are described to introduce the recent studies toward the implementation of a new model for an innovative Flickermeter.
- *Chapter 5*: this chapter illustrates the basis for the implementation of the new model, the two systems implemented during the research activity for the measurement campaigns and their characterization.
- *Chapter 6*: a complete explanation and comments about the obtained results thanks to the measurements campaign with human subject are presented in this chapter.
- *Chapter 7*: in this chapter are presented other tests executed with medical instrumentations like LDF, Electroretinography (ERG).
- *Chapter 8* is devoted to the conclusions.

This thesis represents one of the results obtained in a framework of an international collaboration between the “University of Bologna”, the “Jonh Glenn Research Center” of NASA of Cleveland (Ohio) and the University of Modena and Reggioemilia.

I would like to thank Prof. Lorenzo Peretto for his fundamental guide all along the three years of PhD and his constant support. Acknowledgment are also due to Ing. Roberto Tinarelli and Prof. Luigi Rovati for important discussions on the procedure and on the implementation of the developed systems for the measurement campaigns.

Thank are also due to Dr. Rafat Ansari for his important contribution in this activity.

Acknowledgment are also due to all the people who gave their consensus for the tests.

Finally, I would like to thank all my family for the essential support during the PhD.

**References**

- [1] EN 61000-4-15, “Testing and measurement techniques: Flickermeter-functional and design specification”, Geneva, CH, 1997.
- [2] IEEE Std. 1453, “IEEE recommended practice for measurement and limits of voltage fluctuations and associated light flicker on AC power systems”, New York, USA, 2005.
- [3] EN 50160, “Voltage Characteristics of electricity supplied by public distribution systems”, Geneva, CH, 2004.

## 2. Power Quality in Electrical Systems

### 2.1 Introduction

Electrical energy is a product and, like any other product, should satisfy the proper quality requirements. If electrical equipment is to operate correctly, it requires electrical energy to be supplied at a voltage that is within a specified range around the rated value. A significant part of the equipment in use today, especially electronic and computer devices, requires good power quality (PQ). However, the same equipment often causes distortion of the voltage supply in the installation, because of its non-linear characteristics, i.e. it draws a non-sinusoidal current with a sinusoidal supply voltage. Thus, maintaining satisfactory PQ is a joint responsibility for the supplier and the electricity user.

All customers have to make sure that they obtain an electricity supply of satisfactory quality to avoid the high cost of equipment failures; electrical equipment must also be capable of functioning as required when small disturbances occur. Customers are granted to be safe only if the limits within which power quality may vary can be specified. According to the technical context, such limits should be fixed by standards, by the national regulator, by the customer by means of a power quality contract, by the manufacturer in a device manual or by the grid operator in a guideline. The defined limits must be meaningful, consistent and easy to compare to actual power quality levels. All these different limits have to be accomplished, on the one hand to prevent devices or installations from malfunctioning, on the other hand for clear communication about the quality of supply that is provided or demanded.

The starting point for the definition of the supply-voltage quality is the set of limits defined by the National Regulator and to be met at the point of common coupling with the customer. At the moment, there is no standard for the current quality relevant to that point. In fact the main document dealing with requirements concerning the supplier's side is the European standard EN 50160 [1], which characterizes voltage parameters and their permissible deviation ranges at the customer's point of common coupling in public low voltage (LV) and medium voltage (MV) electricity distribution systems under normal operating conditions.

According to [1] the *supplier* is the party who provides electricity via a public distribution system, and the user or *customer* is the purchaser of electricity from a supplier. The user is entitled to receive a suitable quality of power from the supplier. In practice, the level of PQ is a compromise between user and supplier. Where the available PQ is not sufficient for the user's needs, PQ improvement measures are needed and a cost-benefit analysis should be carried out. However, the cost of poor PQ usually exceeds the cost of measures required for improvement - it is estimated that losses caused by power quality degradation cost EU industry and commerce about €10 billion per annum.

The electric system, characterized in the past by an high level of vertical integration, is the subject of a recent liberalization process which separates the energy production, the management of the transmission network and the power distribution among a plurality of subjects. Beside the classic boundary between the distributor and the user (in high, medium or low voltage systems), all the other new boundaries must be taken into account. This applies in particular to voltage quality, which has to be defined, at least for the main parameters, not only at supply points to the end users, but also at the other boundaries. In facts, the final voltage quality depends on the operating conditions at all levels of the whole process.

However, electrical energy is a very specific product. The possibility for storing electricity in any significant quantity is very limited, so it is consumed at the same instant it is generated. Measurement and evaluation of supplied power quality has to be made at the instant of its consumption. The measurement of PQ is complex, since the supplier and user, whose sensitive electrical equipment is also a source of disturbances, have different perspectives.

The interaction between voltage and current makes it hard to separate the customer as receiving and the network company as supplying a certain level of PQ. The voltage quality (for which the network is often considered responsible) and current quality (for which the customer is often considered responsible) are affecting each other by mutual interaction. The effects of insufficient PQ are normally expressed in terms of emission, immunity and compatibility. The emission is defined as the causal disturbance, such as the offset of a voltage from its nominal value. The immunity is the degree at which the equipment will be able to function as planned in spite of the emission. The compatibility level is the level at which the risk of the equipment malfunctioning is sufficiently low. On the user's side, it is the quality of power available to the user's equipment that is important. Correct equipment operation requires the level of electromagnetic influence on equipment to be maintained below certain limits. Equipment is influenced by disturbances on the supply and by other equipment in the installation, as well as itself influencing the supply. These problems are summarized in the EN 61000 series [7-15] of EMC standards, in which limits of conducted disturbances are characterized.

## 2.2 Power quality

“Power Quality” is the term most utilities use to describe the service seen by consumers at their home or office. In order to effectively describe what's happening, we need to clarify the type of the events:

- Interruptions: can be either momentary or of long duration;
- Voltage sag: also commonly known as under-voltage;
- Voltage swell: known as over-voltage;

- Transients: short duration voltage spikes;
- Distortion: commonly referred to as harmonic distortion;
- Noise: a form of signal distortion that may cause data loss.

Power quality variations fall into two basic categories:

- 1. Disturbances. Disturbances are measured by triggering on an abnormality in the voltage or the current. Transient voltages may be detected when the peak magnitude exceeds a specified threshold. RMS voltage variations (e.g. sags or interruptions) may be detected when the RMS variation exceeds a specified level.
- 2. Steady State Variations. These include normal RMS voltage variations and harmonic distortion. These variations must be measured by sampling the voltage and/or current over time. The information is best presented as a trend of the quantity (e.g. voltage distortion) over time and then analyzed using statistical methods (e.g. average distortion level, 95% probability of not being exceeded).

In the past, measurement equipment has been designed to handle either the disturbances (e.g. disturbance analyzers) or steady state variations (e.g. voltage recorders, harmonics monitors). With advances in processing capability, new instruments have become available that can describe the full range of power quality variations.

### **2.2.1. Steady State Voltage Characteristics**

There is no such thing as steady state on the power system. Loads are continually changing and the power system is continually adjusting to these changes. All of these changes and adjustments result in voltage variations that are referred to as long duration voltage variations. These can be undervoltages or overvoltages, depending on the specific circuit conditions. Characteristics of the steady state voltage are best expressed with long duration profiles and statistics. Important characteristics include the voltage amplitude and unbalance. Harmonic distortion is also a characteristic of the steady state voltage but this characteristic is treated separately because it does not involve variations in the fundamental frequency component of the voltage. Most end use equipment is not very sensitive to these voltage variations, as long as they are within reasonable limits.

### **2.2.2 Transients**

The term transients is normally used to refer to fast changes in the system voltage or current. Transients are disturbances, rather than steady state variations such as harmonic distortion or voltage unbalance. Disturbances can be measured by triggering on the abnormality involved. For transients, it could be the peak magnitude, the rate of rise, or

just the change in the waveform from one cycle to the next. Transients can be divided into two sub-categories, impulsive transients and oscillatory transients, depending on their characteristics. Transients are normally characterized by the actual waveform, although summary descriptors can also be developed (peak magnitude, primary frequency, rate-of rise, etc.).

Figure 2.1 gives a capacitor switching transient waveform. This is one of the most important transients that is initiated on the utility supply system and can affect the operation of end user equipment. Transient problems are solved by controlling the transient at the source, changing the characteristics of the system affecting the transient or by protecting equipment so that it is not impacted. For instance, capacitor switching transients can be controlled at the source by closing the breaker contacts close to a voltage zero crossing. Magnification of the transient can be avoided by not using low voltage capacitors within the end user facilities. The actual equipment can be protected with filters or surge arresters.

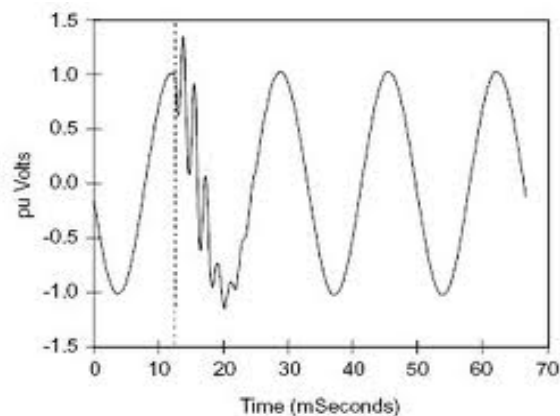


**Figure 2.1.** Disturbance due to a Capacitor switching.

### 2.2.3 Harmonic Distortion

Harmonic distortion of the voltage and current results from the operation of nonlinear loads and devices on the power system. The nonlinear loads that cause harmonics can often be represented as current sources of harmonics. The system voltage appears stiff to individual loads and the loads draw distorted current waveforms. Harmonic voltage distortion results from the interaction of these harmonic currents with the system impedance. The harmonic standard [4], has proposed two criteria for controlling harmonic levels on the power system. In the first case the end users must limit the harmonic currents injected onto the power system. In the second solution the power supplier will control the harmonic voltage distortion by making sure system

resonant conditions do not cause excessive magnification of the harmonic levels. Harmonic distortion levels can be characterized by the complete harmonic spectrum with magnitudes and phase angles of each individual harmonic component. It is also common to use a single quantity, the *Total Harmonic Distortion*, as a measure of the magnitude of harmonic distortion. For currents, the distortion values must be referred to a constant base (e.g. the rated load current or demand current) rather than the fundamental component. This provides a constant reference while the fundamental can vary over a wide range. Harmonic distortion is a characteristic of the steady state voltage and current. It is not a disturbance. Therefore, characterizing harmonic distortion levels is accomplished with profiles of the harmonic distortion over time (e.g. 24 hours) and statistics.

#### **2.2.4 Short Duration Voltage Variations**

Short duration voltage variations include variations in the fundamental frequency voltage that last less than one minute. These variations are best characterized by plots of the RMS voltage vs. time but it is often sufficient to describe them by a voltage magnitude and a duration that the voltage is outside of specified thresholds. It is usually not necessary to have detailed waveform plots since the RMS voltage magnitude is of primary interest. The voltage variations can be a momentary low voltage (voltage sag), high voltage (voltage swell), or loss of voltage (interruption). Interruptions are the most severe in terms of their impacts on end users but voltage sags can be more important because they may occur much more frequently. A fault condition can cause a momentary voltage sag over a wide portion of the system even though no end users may experience an interruption. This is true for most transmission faults. Many end users have equipment that may be sensitive to these kinds of variations. Solving this problem on the utility system may be very expensive so manufacturers are developing ride through technologies with energy storage to handle these voltage variations on the end user side.

A voltage dip is specified in terms of duration and retained voltage, usually expressed as the percentage of nominal RMS voltage remaining at the lowest point during the dip. A voltage dip means that the required energy is not being delivered to the load and this can have serious consequences depending on the type of load involved. Voltage sags - longer-term reductions in voltage – are usually caused by a deliberate reduction of voltage by the supplier to reduce the load at times of maximum demand or

by an unusually weak supply in relation to the load. Motor drives, including variable speed drives, are particularly susceptible because the load still requires energy that is no longer available except from the inertia of the drive. In processes where several drives are involved, individual motor control units may sense the loss of voltage and shut down the drive at a different voltage level from its peers and at a different rate of deceleration resulting in complete loss of process control. Data processing and control equipment is also very sensitive to voltage dips and can suffer from data loss and extended downtime.

There are two main causes of voltage dips: starting of large loads either on the affected site or by a consumer on the same circuit and faults on other branches of the network. When heavy loads are started, such as large drives, the starting current can be many times the normal running current. Since the supply and the cabling of the installation are dimensioned for normal running current the high initial current causes a voltage drop in both the supply network and the installation. The magnitude of the effect depends on how 'strong' the network is, that is, how low the impedance is at the point of common coupling (PCC) and on the impedance of the installation cabling. Dips caused by starting currents are characterized by being less deep and much longer than those caused by network faults – typically from one to several seconds or tens of seconds, rather than less than one second. The extent of a voltage dip at one site due to a fault in another part of the network depends on the topology of the network and the relative source impedances of the fault, load and generators at their common point of coupling.

The duration of the dip depends on the time taken for the protective circuits to detect and isolate the fault and is usually of the order of a few hundred of milliseconds. Since faults can be transitory, for example when caused by a tree branch falling onto a line, the fault can be cleared very soon after it has occurred. If the circuit were to be permanently disconnected by the protection equipment then all consumers on the circuit would experience a blackout until the line could be checked and reconnected. Autoreclosers can help to ease the situation, but also cause an increase in the number of dips. An autorecloser attempts to reconnect the circuit a short time (less than 1 second) after the protection equipment has operated. If the fault has cleared, the autoreclose will succeed and power is restored. Loads on that circuit experience a 100 % dip between disconnection and autoreclose while other loads see a smaller, shorter dip between the fault occurring and being isolated, as discussed above. If the fault has not cleared when

the autorecloser reconnects, the protective equipment will operate again; the process can be repeated according to the program set for the particular autorecloser. Each time it reconnects the faulty line another dip results, so that other consumers can experience several dips in series. Utility performance in deregulated markets is partly - in some countries, such as UK, solely - judged on the average 'customer minutes lost', taking into account interruptions exceeding, typically, one minute. Minimizing this statistic has resulted in the widespread application of autoreclosers and an increase in the probability of dips. In other words, long term availability has been maximized but at the expense of quality.

Electronic equipment power supplies, such as those used in personal computers (PC) and programmable logic controllers (PLC) employ a reservoir capacitor to smooth out the peaks of the full wave rectified waveform, so they should be inherently resilient to short duration dips. The larger the capacitor, and the greater the difference between the stored capacitor voltage and the minimum required for the internal voltage converters to operate, the better the resilience will be. Designers will always try to reduce the size of the capacitor to a minimum to reduce size, weight and cost while ensuring that the charge stored is just sufficient at minimum voltage and maximum load. For good dip resilience a much larger capacitor is required, at least twice as large to enable the equipment to ride through one cycle, and 100 times as large if a one-second ride through was required. An alternative design strategy is to keep the minimum input voltage as low as possible to maximize the hold up time of the system. This is the approach taken, by default, in equipment designed to work over a wide range of voltage. For shallow dips, where there is considerable retained voltage, there are several established automatic voltage regulator technologies including electro-mechanical and electromagnetic devices. Because there is no need for stored energy, these devices can be used for long duration events such as under and over voltage. Where heavy loads or deep dips are concerned a Dynamic Voltage Restorer is used. This device is series coupled to the load and generates the missing part of the supply; if the voltage dips to 70 %, the Restorer generates the missing 30 %. Voltage Restorers are normally expected to support the load for a short period and may use heavy-duty batteries, super capacitors or other forms of energy storage such as high-speed flywheels, hence they cannot be used to correct long term under and over voltage.

## 2.3 Power Quality Evaluation

Systematic procedures for evaluating power quality concerns can be developed but they must include all levels of the system, from the transmission system to the end user facilities. Power quality problems show up as impacts within the end user facility but may involve interaction between all levels of the system. A consistent set of definitions for different types of power quality variations is the starting point for developing evaluation procedures. The definitions permit standardized measurements and evaluations across different systems. A data analysis system for power quality measurements should be able to process data from a variety of instruments and support a range of applications for processing data. With continuous power quality monitoring, it is very important to be able to summarize variations by means of time trends and statistics as well as characterize individual events. Many instruments and on-line monitoring equipment now include the capability to sample waveforms and perform FFT calculations. The capabilities of these instruments vary widely and the user must be careful that the accuracy and information obtained is adequate for the investigation. The following are some basic requirements for harmonic measurements used to investigate a problem:

- i. Capability to measure both voltage and current simultaneously so that harmonic power flow information can be obtained;
- ii. Capability to measure both magnitude and phase angle of each harmonic component;
- iii. Synchronization and a sampling rate matching the correct and accurate measurement of both harmonic components and transient phenomena;
- iv. Capability to characterize the statistical nature of harmonic distortion levels (harmonics levels change with changing load and/or system conditions).

Harmonic distortion is a continuous phenomena. It can be characterized at a point in time by the frequency spectrums of the voltages and currents. However, for proper representation, measurements over a period of time must be made and the statistical characteristics of the harmonic components and the total distortion determined.

### 2.3.1 Research and Standardization activity

In the field of voltage quality, an intense research activity is conducted at international level; this work gives rise to very important pre-standardization documents, that are often taken as basis for the development of the international standards. In the following the most important working groups and standardization committees are reported, as well as their activity summarized.

*CIGRE/CIREN – Joint Working Group on Voltage Quality:* This Joint Working Group has carried out since many years research activity on the main aspects of voltage quality, i.e.: characterization of the various types of low frequency electromagnetic disturbances (harmonics,

flicker, voltage dips and swells), criteria for their evaluation, measuring methods; assessment of criteria to establish adequate limits for these disturbances; mitigation methods, cost analysis for the various mitigation methods and/or for increasing the immunity of the sensible equipment. Recently some reorganization affected the activity of the group but two important items on the criteria for defining voltage quality held: characterization methods for assessing voltage quality; quality indices and measurement protocols. The final WG Report presents power quality data gathered from several different countries across a number of monitoring points over a number of years. The report provides guidance on the key factors that need to be considered when gathering and presenting data. In so doing the report considers the benefits of consistency but recognizes the inherent differences between different electrical systems and different power quality objectives. The report develops the case for a consistent set of power quality indices and objectives that can be seen as the outer envelope of performance for each power quality parameter. Relevant power quality indices are prerequisites for assessing site and system performance with respect to power quality. Such indices will eventually facilitate the task of system operators with their obligation to routinely report power quality performance. Some site indices have already been defined in standards, but others are still missing - in particular for high and extra-high voltage (HV-EHV) systems. Since system operators are at risk of being exposed to penalty payments for excursions in quality beyond the objective values it is important that the objectives are seen not only as achievable but also as being cost effective for all customers. This adds to the incentive for having well defined and recognized power quality indices. Optimizing the power quality performance of the electrical system is one of the roles of a system operator, the role of the regulator is to ensure that this is carried out in a cost-effective manner in that if customers expect power quality to be an intrinsic characteristic of the product they also want it at the lowest price. Recognizing that historically the electrical systems in different countries have been designed in different ways to cater for national/regional variations, such as different commercial or climatic conditions, it is essential that any sets of internationally agreed power quality objectives also recognize these differences.

*IEEE Distribution Subcommittee - Working Group on Distribution Voltage Quality:*

This Working Group carries out, mainly in USA, a research and development activity similar to that of the CIGRE/CIREN Working Group, with which it has a strict co-operation. The IEEE Subcommittee has prepared some important pre-standards, two of them appear particularly important:

- i. IEEE 1159 [2], which defines indices and criteria for the quality level of the electric energy;
- ii. IEEE 519 [4], regarding the criteria for checking the harmonics content.

Both the standards refer to a third document, the IEEE 1459 [3]. It lists the mathematical expressions that were used in the past, as well as new expressions, and explains the features of the new definitions.

The program of future work includes mainly the revision and possible extension of the above documents.

*EURELECTRIC/UNIPEDA and UIE Experts Groups:* In the field of voltage quality important pre-standardization activities are also conducted within EURELECTRIC (Union of the Electricity Industry) / UNIPEDA (International Union of Producers and Distributors of Electric Energy) and UIE (International Union for the Application of the Electricity). With reference to UNIPEDA, the activity has been carried out by the Expert Group “Characteristics of the product electricity and electromagnetic compatibility” of the Specific Committee on Standardization. With reference to UIE, the activity is carried out by Working Group “Power Quality”, which, at present, in cooperation with the above CIGRE/CIGRE Working Group, is preparing a Guide about the various aspects of voltage quality: types of disturbances and relevant standards; voltage dips and short interruptions; voltage distortion; voltage unbalance; flicker; transient and temporary overvoltages.

The real standardization activity is carried out at the international level by IEC, at the European level by CENELEC, at the national level by CEI.

*IEC Subcommittee “Electromagnetic compatibility - Low frequency phenomena”:* This IEC Subcommittee has prepared a series of standards which are of interest for the definition of voltage quality. They can be classified as follows:

- ✓ series IEC 61000-2-x: standards for the definition of the electromagnetic environments and of the low frequency compatibility levels [7];
- ✓ series IEC 61000-3-x: standards for the limitation of the low frequency disturbances produced by the equipment connected to the distribution network [9];
- ✓ standards [13] and [14]: standards relating to the instrumentation and to the measuring techniques for the flicker and the harmonics;
- ✓ standards [12]: standards relating to the immunity of equipment to low frequency conducted disturbances. Within the Subcommittee, a specific Working Group on voltage quality was set up to prepare a standard defining detailed specifications for the instrumentation and the measuring methodologies.

The work led to [15], which specifies these measuring aspects for the various parameters characterizing voltage quality.

*CENELEC - TC 210 “Electromagnetic compatibility”*: its activity in the field of voltage quality essentially consists in the transposition into European standards of the IEC standards described in the previous clause.

*CENELEC – BTTF 68-6 “Physical characteristics of electrical energy”*: an ad-hoc Task Force of the Bureau Technique prepared, on the basis of a document available within UNIPED, the standard [1], published in its first edition in 1994: presently this is the most important technical reference in Europe for the regulation of voltage quality supplied in medium and low voltage public distribution networks. This standard has also been adopted in Italy by the Italian Electrotechnical Committee as CEI 110-22. The standard EN 50160 was not specifically developed in relation to the European Directive 96/92/EC regarding the liberalization of the electric energy market, but it was conceived as a voluntary technical standard for the definition of voltage quality at the terminals of the energy supply to the medium and low voltage users, as a consequence of the European Directive 85/374/EEC, which considers the electrical energy as a product. The problem of voltage quality for the high voltage users and for the other points of energy exchange is outside the scope of EN 50160. Considering the particular importance of this standard, its content is reported in the following section.

### **2.3.2 Basic definitions of voltage parameters**

In standard [1] several voltage parameters are defined. In the following the most important ones are reported:

- ✓ *Supply voltage* – the RMS value of the voltage at a given moment at the point of common coupling, measured over a given time interval.
- ✓ *Nominal voltage of the system* ( $U_n$ ) – the voltage by which a system is designated or identified and to which certain operating characteristics are referred.
- ✓ *Declared supply voltage* ( $U_c$ ) – is normally the nominal voltage  $U_n$  of the system. If, by agreement between the supplier and the user, a voltage different from the nominal voltage is applied to the terminal, then this voltage is the declared supply voltage  $U_c$ .

- ✓ *Normal operating condition* – the condition of meeting load demand, system switching and clearing faults by automatic system protection in the absence of exceptional conditions due to external influences or major events.
- ✓ *Voltage variation* – is an increase or decrease of voltage, due to variation of the total load of the distribution system or a part of it.
- ✓ *Flicker* – impression of unsteadiness of visual sensation induced by a light stimulus, the luminance or spectral distribution of which fluctuates with time.
- ✓ *Flicker severity* – intensity of flicker annoyance defined by the UIE-IEC flicker measuring method and evaluated by the following quantities: Short term severity ( $P_{st}$ ) measured over a period of ten minutes; Long term severity ( $P_{lt}$ ) calculated from a sequence of 12  $P_{st}$  – values over a two-hour interval.
- ✓ *Supply voltage dip* – a sudden reduction of the supply voltage to a value between 90% and 1% of the declared voltage  $U_c$ , followed by a voltage recovery after a short period of time. Conventionally the duration of a voltage dip is between 10 ms and 1 min. The depth of a voltage dip is defined as the difference between the minimum RMS voltage during the voltage dip and the declared voltage. Voltage changes which do not reduce the supply voltage to less than 90% of the declared voltage  $U_c$  are not considered to be dips.
- ✓ *Supply interruption* – is a condition in which the voltage at the supply terminals is lower than 1% of the declared voltage  $U_c$ . A supply interruption is classified as: prearranged in order to allow the execution of scheduled works on the distribution system, when consumers are informed in advance, or accidental, caused by permanent (a long interruption) or transient (a short interruption) faults, mostly related to external events, equipment failures or interference.
- ✓ *Temporary power-frequency overvoltages* – have relatively long duration, usually of a few power frequency periods, and originate mainly from switching operations or faults, e.g. sudden load reduction, or disconnection of short circuits.
- ✓ *Transient overvoltages* – are oscillatory or non-oscillatory, highly damped, short overvoltages with a duration of a few milliseconds or less, originating from lightning or some switching operations, for example at switch-off of an inductive current.
- ✓ *Harmonic voltage* – a sinusoidal voltage with a frequency equal to an integer multiple of the fundamental frequency of the supply voltage. Harmonic voltages

can be evaluated: individually by their relative amplitude  $U_h$  related to the fundamental voltage  $U_1$ , where  $h$  is the order of the harmonic Voltage Characteristics of Public Distribution Systems; globally, usually by the total harmonic distortion factor THD.

- ✓ *Interharmonic voltage* – is a sinusoidal voltage with frequency between the harmonics, i.e. the frequency is not an integer multiple of the fundamental.
- ✓ *Voltage unbalance* – is a condition where the RMS value of the phase voltages or the phase angles between consecutive phases in a three-phase system are not equal.

The standard [1] considers two groups of parameters characterizing voltage quality; for the first group limit values are indicated, whereas for the second only indicative values. Frequency, amplitude of the voltage (slow variations), rapid variations of the voltage, flicker (voltage fluctuations), harmonic distortions, interharmonics, three phase voltage unbalance and level of communication signals injected on the network, are all parameters belonging to the first group. The second group includes the following other parameters: voltage dips and swells; short and long interruptions; transient and temporary overvoltages.

The standard does not contain detailed information on the instrumentation and on the measuring techniques to be adopted to assess the conformity of voltage quality. However, it gives general suggestions for the various parameters to be measured on the criteria for choosing the value (average value, RMS value, peak value, etc) that characterizes the parameter to be measured. Even the statistical method of evaluation is suggested, as far as the indication of the confidence level that a certain value is not exceeded (e.g.: 95%, 99%, 100%), the time interval necessary to obtain a single measurement (10 ms, 3 s, 10 s, 10 min.) and the observation period (one day, one week, one year).

It does not apply under abnormal operating conditions, such as:

- ✓ conditions arising as a result of a fault;
- ✓ in case of failure of a customer's installation or equipment to comply with the relevant standards or with the technical requirements for the connection of loads;
- ✓ in the event of the failure of a generator installation to comply with relevant standards or with the technical requirements for interconnection with an electricity distribution system;

- ✓ in exceptional situations outside the electricity supplier's control, in particular: exceptional weather conditions and other natural disasters, third party interference, actions of public authorities, industrial action (subject to legal requirements), power shortages resulting from external events.

Actually requirements are not particularly rigorous for the supplier. In fact the numerous situations in which the standard does not apply can excuse the majority of outages and voltage disturbance events that occur in practice. Thus, many suppliers interpret the requirements of EN 50160 as principally informative and claim no responsibility when the limits are exceeded. On the other hand, the consumer's point of view is usually totally different –regarding the limits given as requirements that must be guaranteed by the supplier. However, as mentioned before, for many consumers, even fulfilling the requirements of [1] does not assure a satisfactory level of PQ. In such cases the level of PQ required must be defined in a separate agreement between supplier and consumer.

### 2.3.3 Overview of power quality indices

#### Harmonic Components

Obtaining harmonic indices consists of providing the spectrum of voltage or current over a given window of time; a site index from the spectra over a given period; and eventually a system index from the single site indices. Various methods for obtaining the spectrum are discussed in the technical literature, but the method almost exclusively used in power quality monitoring is the Fourier transform. A number of international standard documents define the measurement process, including [13] and [15].

The method proceeds as follows:

- obtain the spectrum over a 10-cycle (50 Hz systems) or 12-cycle (60 Hz systems) window. The window shall be synchronized to the actual frequency during the measurement;
- the spectra (RMS) are combined to a spectrum over a 3-second interval (150 cycles for 50 Hz systems and 180 cycles for 60 Hz systems) and the so obtained values are referred to as "very short time" indices ( $U_{h,vs}$ );
- the 3-second values are combined to a 10-minute value and referred to as "short time" indices ( $U_{h,sh}$ );

- 3-second and 10-minute values are evaluated over a one-day or a one-week period depending on the index. The 95%, 99% or maximum values of the distributions are used as site-indices.

Other publications propose more specific indices such as:

- Technical report [11]:
  - The greatest 95 % probability daily value of  $U_{h,vs}$  (RMS value of individual harmonic components over "very short" 3 s periods);
  - The maximum weekly value of  $U_{h,sh}$  (RMS value of individual harmonics over "short" 10 min periods);
  - The maximum weekly value of  $U_{h,vs}$ . For measurements it refers to [13]. The minimum measurement period should be one week.
- Standard [15] also refers to [13] for measurements, more specifically to class 1, 10/12-cycle gapless harmonic sub-group measurement. The standard does not specify indices, but various indices are given as guidelines for contractual applications
  - The number, or percentage, of values during the interval that exceed contractual values might be counted;
  - The worst-case values might be compared to contractual values (the measurement interval might be different for this possibility, for example one year);
  - One or more 95 % (or other percentage) probability weekly values for 10-minute values, 95 % (or other percentage) probability daily values for 3-sec time interval values, expressed in percent, might be compared to contractual values.

A minimum assessment period of one week is recommended for 10-min values, and daily assessment of 3-sec values for at least one week. Standard [1], stipulates that during each period of one week, the percentile 95% of the 10- min mean RMS value ( $U_{h,sh}$ ) of each individual harmonic voltage is the quality index to be compared to the relevant voltage characteristic. Other regional or national standards and guidelines also recommend indices that are often similar to those mentioned above.

### **Flicker**

The flickermeter algorithm as defined in [14] results in:

- a 10-minute “short-term flicker severity -  $P_{st}$ ”. This value is obtained from a statistical analysis of the “instantaneous flicker value” in a way which models incandescent lamps and our observation of light intensity variations.

- From the 10-minute value, a 2-hour “long-term flicker severity -  $P_{lt}$ ” is calculated.

Indices of flicker severity ( $P_{st}$  and  $P_{lt}$ ) are expressed in per unit of the irritability threshold of flicker, that is the level of flicker considered irritable by a significant portion of the people involved in the tests. Evaluation techniques might be agreed between parties: the number or percentage of values during the interval that exceed contractual values might be counted, as well as 99 % probability weekly values for  $P_{st}$ , or 95 % probability weekly value for  $P_{lt}$ , might be compared to contractual values.

### Unbalance

Only the fundamental components shall be used: all harmonic components should be eliminated by using DFT algorithm. The processing is defined similar as the above harmonic indices: from 10-cycle (50 Hz) and 12-cycle (60 Hz), to 3-second intervals, to 10-minute intervals. For unbalance also 2-hour values (obtained by combining 10-minute values) are used. The whole measurement and evaluation procedure is defined in detail in [15]. This standard suggests that 10-min and/or 2-hr values be assessed as follows:

- i. The number of values during the measurement interval that exceed contractual values might be counted;
- ii. the worst-case values might be compared to contractual values (the measurement interval might be different for this possibility, for example one year);
- iii. one or more 95 % (or other percentage) probability weekly values, NPS expressed as a percentage of PPS, might be compared to contractual values.

In standard EN 50160 the unbalance index is the 95 % of the 10-min mean RMS values of the negative phase sequence component of the supply voltage to be assessed during each period of one week.

The voltage limits set in ANSI Standard C84.1 at the point of use are at  $\pm 10\%$ , derating motor capacity at levels of unbalance greater than 1% and not exceeding 5%. The derating is based on the thermal effects on motors, and are therefore presumed to be related to long-time measurements rather than short-time measurements. The measurement specified is the difference between the average of the three phase

magnitudes and the voltage that differs the most from that average, divided by the average.

### **Voltage Dips**

The first international definition and measurement method for the most common characterization of voltage dips in terms of magnitude and duration is provided in [15]. For the measurement of dips, such standard states that “the basic measurement of a voltage dip and swell shall be the value of the RMS voltage measured over one cycle and refreshed each half cycle”. From the RMS voltage as a function of time two basic characteristics can be determined:

- retained voltage or the dip depth;
- duration.

A voltage dip is characterized by a pair of data, either retained voltage and duration or depth and duration: the retained voltage is the lowest value measured on any channel during the dip; the depth is the difference between the reference voltage and the retained voltage expressed in % of the reference voltage; the duration of a voltage dip is the time difference between the beginning and the end of the voltage dip.

The choice of a dip threshold is essential for determining the duration of the event. This choice of threshold is also important for counting events, as events are only counted as voltage dips when the RMS voltage drops below the threshold. Dip threshold can be a percentage of either nominal or declared voltage, or a percentage of the sliding voltage reference, which takes into account the actual voltage level prior to the occurrence of a dip. The user shall declare the reference voltage in use.

Voltage dip envelopes may not be rectangular hence, for a given voltage dip, the measured duration depends on the selected dip-threshold value. The shape of the envelope may be assessed using several dip thresholds set within the range of voltage dip and voltage interruption threshold detection. A number of other characteristics for voltage dips are mentioned in an annex to [15] including phase angle shift, point-on-wave, three-phase unbalance, missing voltage and distortion during the dip. The use of additional characteristics and indices may give additional information on the origin of the event, on the system and on the effect of the dip on equipment. Even though several of these terms are used in the power-quality literature there is no consistent set of definitions.

Document [8] also refers to [15] for measurement, but introduces a number of additional recommendations for calculating voltage-dip indices. Recommended values are 90% and 91% for dip-start threshold and dip-end threshold, respectively, and 10% for the interruption threshold. Dips involving more than one phase should be designated as a single event if they overlap in time. The most commonly-referred to index is the System Average RMS variation Frequency Index or SARFI.

The term “RMS variation” is used in US literature to indicate all events in which the RMS voltage deviates significantly (typically seen as more than 10%) from its nominal value. This includes voltage dips, voltage swells and long interruptions.

The SARFI<sub>X</sub> index (where X is a number between 0 and 100%) gives the number of events per year with a duration between 0,5 cycle and 1 minute and a retained voltage less than X%. Thus SARFI<sub>70</sub> gives the number of events with retained voltage less than 70%. Strictly speaking, SARFI values are obtained as a weighted average over all monitor locations within a supply network or within part of the supply network. However the term is also used to refer to the event frequency at one location. By using the weighting factors, more weight can be given to location with more – or more important – load. The weighting factors are in most cases taken to be equal for all locations.

Indices used for transmission interruption reporting differ significantly from utility to utility. The indices used can however be divided into the following categories:

- Number of events: actual number of events and the average number of events over the reporting period, i.e. the frequency of events;
- Duration of events: average total duration of events over the reporting period and average time to restore supply per interruption at each supply point. The availability of the supply is the converse of the duration and it gives an indication of the relative risk of interruptions;
- Severity of events: severity of the interruption events over the reporting period (i.e. the size of load affected) and indices estimating the cost impact per event.

### 2.3.4 Standard Measurement methods of PQ parameters

#### Requirements of EN 50160

The correct operation of electrical equipment requires a supply voltage that is as close as possible to the rated voltage. Even relatively small deviations from the rated value can cause operation at reduced efficiency, or higher power consumption with additional losses and shorter service life of the equipment. Sometimes prolonged deviations can cause operation of protection devices, resulting in outages. Of course, the correct operation of equipment also depends on many other factors, such as environmental conditions and proper selection and installation. Investigation of the independent influence of each supply voltage parameter on equipment operation is easily performed, but when parameters vary simultaneously the situation is much more complex. In some cases, after detailed analysis of the effects of each of the different voltage parameters, results can be superimposed in order to estimate the total influence of many parameters.

The increased concern for power quality has resulted in significant advances in monitoring equipment that can be used to characterize disturbances and power quality variations. In particular, measurement and testing of supply voltage quality according to EN 50160 requires specialized apparatus and measuring methods monitoring, continuously over 7 days, the following parameters:

- ✓ voltage in three phases
- ✓ frequency
- ✓ total harmonic distortion factor  $THD_U$
- ✓ voltage unbalance factor, which is a multiple of positive and negative sequence voltage components
- ✓ fast and slow voltage variations, which are defined as short term ( $P_{st}$ ) and long term ( $P_{lt}$ ) flicker severity factors.

This arrangement also enables measurement of voltage dips and outages, its frequency and duration.

The measured parameters are processed and recorded as 10 minute time-segments (1008 segments over 7 days). For each segment the mean value of the measured parameter is calculated. After the 7-day recording period a so-called “ordered diagram” is produced, which shows the sum of the duration of a given distortion level in the

observed time period. (for frequency measurement, the duration of each single segment is 10 seconds).

### **Requirements of IEC 61000-4 series**

Methods for measurement and interpretation of results for power quality parameters in 50/60 Hz a.c. power supply systems are defined in [15]. Measurement methods are described for each relevant type of parameter in terms that will make it possible to obtain reliable, repeatable and comparable results regardless of the compliant instrument being used and regardless of its environmental conditions. This standard addresses methods for measurements carried out at the monitored point of the system.

Measurement of parameters covered by this standard is limited to those phenomena that can be conducted in a power system. These include the voltage and/or current parameters, as appropriate. The power quality parameters considered in this standard are power frequency, magnitude of the supply voltage, flicker, supply voltage dips and swells, voltage interruptions, transient voltages, supply voltage unbalance, voltage and current harmonics and interharmonics, mains signalling on the supply voltage and rapid voltage changes. Depending on the purpose of the measurement, all or a subset of the phenomena on this list may be measured. The effects of transducers being inserted between the power system and the instrument are acknowledged but not addressed in detail in this standard. Precautions on installing monitors on live circuits are addressed.

Measurements can be performed on single-phase or polyphase supply systems. Depending on the context, it may be necessary to measure voltages between phase conductors and neutral (line-to-neutral) or between phase conductors (line-to-line) or between neutral and earth. The basic measurement time interval for parameter magnitudes (supply voltage, harmonics, interharmonics and unbalance) shall be a 10-cycle time interval for 50 Hz power system or 12-cycle time interval for 60 Hz power system. Measurement time intervals are aggregated over 3 different time intervals. The aggregation time intervals are: 3-s interval (150 cycles for 50 Hz nominal or 180 cycles for 60 Hz nominal), 10-min interval, 2-h interval.

Aggregations are performed by using the square root of the arithmetic mean of the squared input values. Three categories of aggregation are necessary:

- i. Cycle aggregation - The data for the 150/180-cycle time interval shall be aggregated from fifteen 10/12-cycle time intervals. This time interval is not a "time clock" interval; it is based on the frequency characteristic.

- ii. From cycle to time-clock aggregation: The 10-min value shall be tagged with the absolute time. The time tag is the time at the end of the 10-min aggregation. If the last 10/12-cycle value in a 10-min aggregation period overlaps in time with the absolute 10-min clock boundary, that 10/12-cycle value is included in the aggregation for this 10-min interval. On commencement of the measurement, the 10/12-cycle measurement shall be started at the boundary of the absolute 10-min clock, and shall be re-synchronized at every subsequent 10-min boundary.
- iii. Time-clock aggregation: The data for the “2-h interval” shall be aggregated from twelve 10-min intervals.

During a dip, swell, or interruption, the measurement algorithm for other parameters (for example, frequency measurement) might produce an unreliable value. The flagging concept therefore avoids counting a single event more than once in different parameters (for example, counting a single dip as both a dip and a frequency variation) and indicates that an aggregated value might be unreliable. Flagging is only triggered by dips, swells, and interruptions. The detection of dips and swells is dependent on the threshold selected by the user, and this selection will influence which data are "flagged".

**Table 2.1.** Standard measurement methods of the voltage quality parameters.

Parameter	Supply voltage characteristics according to EN 50160	Low voltage characteristics according to EMC standard EN 61000	
		EN 61000-2-2	Other parts
Power frequency	LV, MV: mean value of fundamental measured over 10 s $\pm 1\%$ (49.5 - 50.5 Hz) for 99.5% of week $-6\%/+4\%$ (47- 52 Hz) for 100% of week	2%	
Voltage magnitude variations	LV, MV: $\pm 10\%$ for 95% of week, mean 10 minutes rms values		$\pm 10\%$ applied for 15 minutes
Rapid voltage changes	LV: 5% normal 10% infrequently $P_{It} \leq 1$ for 95% of week  MV: 4% normal 6% infrequently $P_{It} \leq 1$ for 95% of week	3% normal 8% infrequently $P_{st} < 1.0$ $P_{It} < 0.8$	3% normal 4% maximum $P_{st} < 1.0$ $P_{It} < 0.65$ (EN 61000-3-3) 3% (IEC 61000-2-12)
Supply voltage dips	Majority: duration <1s, depth <60%. Locally limited dips caused by load switching on: LV: 10 - 50%, MV: 10 - 15%	urban: 1 - 4 months	up to 30% for 10 ms up to 60% for 100 ms (EN 61000-6-1, 6-2) up to 60% for 1000 ms (EN 61000-6-2)
Short interruptions of supply voltage	LV, MV: (up to 3 minutes) few tens - few hundreds/year Duration 70% of them < 1 s		95% reduction for 5 s (EN 61000-6-1, 6-2)
Long interruption of supply voltage	LV, MV: (longer than 3 minutes) <10 - 50/year		
Temporary, power frequency overvoltages	LV: <1.5 kV rms  MV: $1.7 U_c$ (solid or impedance earth) $2.0 U_c$ (unearthed or resonant earth)		
Transient overvoltages	LV: generally < 6kV, occasionally higher; rise time: ms - $\mu$ s.  MV: not defined		$\pm 2$ kV, line-to-earth $\pm 1$ kV, line-to-line 1.2/50(8/20) Tr/Th $\mu$ s (EN 61000-6-1, 6-2)
Supply voltage unbalance	LV, MV: up to 2% for 95% of week, mean 10 minutes rms values, up to 3% in some locations	2%	2% (IEC 61000-2-12)
Harmonic voltage	LV, MV	6%-5 <sup>th</sup> , 5%-7 <sup>th</sup> , 3.5%-11 <sup>th</sup> , 3%-13 <sup>th</sup> , THD <8%	5% 3 <sup>rd</sup> , 6% 5 <sup>th</sup> , 5% 7 <sup>th</sup> , 1.5% 9 <sup>th</sup> , 3.5% 11 <sup>th</sup> , 3% 13 <sup>th</sup> , 0.3% 15 <sup>th</sup> , 2% 17 <sup>th</sup> (EN 61000-3-2)
Interharmonic voltage	LV, MV: under consideration	0.2%	

**Power frequency**

The frequency reading shall be obtained every 10-s. As power frequency may not be exactly 50 Hz or 60 Hz within the 10-s time clock interval, the number of cycles may not be an integer number. The fundamental frequency output is the ratio of the number of integral cycles counted during the 10-s time clock interval, divided by the cumulative duration of the integer cycles. Before each assessment, harmonics and interharmonics shall be attenuated to minimize the effects of multiple zero crossings.

The measurement time intervals shall be non-overlapping. Individual cycles that overlap the 10-s time clock are discarded. Each 10-s interval shall begin on an absolute 10-s time clock,  $\pm 20$  ms for 50 Hz or  $\pm 16,7$  ms for 60 Hz.

**Magnitude of the supply voltage**

The measurement shall be the RMS value of the voltage magnitude over a 10-cycle time interval for 50 Hz power system or 12-cycle time interval for 60 Hz power system. Every 10/12-cycle interval shall be contiguous with, and not overlap, adjacent 10/12-cycle intervals.

**Classes of measurement performance**

For each parameter measured, two classes of measurement performance are defined.

– *Class A performance*

This class of performance is used where accurate measurements are necessary, for example, for contractual applications, verifying compliance with standards, resolving disputes, etc. Any measurements of a parameter carried out with two different instruments complying with the requirements of class A, when measuring the same signals, will produce matching results within the specified uncertainty. To ensure that matching results are produced, class A performance instrument requires a bandwidth characteristic and a sampling rate sufficient for the specified uncertainty of each parameter.

– *Class B performance*

This class of performance may be used for statistical surveys, trouble-shooting applications, and other applications where low uncertainty is not required.

For each performance class the range of influencing factors that shall be complied with is specified in [15]. Users shall select the class of measurement performance taking account of the situation of each application case. A measurement instrument may have

different performance classes for different parameters. The instrument manufacturer should declare influence quantities which are not expressly given and which may degrade performance of the instrument.

### **Voltage Harmonics**

Table 2.2 provides a summary comparison of harmonic indices between various standards and guidelines. It shows that in most cases the reference standard to perform harmonic measurements is [13]. This part of IEC 61000 is applicable to instrumentation intended for measuring spectral components in the frequency range up to 9 kHz which are superimposed on the fundamental of the power supply systems at 50 Hz and 60 Hz. For practical considerations, this standard distinguishes between harmonics, interharmonics and other components above the harmonic frequency range, up to 9 kHz. This standard defines the measurement instrumentation intended for testing individual items of equipment in accordance with emission limits given in certain standards (for example, harmonic current limits as given in [10]) as well as for the measurement of harmonic currents and voltages in actual supply systems. Instrumentation for measurements above the harmonic frequency range, up to 9 kHz is tentatively defined. Practically, the most common index for harmonic voltage is the so-called short time or 10-min value ( $U_{h,sh}$ ). It is used mainly for voltage characteristics and the level of harmonics to be compared with the objectives is usually the value corresponding to 95% probability of weekly statistics.

Instruments for the harmonic and interharmonic emission measurement or for measurements above the harmonic frequency range up to 9 kHz are considered in the IEC standard. Strictly speaking, harmonic measurements can be performed only on a stationary signal; fluctuating signals cannot be described correctly by their harmonics only. However, in order to obtain results that are inter-comparable, a simplified and reproducible approach is given for fluctuating signals. Two classes of accuracy (I and II) are considered, to permit the use of simple and low-cost instruments, consistent with the requirements of the application. For emission tests, the upper class I is required if the emissions are near to the limit values.

New designs of instrument are likely to use the discrete Fourier transform (DFT), normally using a fast algorithm called fast Fourier transform (FFT). Therefore the standard considers only this architecture but does not exclude other analysis principles. The main instrument for harmonic frequency measurements comprises:

- input circuits with anti-aliasing filter;
- A/D-converter (including sample-and-hold unit);
- synchronization and window-shaping unit;
- DFT-processor providing the Fourier coefficients  $a_m$  and  $b_m$ .

The instrument is complemented by the special parts devoted to current assessment and/or voltage assessment. For full compliance with this standard, the window width shall be 10 (50 Hz systems) or 12 (60 Hz systems) periods with rectangular weighting. Hanning weighting is allowed only in the case of loss of synchronization. This loss of synchronization shall be indicated on the instrument display and the data so acquired shall be flagged. The time window shall be synchronized with each group of 10 or 12 cycles according to the power system frequency of 50 Hz or 60 Hz. The time between the leading edge of the first sampling pulse and the leading edge of the  $(M+1)^{\text{th}}$  sampling

**Table 2.2.** Summary comparison of harmonics indices between different standards and reference documents.

Harmonic voltage indices	Standard /document	Status	Purpose	Very short time indices	Short time indices	Other indices	Period for statistical assessment	Measurement method
International standard or guidelines	IEC 61000-3-6	Technical report type	Indicative planning levels for emission limits	$U_{h,vs}$ 95% daily	$U_{h,s}$ max. weekly	$U_{h,vs}$ max. weekly	One week minimum	IEC 61000-4-7
	IEC 61000-4-30	International Std.	Power quality measurement methods	$U_{h,vs}$ X% as agreed	$U_{h,s}$ X% as agreed		At least one week or more	IEC 61000-4-7
Regional or national standards and guidelines	EN 50160	European Std.	Supply voltage characteristics for public networks		$U_{h,s}$ + THD 95% weekly		One week	IEC 61000-4-7
	ANSI/IEEE E 519	ANSI std. recommended practice	Emission limits and system design methods			95% (no definite indices)	Undefined	No specific method
	NRS 048-	South	Minimum		$U_{h,s}$		One	Specified

	2	African Std.	Std. used by the regulator		+ THD 95% weekly		week min.	method
	EDF Emeraude Contract	(France) PQ contract	Supply voltage characteristic		$U_{h,s}$ + THD max		At least one week or more	IEC 61000-4-7
	ER G5/4	UK National Std.	Planning levels for controlling emissions			$U_{h1}$ min + THD 95% weekly	One week	Specified method
	H. Q. Voltage Characteristics	Voluntary (Quebec)	Supply voltage characteristic		$U_{h,s}$ + THD 95% weekly		One week	IEC 61000-4-7

pulse (where  $M$  is the number of samples) shall be equal to the duration of the specified number of cycles of the power system, with a maximum permissible error of  $\pm 0,03\%$ .

Instruments including a phase-locked loop or other synchronization means shall meet the requirements for accuracy and synchronization for measuring at any signal frequency within a range of at least  $\pm 5\%$  of the nominal system frequency. However, for instruments having integrated supply sources, so that the source and measurement systems are inherently synchronized, the requirement for a working input frequency range does not apply, provided the requirements for synchronization and frequency accuracy are met.

The output shall provide the individual coefficients  $a_m$  and  $b_m$  of the DFT, for the current or voltage, i.e. the value of each frequency component calculated. A further output, not necessarily from the DFT, shall provide the active power  $P$  evaluated over the same time window used for the harmonics. For the harmonic emission measurements according to [10], this power shall not include the d.c. component.

### Flicker

The minimum measurement period should be one week (see [14]). For flicker, indices should be: 1.  $P_{st}$  99% weekly; 2.  $P_{lt}$  99% weekly. Standard [15] also refers to

standard [14] for flicker measurement. Voltage dips, swells, and interruptions shall cause  $P_{st}$  and  $P_{lt}$

**Table 2.3.** Summary comparison of flicker indices between different standards and reference documents

Flicker indices	Standard /document	Status	Purpose	Short time indices	Long time indices	Period for statistical assessment	Measurement method
<b>International standard or guidelines</b>	IEC 61000-3-7	Technical report type	Indicative planning levels for emission limits	$P_{st}$ 99% weekly	$P_{lt}$ 99% weekly	One week minimum	IEC 61000-4-15
	IEC 61000-4-30	International Std.	Power quality measurement methods	$P_{st}$ 99% weekly or X% as agreed	$P_{lt}$ 95% weekly or X% as agreed	At least one week or more as agreed	IEC 61000-4-15
<b>Regional/national standards and guidelines</b>	EN 50160	European Std.	Supply voltage characteristics for public networks		$P_{lt}$ 95% weekly	One week	IEC 61000-4-15
	NRS 048-2	South African Std.	Minimum Std. used by the regulator		$P_{st}$ 95% weekly	One week min.	IEC 61000-4-15
	EDF Emeraude Contract – A2	(France) PQ contract	Supply voltage characteristic		$P_{lt}$ no further specification	At least one week or more	IEC 61000-4-15
	ER P28	UK National Std.	Planning levels for controlling emissions	$P_{st}$ no further specification	$P_{lt}$ no further specification	Sufficient to capture full operating cycle of load	IEC 868
	H. Q. Voltage Characteristics	Voluntary (Quebec)	Supply voltage characteristic		$P_{lt}$ 95% weekly	One week	IEC 61000-4-15

output values to be flagged so that they can later be removed from statistics.  $P_{st}$  or  $P_{lt}$  might be considered. The minimum assessment period should be one week.

The minimum measurement period should be one week (see [14]). For flicker, indices should be: 1.  $P_{st}$  99% weekly; 2.  $P_{lt}$  99% weekly. Standard [15] also refers to

standard [14] for flicker measurement. Voltage dips, swells, and interruptions shall cause  $P_{st}$  and  $P_{lt}$

Table 2.3 provides a summary comparison of flicker indices between various standards and guidelines. The most common reference for flicker measurement is basically standard [14]. The 95% or 99% weekly values of  $P_{st}$  or  $P_{lt}$  indices are mostly in use. Considering that  $P_{lt}$  and  $P_{st}$  values are often correlated by a definite or quasi-constant factor related to the characteristics of the disturbing process, it may be questioned whether it is redundant specifying both indices.

### Unbalance

Table 2.4 summarises the indices relevant to negative sequence voltage unbalance factor ( $U_{neg}$ ). 10-min values are most commonly in use. Although different equations may be used for calculating voltage unbalance factor, results should be similar for a given integration time provided they consider negative sequence voltage.

### Voltage dips

Various methods for reporting dips or sags have been proposed in literature. They can be classified in two categories: methods to characterize site or system performance as such, and methods most suitable to estimate the compatibility between equipment and supply. Magnitude-duration table: Site performance as well as system performance are often described in the form of a voltage-dip table. Different table formats are discussed in [5] but only the so-called density table is commonly used. The columns of the table represent ranges of voltage-dip duration; the rows represent ranges of retained voltage.

**Table 2.4.** summary comparison of flicker indices between different standards and reference documents.

Voltage unbalance indices	Standard /document	Status	Purpose	Very short time indices	Short time indices	Long time indices	Period for statistical assessment
International standard or guidelines	IEC 61000-4-30	International Std.	Power quality measurement methods		$U_{neg,s}$ 95% weekly or as agreed	$U_{neg,l}$ 95% weekly or as agreed	One week minimum
	Cigré 1992 paper 36-203	Cigré 36.05 work	Assessing voltage quality in relation to harmonics, flicker and unbalance	$U_{neg,vs}$ 95% daily	$U_{neg,s}$ max. weekly		A few days including a week end
Regional or national standards and	EN 50160	European Std.	Supply voltage characteristics for public networks		$U_{neg,s}$ 95% weekly		One week

guidelines	NRS 048-2	South African Std.	Minimum Std. used by the regulator		$U_{neg,s}$ 95% daily		One week min.
	EDF Emeraude Contract – A2	(France) PQ contract	Supply voltage characteristic		$U_{neg,s}$ no further specification		At least one week or more
	ER P29	UK National Std.	Planning levels for controlling emissions		Max. of negative sequence measured over 1 minute		Sufficient to represent effect on rotating plant
	H. Q. Voltage Characteristics	Voluntary (Quebec)	Supply voltage characteristic			$U_{neg,l}$ 95% weekly	One week

The choice of the magnitude and duration ranges for voltage-dip tables is a point of discussion. Different publications use different values.

*Voltage-sag coordination chart:* A method for reporting site information from event magnitude and duration is described in [5] and [6]. The method results in the so-called “voltage sag coordination chart”. An example of such a chart is shown in Figure 2.2. This figure is the result of monitoring from 6 years at 20 HV-sites. The chart, as defined in these standards, contains the performance of the supply at a given site, and the voltage tolerance of one or more devices. For the purpose of this document only the supply performance part of the chart is of relevance. The chart gives the number of events per year (sags and interruptions) as a function of the severity of the event. For the example shown here there is on average 1 event per year dropping the voltage below 50% for 100 ms or longer. There is also on average 1 event per year more severe than 80%, 80 ms and on average 0.1 event per year below 70% for longer than 500 ms.

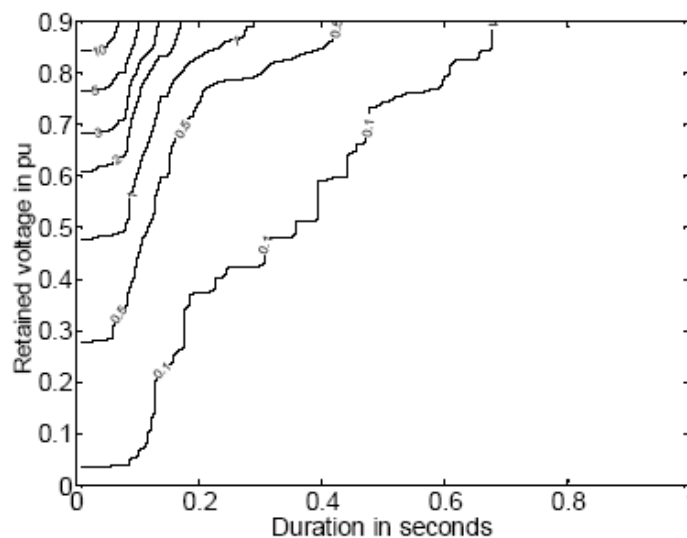


**Figure 2.2.** Voltage-sag coordination chart.

### 2.3.5 Non conventional parameters for PQ measurement

Recently, the worldwide research activity in the field of both electrical systems and electric and electronic measurements has been focused on the detection and localization of the sources of disturbance within a network. The solution to this issue is getting more and more important in the management of electric systems because the location of a disturbing device can be strictly related to the economical and contractual aspects between utility and customers.

Reliable results of power quality monitoring systems depend on the correctness of the theoretical model of the electric network and of the installed devices. First of all, the sinusoidal balanced steady-state condition can be assumed no longer for modelling the whole electrical system, even though the 50 Hz steady state is considered as usual working condition for designing the devices and for the most popular simulation and measurement techniques. Considering for example the electric lines model: the simple 4-pole tap parameters model used correctly for a 50 Hz short electric line (220 kV, 100 km), has to be switched to a more complicated frequency-dependent model if the signal has a 2500 Hz frequency. The equivalent line length in this case is 5000 km. Hence, the model of the system has to be adapted in function of the type of disturbance under test.

When the presence and the main characteristics of a disturbance affecting the network are known, its propagation along the lines and loads has to be analyzed. In doing this, the main issue is the mathematical representation of the interaction between the device generating the disturbance and the system affected by its effects. Unfortunately, in most cases the direct method is not correct: it would consist in analyzing the disturbance contribution of the load under test by itself and then injecting the disturbance into the system to check its behavior without the considered load be installed. The interactions have no significant effect on the measurement instrumentation, but can affect the measurement procedure and/or the results interpretation.

The scientific literature proposes techniques based on different operating principles. No one of them, anyway, has been approved yet by the entire scientific community and by the governments, in facts each proposed approach can register and show some critical aspects of the network under test but can be misleading about other aspects. Some surveys or evaluations about the location methods proposed in case of periodic disturbances are reported in [17-24]. Instead of describing the theory standing beside

each approach, it may be worthy to underline their common characteristic: most of the methods locating a source of disturbance in a network depend strongly on the measurement system chosen to implement it. For example, let's consider the techniques based on the evaluation of the sign of the harmonics active power contribution; the source of harmonic disturbances is assumed to be the load if the harmonic active power is negative, otherwise it is assumed to be the electric system if the harmonic active power is positive. The approach is suggested by the standard [13] aiming at recognizing the load responsible for the distortion affecting the line voltages, hence it is implemented in numerous commercial instruments designed for Power Quality monitoring, even if the scientific community showed the technique to be weak, mainly due to the fact that a load can be classified as polluting or polluted depending on the operation of all the other loads connected to the same power network.

Anyway, the method based on the sign of harmonic power components, compensated in its wrong aspects, is the most popular for the location of periodic disturbance sources. Hence, attention must be focused on the metrological characteristics of instrumentation used for the application of the method. In particular, the conditioning block, i.e. voltage and current transducers, must be carefully chosen in order to avoid that their phase error, by varying with frequency, leads to wrong evaluation of the harmonic components flow. On the basis of the sign of the harmonic active powers displayed by the instrument the operator would then mistake in assessing responsibilities for the voltage power quality degradation.

Often research groups present methods for the location of the source of disturbances based on distributed measurement systems; the analysis of data simultaneously captured in numerous points of the monitored network gives much more information on the system conditions. By the metrological point of view, distributed measurements introduce new uncertainty sources respect to spot measurements, such as lack of synchronization and data transmission delay.

## 2.4 European Scenario: standards, guides and PQ level.

There is a worldwide trend of countries reforming their power sectors: liberalization and privatization have been introduced and a new approach is taken to the regulation of the remaining network monopolies. Generally, the main objectives of power sector reform have been to improve efficiency and quality levels. Regulators are assigned the task to attain objectives that are beneficial for society, and these typically include the promotion of high economic efficiency and adequate levels of quality.

Reliability is the most important quality feature in electricity distribution, in fact it is considered the core value of electricity service provision. Any service interruption temporarily ceases the provision of electricity therewith directly affects consumers. Network reliability means the continuous availability of electricity for the consumer. It is characterized by the number of outages for a customer and the duration of these outages. To most customers, it represents the most visible and sensible issue concerning the quality of supply. Therefore many regulators prioritize network reliability when starting regulating quality of supply. The situation of distribution and transmission networks is very different, as the first ones are characterized with many outages with relatively long duration and affecting a limited number of customers, whereas the latter ones are affected by rare outages, usually short in duration but involving many customers. The most interruptions are caused in the low voltage (LV) grid, followed by medium voltage (MV) grids. A survey by the Italian regulator in 1998 showed that within Italy the MV grids are responsible for 85% of the total minute lost, followed by the LV grid (12%) and the HV grids (3%).

As mentioned above, while EN 50160 gives general limits for public supply networks, various European countries have additional rules governing supply conditions. Many of these national regulations cover areas not included in EN 50160, such as the maximum permissible harmonic load to be connected to the PCC.

The German national standard VDE 0100 states that the voltage parameters defined in DIN EN 50160 reflect extreme situations in the network and are not representative of typical conditions. In planning networks the recommendations of VDE 0100 should be followed: it gives maximum values (per unit) for phase-angle controlled resistive loads (1700 VA single-phase, 3300 VA two-phase and 5000 VA balanced three-phase) and for uncontrolled rectifier loads with capacitive smoothing (300 VA single phase, 600

VA two-phase and 1000 VA balanced three-phase). The equipment standard VDE 0838 (EN 60555) is also quoted.

In Poland, the rules of electrical energy distribution established by the government give the fundamental parameters of the supply voltage and do not refer to EN 50160.

Additionally, consumers are divided into six groups, for which separate, permissible total annual outage times are defined. The document also deals in detail with various economic aspects of the energy market, principles of settlement between network and distribution companies etc.

In Italy there is an important document dealing with the continuity of supplied energy [16]. The Italian Regulatory Authority for Electricity and Gas (AEEG) has in fact set out a uniform system of service continuity indicators and has put in place a system of incentives and penalties in order to progressively bring continuity levels up to meet European standards. The Authority has divided the national territory into 230 geographical zones, sub-divided by areas of population density and has set improvement targets for each area on the basis of the previous year's performance. Utilities that succeed in improving by more than the required rate can recover the higher costs sustained. Conversely, companies have to pay a penalty if they fail to meet the improvement target. Interruptions due to third parties are not included in the calculation. The overall performance target is to bring continuity levels up to national benchmark levels based on European standards: 30 minutes of interruptions overall per user per year in large cities (high density); 45 minutes in medium-sized towns (medium density); and 60 minutes in rural areas (low density). Other countries have similar regimes imposed by the regulatory authorities.

The UK has a number of documents making up the distribution code. One of the most important is G5/4, discussed elsewhere in this Guide, which regulates the connection of harmonic loads to the point of common coupling. Measures to encourage the improvement of continuity are the responsibility of the Office of Gas and Electricity Markets (OFGEM).

Most European countries are collecting data on SAIFI (System Average Interruption Frequency Index) and SAIDI (System Average Interruption Duration Index): in their formulas the number of customers is used as a basis for weighting, but Austria, France and Spain are using the installed capacity (in MVA) for the same purpose, that is more consistent as weighting factor because it corresponds to the actual electric power that can be absorbed in each node. In MV networks the difference of customer size is

reflected in this case, and for operators it is easier to count capacity than the number of clients. For distribution networks, SAIDI and SAIFI indicators are used by regulators in Great Britain, Hungary, Italy, Norway, Czech Republic, Greece, Portugal, France, Lithuania, Sweden, Estonia, Ireland, Germany and the Netherlands. Although different countries are using slightly different definitions, in Europe SAIFI and SAIDI are well accepted. For transmission networks only a few European countries are collecting the same indices (Czech Republic, France, Portugal, Norway and Italy). Actually regulators prefer energy related indicators for monitoring reliability in this case, because they generally only have a few customers who are connected directly to their networks.

For interruptions with duration shorter than three minutes the MAIFI (Momentary Average Interruption Frequency Index) is used. For a customer, short interruptions are especially unpleasant in case of working with computers, as even an interruption of several seconds can lead to high costs. Among regulators, monitoring short interruptions is increasing, but still this phenomenon is registered by a limited number of countries, i.e. Finland, France, Hungary, Great Britain and Italy, some of them on both transmission and distribution networks. Probably the main reason for this is that for distribution companies it is not easy to measure short interruptions because they don't need human intervention. Actually, interruptions longer than 3 minutes can be reported manually as number of outages, whereas for short interruptions automatic monitoring equipment should be installed.

By comparing the data on SAIFI of the countries within Europe to establish their reliability performance, it shows that countries like Portugal and Finland have higher SAIFI functions than the other countries. Anyway countries like UK, Ireland and Netherlands have a higher average duration per outage. Based on the SAIDI, the Netherlands has the highest reliability and Portugal the lowest one. Although the SAIFI is different between UK and Italy, the reliability based on the SAIDI is equal for both of them.

In most countries outages caused by faults in other networks are considered as being caused outside of area of responsibility of the network operator. Because of its nature, the so-called Force Majeure is more difficult to assess, but should not be blamed to the operator. On the other hand, not including such exceptional and severe circumstances in quality regulation could lead to serious debts or even bankrupt of the network operator. Therefore, these events could be better monitored separately.

Outages caused by third parties, i.e. externally caused outages, and internally caused outages are not always easy to distinguish. Moreover, externally caused outages could be influenced by the network operator into some extent. For example, the operator could protect his system better to external faults or could provide better information to parties that potentially hurt the system. Moreover, the duration of the outage can be influenced largely by the network operator because he is restoring power supply.

Climate and weather influence the quality of supply, especially in case of overhead networks. The climate is a factor that could not be changed by the network operator, however he is the only party who is able to optimize expenditure and the final quality. Traditionally, the trade-off between quality of supply and network cost is different for rural area and urban areas. This results in more meshed underground networks in urban areas, and hence to a better quality of supply. In quality of supply regulation often urban and rural networks are treated differently. Some European countries collect SAIDI and SAIFI data separately for different customer densities as well. Italy and Lithuania use the number of inhabitants of municipalities as the characteristic for classification, whereas Spain, Portugal and Latvia use a classification based on customers instead of inhabitants. Within the UK each company has to report about their availability. Advanced quality regulation should take into account both the energy consumed by the customer and the vulnerability of the customer. Of course, this could not be done for every individual customer connected to the distribution network, however a compromise should be create customer groups and collect quality data separately for different groups. Optimal quality is achieved if the additional costs to provide higher quality are equal to the resulting decrease in interruption costs experienced by the consumers. If quality is higher than the optimum, there is a welfare loss as consumers would be provided a level of quality where the additional costs of providing this high quality exceed the associated reduction in interruption costs. Conversely, if quality is below the optimum, there is also a reduction in interruption costs.

The cost of an interruption is driven by a number of factors, first of all its duration. For the industrial sector it has been found that the cost per hour of interruption decrease with duration, suggesting that there is a large initial fixed cost component and a variable component that decreases with duration.

Another factor influencing the cost of an interruption is the reliability level at which the customer is being supplied. Generally, the higher the reliability level the more severe the impact of an interruption will be. As the frequency of interruptions increases,

consumers can make a better trade-off between expected interruption costs and the adaptive response costs thus minimizing total interruption costs. Interruption costs vary also with the time of the year, day of the week and time of the day.

The regulatory cap control framework provides companies with strong incentives to avoid over-investments, reduce costs and to improve efficiency. This may have strong implications on the short- and long-term reliability of the system. Therefore, regulators will need to accompany price regulation to protect customers against a decrease in quality and performance standards below certain limits. The introduction of the quality of supply regulation is in line with the main task of a regulator, the protection of customers from monopoly power of the network operators. In doing so, quality regulation helps to overcome incentives to reduce quality that are provided within the system of cap regulation. Thus, quality regulation is a necessary component of price regulation to balance the incentives to cut cost in order to provide the amount of quality the customers expect and are willing to pay for. Even though the quality reduction may cause additional cost for network users, the monopoly network operator may still find it more profitable to cut costs at the expense of quality. The quality of supply is just as important as prices to customers. If standard services fall but prices remain the same, consumers are effectively suffering from an increase in prices. Another benefit of quality regulation is that it provides better guidance to the regulated companies in developing and implementing their quality policy. Even if providing high quality is important to the network service providers, this does not answer the question of how high this quality should actually be.

### **2.4.1 Reliability regulation**

Reliability is a measure for the ability of the network to continuously meet the demand from customers [25]. For its regulation three methods can be distinguished:

- a) Performance publication – indirect method;
- b) Standards;
- c) Incentive schemes.

a) performance publication is widely used by regulators. The regulator requires the companies to disclose information about trends in its quality performance to the public. Overviews of the company's quality performance are then provided, for example, in the company's annual reports, in dedicated regulatory publication or on the company's website. Additionally, the regulator can oblige the regulated service provider to take

into consideration the views of customer representation groups or include customers in the advisory or supervisory boards. Performance publication is relatively simple to implement and requires limited regulatory involvement. The basic idea is to expose the company to public scrutiny by providing customers with information about the company's performance. The assumption is that the company would then be inclined to match its quality to customer demand because of its reputation.

b) standards put a floor to the performance level of the company. Violation of the standard can lead to a fine or tariff rebate. Examples of such standards are customer minutes lost, percentage of customers with outage, or some aggregated quality index. In regulation there is a distinction between overall standards and guaranteed standards. Overall ones are levels of performance set by the regulator and companies must do their utmost to comply with them. They are not measured with respect to performance for individual customers. Guaranteed ones are levels of performance which must be achieved in each individual delivery of a specified service. Customers who fail to receive the required level of service under a guaranteed standard may be entitled to receive a penalty payment.

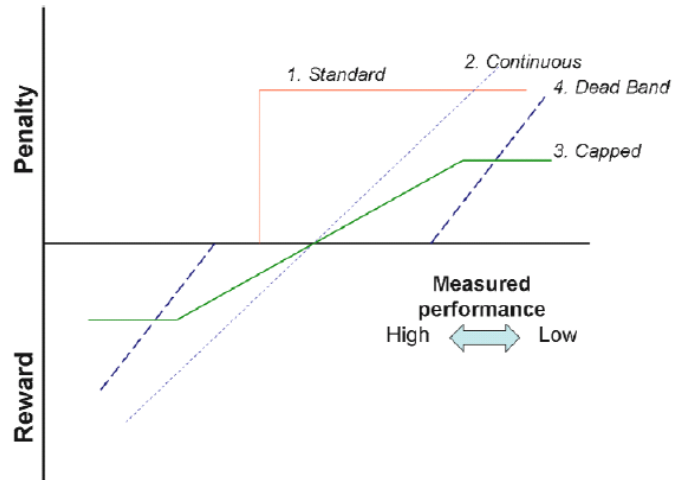
Standards can be defined per region or zone. In this case, the standard is called a zonal standard. Usually, zones with higher customer density, such as urban areas, have a higher standard to reflect the higher costs involved in supplying customers living in rural and less densely populated zones. Consequently, the minimum standard for urban zones would be set higher than for rural ones. Within the regulatory practice standards tend more and more to be set as guaranteed standards since they are easier to measure and to document. Guaranteed standards intend to protect the single customer and do not incentive the average performance of the regulated network operator. Standards are used to set limits for commercial quality and reliability.

The main problem of a standard is that it imposes a discrete and not continuous relationship between quality and price. The company either pays a fine or it does not, depending on whether it violates the set standard: there is nothing in between. The question is at what level the standard should be set, and what the level of the fine should be. These two need to be low enough to be defensible and high enough to be effective. If they are set too high the standard may severely punish the company for not meeting unrealistic targets. If the standard is set too low, quality degradation may occur.

Quality incentive schemes can be considered as an extension of a standard. Alternatively, a standard can be considered as a special case of quality incentive

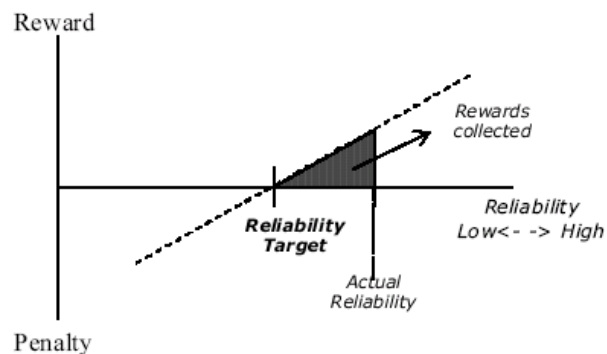
scheme. The price and quality are closely related and the company's performance is compared to some quality target: deviations result in either a penalty or a reward there are many variations of quality incentive schemes. Price and quality can be mapped continuously, in a discrete way, or a combination of these; the level of the penalty can be capped, dead bands can be applied.

Figure 2.3 shows some examples, where the x-axis represents the measured quality level, the y-axis the penalty or reward.



**Figure 2.3.** Penalties/Rewards in function of quality.

Quality incentive schemes can be used for all kind of quality indicators. The measured performance can be expressed for example in terms of SAIDI or SAIFI. The Dutch regulator has introduced a quality incentive scheme that refers to these indices. Figure 2.4 reports the Dutch incentive scheme.



**Figure 2.4.** Quality incentives scheme for SAIDI and SAIFI.

Beside the three methods of quality regulation that are normally applied together regulatory practice is facing more and more tendency towards so-called integrated price-quality regulation. It solves the trade off between cost and quality by explicitly

considering quality as a cost component within the benchmarking since it can be assumed that higher quality leads to higher cost and vice versa. By doing so, quality is taken into account while comparing the efficiency of the network operators within the analysis of data with a method to compare firms using multiple input and output factors. Up to this point only short time measurement and short time implications of price regulation on reliability have been considered. Anyway, given the long term nature of investment decisions and the effects of a continuous maintenance, short term decisions on quality have a deep impact on future cost and quality that cannot be under control just with short time measurements. Long term analysis and assessment of reliability is becoming more and more important. Regulators should be aware of the interaction between short term incentives and long term consequences of their decision and use of additional tools to evaluate them. Long time reliability control should be in line with the general regulatory approach. It comes clear that cap regulation provides strong incentives to reduce cost more than obliged by the regulator in order to realize efficiency gains, leading to an overall decrease in quality of supply and quality restriction for certain customer groups. Quality regulation is important as a part of incentive regulation in order to ensure appropriate solutions for the cost-quality trade off respecting the customers demand for reliability.

By applying the above three methods the cost-quality trade off is not immediately solved. Hence, regulators introduce integrated price-quality regulation that considers the quality provided in the efficiency analysis. Moreover, the long-term aspects of quality become more and more a challenge for regulators to implement a balanced system that ensures the consistency of short time efficiency incentives and long term reliability.

### **2.4.2 Voltage quality regulation**

In many countries voltage quality is regulated to some extent, often using industrial standards or accepted practice to provide indicative levels of relevant performance. The main difference in voltage quality and network reliability is that until a certain voltage quality level the customer is not affected by a not perfect performance, whereas the same customer is affected by any interruption of the power supply. The customer does not have interest in improving the voltage quality as long as it stands within certain limits, while the customer has interest in avoiding all interruptions in the power supply.

In most European countries the voltage quality is not an issue for a large majority of the customers in distribution networks. This means that these customers will basically

not benefit from improvements in the voltage quality. However, as connected equipment is not working due to the lack of voltage quality, improvement of the quality has a value to the customer. Because some equipment is more vulnerable to lack of technical quality than other equipment, some clients will value this quality increase differently. Therefore, it is hard to assess the value of technical quality and its individual dimensions than the value of prevented interruptions. This is the second main difference between voltage quality and network reliability.

A third difference is the cause of the lack of quality. While power interruptions for the customer are mainly caused in the electricity network or the connection of the customer, voltage quality is largely influenced by other customers. Harmonic distortion is caused by electronic equipment connected to the network and voltage dips could be caused by short circuits in the network or by welding apparatus. Hence the network operator should not pay for every single decrease of voltage quality, but it should be able to keep the voltage quality at least on acceptable levels by applying maximum disturbance levels and checking customers on keeping them. In most countries minimum standards are defined for voltage quality. This way if a minimum level of quality is met, the customer is not interested in a better quality, anyway the network operator is responsible for meeting a minimum of quality in his system. Since there is a large difference regarding the influence of lack of quality for different type of customers, some customers need higher quality than the minimum standard levels. In most cases, this is regulated by connection contracts. Dutch network operators are investigating a transparent classification system for the delivered voltage quality on the point of common coupling. Actually, the minimum standards are usually based on an international accepted standards, as the European EN 50160 “the characteristic of the supply voltage concerning: frequency, magnitude, waveform and symmetry of the phases”. Mostly these minimum standards for voltage quality are included in the grid code or the distribution code. Although EN 50160 gives indicative values for many of the phenomena, it is only applicable to voltage levels up to 35 kV. For higher voltage levels no standard exists; in the Netherland, Italy and Portugal some criteria from EN 50160 are extended to voltage levels up to 50 kV or higher.

In some countries, voltage quality standards introduced by regulators differ from the limits prescribed by EN 50160; in an increasing number of EU countries the EN reference levels are not found to be satisfactory both by regulators and customers. The CEER Benchmarking report and the Cigré workgroup on PQ both highly recommend

that EN 50160 should be revised, taking into account both the actual levels of voltage quality in European transmission and distribution networks, the evaluation of customer's needs. Like network reliability, the voltage quality in distribution networks is influenced as well by the voltage quality in the interconnected transmission and distribution networks. A difference however is that where interruptions in the power supply could be related to a cause in a network, voltage quality is the result of many different causes which are changed during transmission and transformation. Thus, it is hard to identify the network owner who should be responsible for the level of power quality.

### 2.4.3 Monitoring the voltage quality within EU

A good knowledge of the real situation is a preliminary step towards any kind of regulatory intervention. Therefore, a growing number of European countries have monitoring systems installed or plan to install them in the near future, as shown in Table 2.5. Monitoring systems within a number of EU countries are based on a sampling either of transmission-distribution interface points or customer connection points.

**Table 2.5.** Monitoring system in European Countries.

VOLTAGE QUALITY MONITORING SYSTEM	COUNTRIES
Monitoring at both transmission and distribution levels	Italy, Norway, Portugal, Slovenia, the Netherlands
Monitoring only at transmission level	Czech republic
Monitoring only at distribution level	Hungary
Proposal stage	Spain and Sweden

In Norway a monitoring system has been applied for several years. From 2006 mandatory voltage quality monitoring started: each network company is obliged to monitor quality parameters continuously in different characteristic parts of its power system.

In Hungary the regulator owns 400 voltage quality recorders that are installed each semester in one of the six distribution companies, at low voltage only. The regulator chooses the network points randomly, in a way that does not depend on previous events or complains.

In Portugal there are 61 points monitored on the transmission grid (40 for 4 weeks and the rest all year long); in distribution system, all 423 substations in MV and 1270 power transformation stations in LV have been monitored for 3 years.

In Slovenia distribution and transmission companies are obliged to measure voltage quality parameters; monitoring is implemented in high voltage covering all the substations and about 10% of MV systems.

In Italy at the end of 2004 the regulator asked the transmission company to install about one hundred voltage quality recorders; as for distribution, a voltage quality monitoring system of 400 points is working in about 10% of MV bus-bars in HV/MV transformers.

In Spain the distribution companies and the regulator have been working on a procedure for controlling and measuring voltage quality; 10% of the busbars in MV of each province is involved.

In Czech Republic a monitoring systems is going to be installed at the interconnection points between transmission and distribution networks.

In the Netherlands the grid operators measure at 150 points (50 points at HV, 50 points at MV and 50 points at LV) the quality for one week each. Every year these points are selected randomly in such a way that does not depend on previous events or complains. The measuring devices are owned by the federation of energy companies in the Netherlands. With a limited number of measuring equipment 150 network points can be monitored. The grid operators started in 2005 with measuring the voltage dips at 20 EHV stations and 20 HV stations for a period of one year.

Although these monitoring systems within several countries are different from each other in many respects, a common point is that at least voltage magnitude, dips and harmonic distortion of the voltage waveform are monitored. The number and location of voltage recorders is quite different from one country to another.

As for individual voltage quality measurements, one case deserves special attention. In France the main distribution companies offer their customers customized contracts with assigned power quality levels. If the customer claims for better contractual levels than normal ones, he can ask the operator for customized contractual levels in is contract, paying an extra charge. Customers having customized contracts must be monitored by a recorder installed and owned by the customers themselves or by the operator. In distribution networks about 16% of MV customers have a power quality

recorder, whereas in the transmission networks the monitoring involves about 12% of EHV and HV customers.

In comparison to regulation of reliability, the regulation of voltage quality is less advanced. Where some European countries are using complex and highly effective regulations (e.g. incentive regulation) for reliability, for regulation of voltage quality most regulators rely on indirect measurements or minimum standards at most.

As definitions and procedures are in place, the reliability measurement is quite immediate, no special measurement equipment needs to be installed to collect duration of the power interruption and the number of affected customers, or the total amount of interrupted power. This is different for most dimensions of voltage quality, which need to be measured with specialized measurement devices. An important issue is that the voltage quality is different for every connection point in the network. Because it is not feasible to measure everywhere, statistical techniques are needed to report on average voltage quality of individual sensitive customers. In contradiction to this, reliability can be measured by just sorting out and summing all individual outage statistics. One more difference between reliability and power quality is the cause of their lack. For interruptions in most cases the cause could be found in one or more events in the public electricity network, whereas voltage quality is influenced by both conditions in the public electricity network and at the client site. Steel manufacturers are well known producers of voltage dips that are “exported” from their plants to the network, influencing the voltage quality of other clients. Although the network operator should be responsible for the voltage quality in its network, this aspect makes the voltage quality regulation a more complex issue.

In a number of EU countries (Italy, Norway, Portugal, Slovenia, Czech Republic, Hungary and the Netherlands) voltage quality monitoring systems are installed or currently under commissioning. Most countries apply recorders on both transmission and distribution, while Hungary, e.g., is interested in quality only of low voltage. Anyway, in most countries there is no systematic monitoring system for voltage quality, but a clear trend shows that the number of countries with monitoring systems is increasing.

For the measurement of system quality, in Norway, Hungary, Portugal, Slovenia, Netherlands, Italy and Spain a measurement program is or is planned to be installed. The program statistically determines parameters that provide general picture of voltage quality of the system by using a large set of voltage quality meters. For example, in

Hungary 400 devices are installed in the low voltage network, for one semester at each place. In Portugal 1270 low voltage substations 423 medium voltage substations and 61 points in the transmission grid are monitored. Although measurement schemes are installed more and more, results of voltage quality are not yet easily accessible for the average client.

#### **2.4.4 Minimum standards**

Since voltage quality is an individual indicator, in almost all European countries a set of minimum standards are introduced to define the minimum voltage quality for individual connection points to be delivered by the network operator. Many EU countries apply EN 50160 as the minimum standard for voltage quality even if this standard is recognized to be not perfect. One important disadvantage is that EN 50160 is valid only for voltage levels up to 35 kV, but in many countries the same or similar levels for higher voltage networks are used. Moreover, EN 50160 only provides mandatory standards for a limited number of Power Quality indicators, while for others only indicative values are provided. In addition to this, many standards are defined for 95% of the time, leaving out the rest of the time. Finally, sometimes EN 50160 is considered to be too weak.

Although EN 50160 is very common for European Regulators, a number of them is adapting their minimum standards on voltage quality so that the relevant disadvantages are overcome. E.g. Norway has adapted voltage quality standards on supply voltage variations, flicker severity, rapid voltage changes, voltage unbalance and harmonic distortion. The Norwegian standards are now made better compatible to immunity levels of equipment. Also France, the Netherlands and Portugal have adapted some of the EN 50160 standards. Currently several institutions such as Cigré and Cired are discussing improvements to the standard EN 50160.

If one issue is having sensible standards, another one is how to deal with voltage quality that does not meet the minimum standards. A large number of countries (Austria, Belgium, Czech Republic, Estonia, France, Latvia, Norway and Poland) distribution network operators have the obligation to verify voltage quality complaints of individual customers. Generally, this is done on customer's expenses, but sometimes customers only pay if the voltage quality meets the standards. Usually, not meeting the voltage quality standards does not lead to penalties and only leads to the obligation for the network operator to improve quality in order to fulfill the minimum standards.

Some countries have installed a complaint procedure, which includes a maximum response time for the network operators on power quality complaints of the customer. Sometimes a penalty payment is needed if the network operator exceeds this set time. In the U.K. in case of voltage complaint by a customer, the distribution network operator must visit the customer within 7 working days or send a substantive reply within 5 days. If the operator fails meeting this standard, the customer is provided with a payment of £ 20. similar complaint procedures exist in Norway, Hungary, Ireland, Italy, Latvia, Portugal and Slovenia. Penalties applied in these countries range from 8 Euro for 7 working days in Hungary (in case of domestic customers) to 75 Euro for 15 working days in Portugal (Medium and High voltage customers).

Hungary and Ireland apply also a standard for the correction of voltage quality problems. In the first country the operators need to pay a penalty of 20 to 120 Euro (depending on the size of the customer) if voltage complaints are not compensated within 12 months. In the second country a payment of 50 Euro is needed after three months.

#### **2.4.5 Incentive schemes**

Unlike power quality regulation with regard to reliability, currently no regulators are applying incentive regulation for voltage quality. However, some countries are applying so-called “power quality contracts”, i.e. individual contracts between network operator and customer agree on voltage quality standards which are different from the usual standard. In France network operators usually offer all customers such contracts, which could be customized to the desired quality level. The payment is related to the work that has to be done by the operator in order to meet these standards. While this contract is pretty popular for reliability (for which 1000 over 100,000 MV customers have a contract) only 92 customers have a contract with customized contractual levels on voltage quality. Because of different reasons, incentive regulation schemes are not yet in place for quality regulation. Since interruptions are considered to be more important by the majority of customers, regulators started with incentive regulation for reliability. On the other hand, some investigations show that costs of lack of quality are significant, e.g. Norwegian investigation shows that customers costs associated with short interruptions and voltage dips in Norway are similar to the customers costs related to long interruptions. However, some issues need to be addressed before being able to implement incentive regulation. Main issues are:

- ✓ Measurement of short interruptions and long and deep voltage dips;
- ✓ Determining customers costs in case of short interruptions and long and deep voltage dips.

**Table 2.6.** Methods for quality regulation in Europe.

Method	APPLIED FOR VOLTAGE QUALITY	Objective
Indirect	Monitoring voltage quality by large measurement programs	Monitor long term development
Standards	Individual guaranteed standards based on EN 50160	Protection of individual customer groups
	Quality contracts	Meeting voltage quality requirements of individual customers
Incentive scheme	Not applied	Ensuring an average voltage quality level

Table 2.6 provides a high-level overview of the methods used for quality regulation in Europe, categorized in indirect methods, minimum standards and incentive regulation. In some countries large voltage quality monitoring systems are installed. Using results relevant to more than one year the long term developments of voltage quality of the system could be monitored.

Since equipment at the customers will get more sensitive for lack of voltage quality it can be expected that the regulators will extend regulation on voltage quality. A better insight in costs at customers due to lack of voltage quality, characteristic of regulation, individually for the different parameters of voltage quality could be helpful for them. It is important to consider all voltage quality parameters individually, e.g. regulating on voltage dips will be different from regulating on harmonics [26].

**References**

- [1] EN 50160, “*Voltage characteristics of electricity supplied by public distribution systems*”, CENELEC, Bruxelles (Belgium), 1999;
- [2] IEEE std 1159-1995, “*Recommended practice for monitoring electric power quality*”, The IEEE, Piscataway (USA), Nov. 1995;
- [3] IEEE Trial-Use Std 1459-2000, “*Definitions for the measurements of electric power quantities under sinusoidal, nonsinusoidal, balanced or unbalanced conditions*”, The IEEE, New York (USA), June 2000;
- [4] IEEE Trial-Use Std 519-1992, “*Recommended Practices and Requirements for Harmonic Control in Electrical Power Systems*” The IEEE, Piscataway (USA), June 1992;
- [5] IEEE Std 493-2007, “*IEEE Recommended Practice for the Design of Reliable Industrial and Commercial Power Systems*”, The IEEE, Piscataway (USA), 2007;
- [6] IEEE Std 1346-1998, “*Recommended Practice for Evaluating Electric Power System Compatibility with Electronic Process Equipment*”, The IEEE, Piscataway (USA), May 1998;
- [7] IEC 61000-2-X, “*Electromagnetic compatibility (EMC): Environment*”, 2002;
- [8] IEC 61000-2-8, “*Electromagnetic compatibility (EMC): Environment – Voltage dip and short interruption on public electric power supply system with statistical measurements results*”;
- [9] IEC 61000-3-X, “*Electromagnetic compatibility (EMC): Limits*”;
- [10] IEC 61000-3-2, “*Electromagnetic compatibility (EMC): Limits for harmonic current emissions (equipment input current  $\leq 16$  A per phase)*”;
- [11] IEC 61000-3-6, “*Electromagnetic compatibility (EMC) – Part 3: Limits – Assessment of emission limits for distorting load in MV and HV power systems*”;
- [12] IEC 61000-4-X, “*Electromagnetic compatibility (EMC): Testing and Measurements techniques*”, 2002;
- [13] IEC 61000-4-7, “*Electromagnetic compatibility (EMC) – Part 4-7: Test and Measurements techniques – General guide on harmonics and inter-harmonics measurements and instrumentation for power supply systems and equipment connected thereto*”;
- [14] IEC 61000-4-15, “*Electromagnetic compatibility (EMC) – Part 4-15: Test and Measurements techniques – Flickermeter – Functional and design specifications*”;

- [15] IEC 61000-4-30, “*Electromagnetic compatibility (EMC) – Part 4-30: Test and Measurements techniques – Power quality measurements methods*”;
- [16] Autorità per l’Energia Elettrica e il Gas: “*Testo integrato delle disposizioni dell’Autorità in materia di qualità dei servizi di distribuzione, misura e vendita dell’energia elettrica*”, Delibera 30 gennaio 2004, n.4/04;
- [17] E. J. Davis, A. E. Emanuel, D. J. Pileggi, “*Evaluation of single-point Measurements Method for Harmonic Pollution Cost Allocation*”, IEEE Trans. on Power Delivery, vol. 15, n. 1, 2000, pp. 14-18;
- [18] P. J. Rens, P. H. Swart, “*On Techniques for the Localization of Multiple Distortion Sources in three-phase Networks: Time Domain Verification*”, ETEP, Vol. 11, No 5, 2001, pp. 317-332;
- [19] C. Muscas, “*Assessment of Electric Power Quality: Indices for Identifying Disturbing Loads*”, ETEP, Vol. 8, No. 4, 1998, pp. 287-292;
- [20] L. Cristaldi, A. Ferrero, S. Salicone, “*A distributed Measurement System for Electric Power Quality Measurement*”, IEEE Trans. on Instr. and Meas., Vol. 51, No. 4, 2002, pp. 19-23;
- [21] D. Castaldo, A. Testa, A. Ferrero, S. Salicone, “*An Index for Assessing the Responsibility for Injecting Periodic Disturbances*”, L’energia elettrica, vol. 81, 2004, “Ricerche”;
- [22] A. Ferrero, R. Sasdelli, “*Revenue and Harmonics: a Discussion about New Quality Oriented Measurement Methods*”, Proc. Of the 9<sup>th</sup> intern. Conference on metering and tariffs for energy supply, Publication 462, Birmingham, UK, 1999, pp. 46-50;
- [23] R. Sasdelli, C. Muscas, L. Peretto, “*A VI-based measurement system for sharing the customer and supply responsibility for harmonic distortion*”, IEEE Trans. on Instr. And Meas., 1998, Vol. 47, No. 5, pp. 1335-1340;
- [24] C. Muscas, L. Peretto, S. Sulis, R. Tinarelli, “*Implementation of multi-point Measurement Techniques for PQ Monitoring*”, Proc. Of the 21st IEEE IMTC/04, Como(Italy), 2004, vol. 3, pp. 1626-1631;
- [25] K. Keller, B.F.C Franken, “*Quality of Supply and Market Regulation; survey within Europe*”, KEMA Consulting by order of the European Copper Institute, Arnhem, The Netherlands, December 2006.
- [26] PhD Thesis “*Development and Characterization of a distributed measurement system for the evaluation of voltage quality in electric power networks*”, Elisa Scala.

## 3. The human visual system

### 3.1 Anatomy and function

The human eye is a complex anatomical device able to give many times more information about surroundings than all other senses combined. Its structure is remarkable, not only for what it can do, but also because the eye is the only part of the body where nerves and tiny blood vessels can be seen directly, and by its inspection it is possible to provide important clues about the health of the entire body. Like a camera, it is able to refract light and produce a focused image that can stimulate neural responses and enable the ability to see. It is essentially an opaque eyeball, shown in figure 3.1, filled with a water like fluid. In the front of the eyeball is a transparent opening

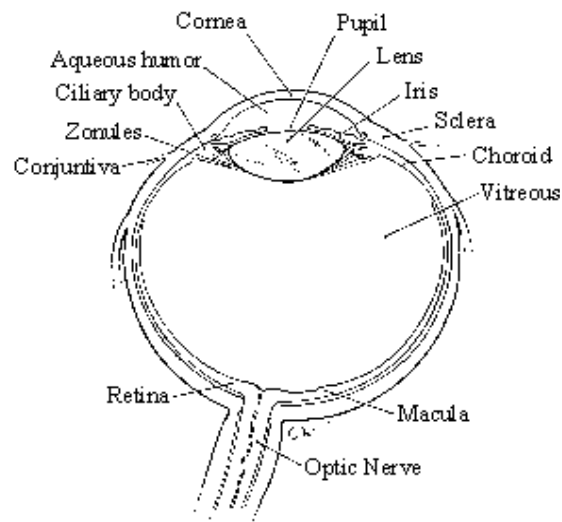


Figure 3. 1 The human eye.

known as the cornea. That is a thin membrane that has the dual purpose of protecting the eye and refracting light as it enters the eye. After light passes through the cornea, a portion of it goes through an opening known as the pupil. Rather than being an actual part of the eye's anatomy, the pupil is merely an opening. The pupil is the black portion in the middle of the eyeball. Its black appearance is attributed to the fact that the light that the pupil allows to enter the eye is absorbed on the retina (and elsewhere) and does not exit the eye. Like the aperture of a camera, the size of the pupil opening can be adjusted by the dilation of the iris. The iris is the colored part of the eye; it is a diaphragm that is capable of stretching and reducing the size of the opening. In bright-light situations, the iris adjusts its size to reduce the pupil opening and limit the amount of light that enters the eye. Also, in dim-light situations, the iris adjusts so as to maximize the size of the pupil opening and increase the amount of light that enters the eye. Light that passes through the pupil opening, will enter the crystalline lens. This one is made of layers of a fibrous material that has an index of refraction of roughly 1.40. Unlike the lens on a camera, the lens of the eye is able to change its shape and thus serves to fine-tune the vision process. The lens are attached to the ciliary muscles which

relax and contract in order to change the shape of the lens. By carefully adjusting the lenses shape, the ciliary muscles assist the eye in the critical task of producing an image on the back of the eyeball. The inner surface of the eye is known as the retina. The retina contains the rods and cones that serve the task of detecting the intensity and the frequency of the incoming light. An adult eye is typically equipped with up to 120 million rods that detect the intensity of light and about 6 million cones that detect the frequency of light. These photoreceptors send nerve impulses to the brain, that travel through a network of nerve cells. There are as many as one million neural pathways from the rods and cones to the brain. This network of nerve cells is bundled together to form the optic nerve on the very back of the eyeball.

The dimensions of the eye are reasonably constant, varying among normal individuals by only a millimeter or two; the vertical diameter is about 24 mm and is usually less than the transverse diameter. At birth that diameter is about 16 to 17 mm; it increases rapidly to about 22.5 to 23 mm by the age of three years; between three and 13 the globe attains its full size. The weight is about 7.5 grams and its volume 6.5 mm<sup>3</sup>. [1]

## **3.2 How the eye works**

### **3.2.1 The iris and the pupil**

The iris is the only visible portion to superficial inspection, appearing as a perforated disc, the central hole, or pupil, varying in size according to the surrounding illumination and other factors. A prominent feature is the collarette at the inner edge, representing the place of attachment of the embryonic pupillary membrane that, in embryonic life, covers the pupil; it is typically defined as the region where the sphincter muscle and dilator muscle overlap. As with the ciliary body, with which it is anatomically continuous, the iris consists of several layers: namely, an anterior layer of endothelium, the stroma; and the posterior iris epithelium. The stroma contains the blood vessels and the sphincter and dilator muscles; in addition, the stroma includes pigment cells that determine the color of the eye. In the back, the stroma is covered by a double layer of epithelium, the continuation forward of the ciliary epithelium; here, however, both layers are heavily pigmented and serve to prevent light from passing through the iris tissue, confining the optical pathway to the pupil. The cells of the anterior layer of the iris epithelium have projections that become the fibres of the dilator muscle; these projections run radially, so that when they contract they pull the iris into folds and

widen the pupil; by contrast, the fibres of the sphincter pupillae muscle run in a circle around the pupil, so that when they contract the pupil becomes smaller.

When bright light is shone on the eye light sensitive cells in the retina, including rod and cone photoreceptors and melanopsin ganglion cells, will send signals to the oculomotor nerve, specifically the parasympathetic part coming from the Edinger-Westphal nucleus, which terminates on the circular iris sphincter muscle. When this muscle contracts, it reduces the size of the pupil. This is the pupillary light reflex (figure. 3.2), which regulates the intensity of light entering the eye and it is an important test of brainstem function. Furthermore, the pupil will dilate if a person sees an object of interest.

The pupil gets wider in the dark but narrower in light. When narrow, the diameter is 3 to 4 mm. In the dark it will be the same at first, but will approach the maximum distance for a wide pupil 5 to 9 mm. In any human age group there is however considerable variation in maximal pupil size. For example, at the peak

age of 15, the dark-adapted pupil can vary from 5 to 9 mm with different individuals. After 25 years of age the average pupil size decreases, though not at a steady rate. At this stage the pupils do not remain completely still, therefore may lead to oscillation, which may intensify and become known as 'hippus'. When only one eye is stimulated, both eyes contract equally. The constriction of the pupil and near vision are closely tied. In bright light, the pupils constrict to prevent aberrations of light rays and thus attain their expected acuity; in the dark this is not necessary, so it is chiefly concerned with admitting sufficient light into the eye.

A pupillary constriction will also occur when a person looks at a near object (the near reflex). Thus, accommodation and pupillary constriction occur together reflex and are excited by the same stimulus. The function of the pupil is clearly that of controlling the amount of light entering the eye, and hence the light reflex. The constriction occurring

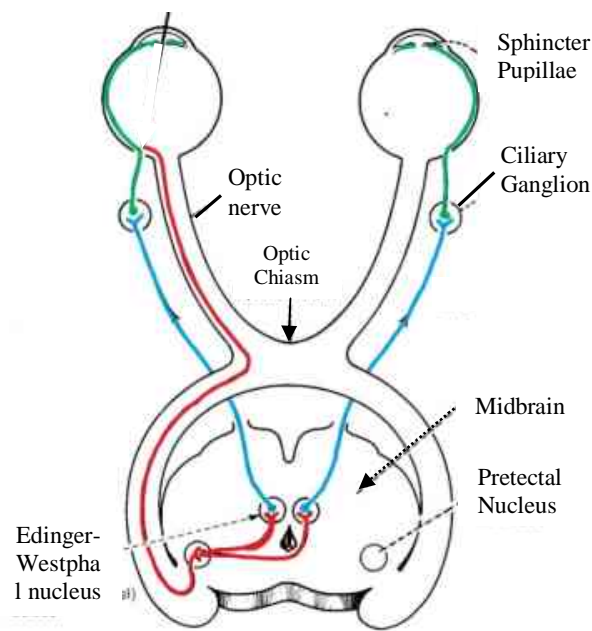


**Figure 3.2** Pupillary light reflex.

during near vision suggests other functions, too; thus, the aberrations of the eye (failure of some refracted rays to focus on the retina) are decreased by reducing the aperture of its optical system. In the dark, aberrations are of negligible significance, so that a person is concerned only with allowing as much light into the eye as possible; in bright light high visual acuity is usually required, and this means reducing the aberrations. The depth of focus of the optical system is increased when the aperture is reduced, and the near reflex is probably concerned with increasing depth of focus under these conditions. Dilation of the pupil occurs as a result of strong psychical stimuli and also when any sensory nerve is stimulated; dilation thus occurs in extreme fear and in pain.

The muscles of the iris have been described earlier. It is clear from their general features that constriction of the pupil is brought about by shortening of the circular ring of fibres—the sphincter; dilation is brought about by shortening of the radially oriented fibres. The sphincter is innervated by parasympathetic fibres of the oculomotor nerve, with their cell bodies in the Edinger-Westphal nucleus, as are the nerve cells controlling accommodation; thus, the close association between the accommodation and pupillary reflexes is reflected in a close anatomical contiguity of their motor nerve cells.

The sensory pathway in the light reflex involves the rods and cones, bipolar cells, and ganglion cells. As indicated earlier, a relay centre for pupillary responses to light is the pretectal nucleus in the midbrain. There is a partial crossing-over of the fibres of the pretectal nerve cells so that some may run to the motor nerve cells in the Edinger-Westphal nucleus of both sides of the brain, and it is by this means that illumination of one eye affects the other. The Edinger-Westphal motor neurons have a relay point in the ciliary ganglion, a group of nerve cells in the eye socket, so that its electrical stimulation causes both accommodation and pupillary constriction; similarly, application of a drug, such as pilocarpine, to the cornea will cause a constriction of the pupil and also a spasm of accommodation; atropine, by paralyzing the nerve supply, causes dilation of the pupil and paralysis of accommodation (cycloplegia).

The dilator muscle of the iris is activated by sympathetic nerve fibres. Stimulation of the sympathetic nerve in the neck causes a powerful dilation of the iris; again, the influx of adrenalin into the blood from the adrenal glands during extreme excitement results in pupillary dilation.

Many involuntary muscles receive a double innervation, being activated by one type of nerve supply and inhibited by the other; modern experimentation indicates that the iris muscles are no exception, so that the sphincter has an inhibitory sympathetic nerve

supply, while the dilator has a parasympathetic (cholinergic) inhibitor. Thus, a drug like pilocarpine not only activates the constrictor muscle but actively inhibits the dilator. A similar double innervation has been described for the ciliary muscle. In general, any change in pupillary size results from a reciprocal innervation of dilator and constrictor; thus, activation of the constrictor is associated with inhibition of the dilator and vice versa [1,2,3].

### 3.2.2 The sclera and the cornea

The sclera, the "white" of the eye, is the tough outer coating that gives the eye its spherical shape (the eyelids conceal much of its shape); it is the opaque, fibrous, protective, outer layer of the eye containing collagen and elastic fiber. The sclera is covered by the conjunctiva, a thin membrane, translucent like waxed paper, that also lines the undersides of the eyelids. The conjunctiva, along with the lacrimal glands, makes tears, which keep the eye moist. But it is probably best known for its tendency to get inflamed when it is infected or irritated. This condition, called conjunctivitis, is very common and is generally only an annoyance. The sclera is perforated by many nerves and vessels passing through the posterior sclera foramen, the hole that is formed by the optic nerve. At the optic disc the outer two-thirds of the sclera continues with the *dura mater* (outer coat of the brain) via the dural sheath of the optic nerve. The inner third joins with some choroidal tissue to form a plate (lamina cribrosa) across the optic nerve with perforations through which the optic fibers (fasciculi) pass. The thickness of the sclera varies from 1 mm at the posterior pole to 0.3 mm just behind the rectus muscle insertions. The sclera's blood vessels are mainly on the surface. Along with the vessels of the conjunctiva, those of the sclera render the inflamed eye bright red. The cornea is in front of the iris and it is a very sensitive structure. Though it is part of the same layer as the sclera, it is different in that the cornea is transparent. Light must pass through it to get to the pupil and the inside of the eye.

Although the cornea is clear and seems to lack substance, it is a highly organized group of cells and proteins. Unlike most tissues in the body, the cornea contains no blood vessels to nourish or protect it against infection. Instead, the cornea receives its nourishment from the tears and aqueous humor that fills the chamber behind it. The cornea must remain transparent to refract light properly, and the presence of even the tiniest blood vessels can interfere with this process. To see well, all layers of the cornea must be free of any cloudy or opaque areas.

The corneal tissue is arranged in five basic layers, each having an important function.

These five layers are:

- **Epithelium**: The cornea's outermost region, comprising about 10% of the tissue's thickness. The epithelium functions primarily to: (1) Block the passage of foreign material, such as dust, water, and bacteria, into the eye and other layers of the cornea; and (2) Provide a smooth surface that absorbs oxygen and cell nutrients from tears, then distributes these nutrients to the rest of the cornea. The epithelium is filled with thousands of tiny nerve endings that make the cornea extremely sensitive to pain when rubbed or scratched. The part of the epithelium that serves as the foundation on which the epithelial cells anchor and organize themselves is called the basement membrane.
- **Bowman's Layer**: A transparent sheet of tissue composed of strong layered protein fibers called collagen. Once injured, Bowman's layer can form a scar as it heals. If these scars are large and centrally located, some vision loss can occur.
- **Stroma**: A layer accounting for 90% of the cornea's thickness, consisting primarily of water (78%) and collagen (16%), and does not contain any blood vessels. Collagen gives the cornea its strength, elasticity, and form. The collagen's unique shape, arrangement, and spacing are essential in producing the cornea's light-conducting transparency.
- **Descemet's Membrane**: A thin but strong sheet of tissue that serves as a protective barrier against infection and injuries. It is composed of collagen fibers (different from those of the stroma) and is made by the endothelial cells that lie below it. Descemet's membrane is regenerated readily after injury.
- **Endothelium**: The extremely thin, innermost layer of the cornea. Endothelial cells are essential in keeping the cornea clear. Normally, fluid leaks slowly from inside the eye into the middle corneal layer (stroma).

The endothelium's primary task is to pump this excess fluid out of the stroma. Without this pumping action, the stroma would swell with water, become hazy, and ultimately opaque. In a healthy eye, a perfect balance is maintained between the fluid moving into the cornea and fluid being pumped out of the cornea. Once endothelium cells are destroyed by disease or trauma, they are lost forever. If too many endothelial cells are destroyed, corneal edema and blindness ensue, with corneal transplantation the only available therapy. [4,5]

### 3.2.3 The choroid, the ciliary body, and the lens

Hidden beneath the sclera is a second layer, the choroid. Its function is to supply blood to the other parts of the eye, especially the retina. In fact, blood vessels in the choroid are more densely packed than anywhere else in the body. The retina needs a rich supply of blood for two reasons. First, it is metabolically active and therefore needs a great deal of energy. Second, the focusing of light onto the retina creates heat, much like the focusing of the sun's light by a magnifying lens. The rich blood supply of the choroid carries this heat away and protects the eye from injury.

The choroid is of blood vessels and connective tissue between the sclera and retina, as shown in figure 3.3. Also in this layer is the ciliary body, which lies just behind the junction of the cornea and the sclera. Like the iris, the ciliary body is a muscular structure, but its central opening is much larger. The ciliary body produces aqueous humor.

The lens, made of nearly pure protein, is a transparent structure with two convex surfaces. Special "guy-wires" called zonules connect the lens to the ciliary body and suspend it so it is centered behind the pupil. When the ciliary body constricts, it relaxes the pull on the zonules so that the shape of the lens changes. This process, called accommodation, focuses light on the retina so we can see near objects clearly. When the muscles of the ciliary body are relaxed, tension is placed on the zonules and the focus of the lens is readjusted so we can see things at a distance. Often in older people, and occasionally even in children, the normally transparent lens becomes cloudy. If it interferes with vision, this clouding of the lens is called a cataract [6].

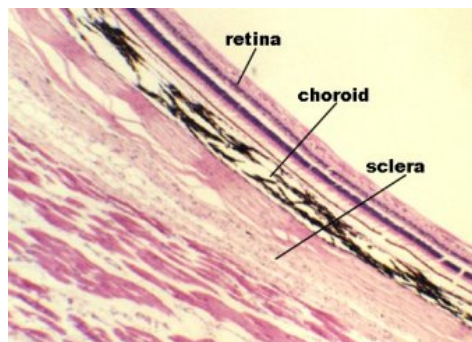
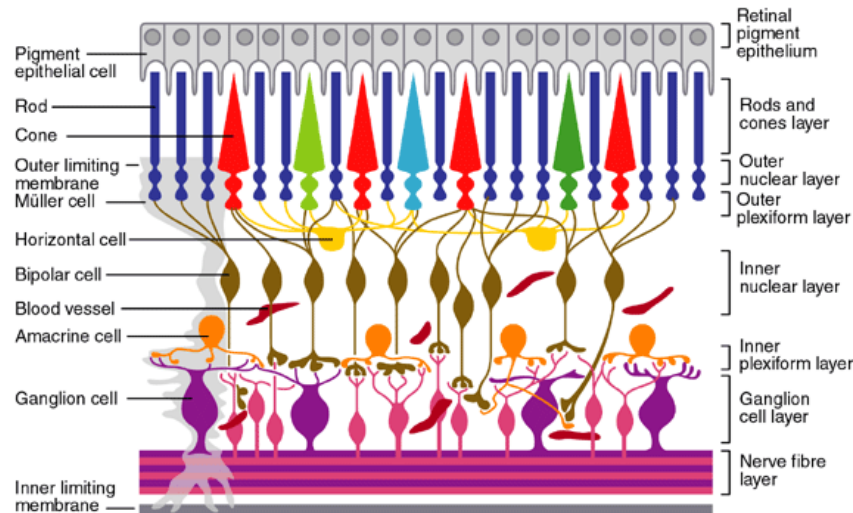


Figure 3.3 Eye layers.

### 3.2.4 The retina

The inner tunic of the rear portion of the globe, as far forward as the ciliary body, is the retina (figure. 3.3), including its epithelia or coverings. These epithelia continue forward to line the remainder of the globe. Separating the choroid (the middle tunic of the globe) from the retina proper is a layer of pigmented cells, the pigment epithelium of the retina; this acts as a restraining barrier to the indiscriminate diffusion of material from the blood in the choroid to the retina. The retina ends at the 'ora serrata', where



**Figure 3.4** Cellular organization of the retina.

the ciliary body begins (3.1). The pigment epithelium continues forward as a pigmented layer of cells covering the ciliary body; farther forward still, the epithelium covers the posterior surface of the iris and provides the cells that constitute the dilator muscle of this diaphragm. Next to the pigment epithelium of the retina is the neuroepithelium, or rods and conor rods and cones. Their continuation forward is represented by a second layer of epithelial cells covering the ciliary body, so that by the ciliary epithelium is meant the two layers of cells that are the embryological equivalent of the retinal pigment epithelium and the receptor layer (rods and cones) of the retina. This unpigmented layer of the ciliary epithelium is continued forward over the back of the iris, where it acquires pigment and is called the posterior iris epithelium.

The retina is the part of the eye that receives the light and converts it into chemical energy. The chemical energy activates nerves that conduct the messages out of the eye into the higher regions of the brain. The retina is a complex nervous structure, being, in essence, an outgrowth of the forebrain.

Ten layers of cells in the retina can be seen microscopically. In general, there are four main layers: (1) next to the choroid is the pigment epithelium, already mentioned; (2) above the epithelium is the layer of rods and cones, the light-sensitive cells. The changes induced in the rods and cones by light are transmitted to (3) a layer of neurons (nerve cells) called the bipolar cells. These bipolar cells connect with (4) the innermost layer of neurons, the ganglion cells; and the transmitted messages are carried out of the eye along their projections, or axons, which constitute the optic nerve fibres. Thus, the optic nerve is really a central tract, rather than a nerve, connecting two regions of the nervous system, namely, the layer of bipolar cells, and the cells of the lateral geniculate

body, the latter being a visual relay station in the diencephalon (the rear portion of the forebrain). The arrangement of the retinal cells in an orderly manner gives rise to the outer nuclear layer, containing the nuclei of the rods and cones; the inner nuclear layer, containing the nuclei and perikarya (main cell bodies outside the nucleus) of the bipolar cells, and the ganglion cell layer, containing the corresponding structures of the ganglion cells. The plexiform layers are regions in which the neurons make their interconnections. Thus, the outer plexiform layer contains the rod and cone projections terminating as the rod spherule and cone pedicle; these make connections with the dendritic processes of the bipolar cells, so that changes produced by light in the rods and cones are transmitted by way of these connections to the bipolar cells. (The dendritic process of a nerve cell is the projection that receives nerve impulses to the cell; the axon is the projection that carries impulses from the cell). In the inner plexiform layer are the axons of the bipolar cells and the dendritic processes of the ganglion and amacrine cells. The association is such as to allow messages in the bipolar cells to be transmitted to the ganglion cells, the messages then passing out along the axons of the ganglion cells as optic nerve messages.

The photosensitive cells are, in the human and in most vertebrate retinas, of two kinds, called rods and cones (figure 3.4), the rods being usually much thinner than the cones but both being built up on the same plan. The light-sensitive pigment is contained in the outer segment, which rests on the pigment epithelium. Through the other end, called the synaptic body, effects of light are transmitted to the bipolar and horizontal cells. When examined in the electron microscope, the outer segments of the rods and cones are seen to be composed of stacks of disks, apparently made by the infolding of the limiting membrane surrounding the outer segment; the visual pigment, located on the surfaces of these disks, is thus spread over a very wide area, and this contributes to the efficiency with which light is absorbed by the visual cell.

The arrangement of the retina makes it necessary for light to pass through the layers not sensitive to light first before it reaches the light-sensitive rods and cones. The optical disadvantages of this arrangement are largely overcome by the development of the fovea centralis, a localized region of the retina, close to the optic axis of the eye, where the inner layers of the retina are absent. The result is a depression, the foveal pit, where light has an almost unrestricted passage to the light-sensitive cells. It is essentially this region of the retina that is employed for accurate vision, the eyes being directed toward the objects of regard so that their images fall in this restricted region. If the object of

interest is large, so as to subtend a large angle, then the eye must move rapidly from region to region so as to bring their images successively onto the fovea; this is typically seen during reading. In the central region of the fovea there are cones exclusively; toward its edges, rods also occur, and as successive zones are reached the proportion of rods increases while the absolute density of packing of the receptors tends to decrease. Thus, the central fovea is characterized by an exclusive population of very densely packed cones; here, also, the cones are very thin and in form very similar to rods. The region surrounding the fovea is called the parafovea; it stretches about 1,250 microns from the centre of the fovea, and it is here that the highest density of rods occurs. Surrounding the parafovea, in turn, is the perifovea, its outermost edge being 2,750 microns from the centre of the fovea; here the density of cones is still further diminished, the number being only 12 per hundred microns compared with 50 per hundred microns in the most central region of the fovea. In the whole human retina there are said to be about 7,000,000 cones and from 75,000,000 to 150,000,000 rods.

The fovea is sometimes referred to as the macula lutea (“yellow spot”); actually this term defines a rather vague area, characterized by the presence of a yellow pigment in the nervous layers, stretching over the whole central retina—i.e., the fovea, parafovea, and perifovea.

The blind spot in the retina corresponds to the optic papilla, the region on the nasal side of the retina through which the optic nerve fibres pass out of the eye.

Although the rods and cones may be said to form a mosaic, the retina is not organized in a simple mosaic fashion in the sense that each rod or cone is connected to a single bipolar cell that itself is connected to a single ganglion cell. There are only about 1,000,000 optic nerve fibres, while there are at least 150,000,000 receptors, so that there must be considerable convergence of receptors on the optic pathway. This means that there will be considerable mixing of messages. Furthermore, the retina contains additional nerve cells besides the bipolar and ganglion cells; these, the horizontal and amacrine cells, operate in the horizontal direction, allowing one area of the retina to influence the activity of another. In this way, for example, the messages from one part of the retina may be suppressed by a visual stimulus falling on another, an important element in the total of messages sent to the higher regions of the brain. Finally, it has been argued that some messages may be running the opposite way; they are called centrifugal and would allow one layer of the retina to affect another, or higher regions of the brain to control the responses of the retinal neurons. In primates the existence of

these centrifugal fibres has been finally disproved, but in such lower vertebrates as the pigeon, their existence is quite certain.

The pathway of the retinal messages through the brain is described later in this chapter; it is sufficient to state here that most of the optic nerve fibres in primates carry their messages to the lateral geniculate body, a relay station specifically concerned with vision. Some of the fibres separate from the main stream and run to a midbrain centre called the pretectal nucleus, which is a relay centre for pupillary responses to light. [1]

### **3.2.5 The aqueous humour**

The aqueous humour is a clear colorless fluid with a chemical composition rather similar to that of blood plasma (the blood exclusive of its cells) but lacking the high protein content of the latter. Its main function is to keep the globe reasonably firm. It is secreted continuously by the ciliary body into the posterior chamber, and flows as a gentle stream through the pupil into the anterior chamber, from which it is drained by way of a channel at the limbus; that is, the juncture of the cornea and the sclera. This channel, the canal of Schlemm, encircles the cornea and connects by small connector channels to the blood vessels buried in the sclera and forming the intrascleral plexus or network. From this the blood, containing the aqueous humour, passes into more superficial vessels; it finally leaves the eye in the anterior ciliary veins. The wall of the canal that faces the aqueous humour is very delicate and allows the fluid to percolate through by virtue of the relatively high pressure of the fluid within the eye. Obstruction of this exit, for example, if the iris is pushed forward to cover the wall of the canal, causes a sharp rise in the pressure within the eye, a condition that is known as glaucoma. Often the obstruction is not obvious, but is caused perhaps by a hardening of the tissue just adjacent to the wall of the canal—the trabecular meshwork, in which case the rise of pressure is more gradual and insidious. Ultimately the abnormal pressure damages the retina and causes a variable degree of blindness. The normal intraocular pressure is about 15 mm of mercury above atmospheric pressure, so that if the anterior chamber is punctured by a hypodermic needle the aqueous humour flows out readily. Its function in maintaining the eye reasonably hard is seen by the collapse and wrinkling of the cornea when the fluid is allowed to escape. An additional function of the fluid is to provide nutrition for the crystalline lens and also for the cornea, both of which are devoid of blood vessels; the steady renewal and drainage serve to bring into the eye

various nutrient substances, including glucose and amino acids, and to remove waste products of metabolism [1].

### 3.2.6 The vitreous body

The vitreous body is a semisolid gel structure that is remarkable for the small amount of solid matter that it contains. The solid material is made up of a form of collagen, vitrosin, and hyaluronic acid (a mucopolysaccharide). Thus, its composition is rather similar to that of the cornea, but the proportion of water is much greater, about 98% or more, compared with about 75% for the cornea. The jelly is probably secreted by certain cells of the retina. In general, the vitreous body is devoid of cells, in contrast with the lens, which is packed tight with cells. Embedded in the surface of the vitreous body, however, there is a population of specialized cells, the hyalocytes of Balazs, which may contribute to the breakdown and renewal of the hyaluronic acid. The vitreous body serves to keep the underlying retina pressed against the choroid [1].

### 3.2.7 The crystalline lens

The crystalline lens is a transparent body, flatter on its anterior than on its posterior surface, and suspended within the eye by the zonular fibres of Zinn attached to its equator; its anterior surface is bathed by aqueous humour, and its posterior surface by the vitreous body. The lens is a mass of tightly packed transparent fibrous cells, the lens fibres, enclosed in an elastic collagenous capsule. The lens fibres are arranged in sheets that form successive layers; the fibres run from pole to pole of the lens, the middle of a given fibre being in the equatorial region. On meridional (horizontal) section, the fibres are cut longitudinally to give an onion-scale appearance, whereas a section at right-angles to this—an equatorial section—would cut all the fibres across, and the result would be to give a honeycomb appearance. The epithelium, covering the anterior surface of the lens under the capsule, serves as the origin of the lens fibres, both during embryonic and fetal development and during infant and adult life, the lens continuing to grow by the laying down of new fibres throughout life [1].

### **3.2.8 Accommodation**

#### **Effects of accommodation**

The image of an object brought close to the eye would be formed behind the retina if there were no change in the focal length of the eye. This change to bring the image of an object upon the retina is called accommodation. The point nearer than which accommodation is no longer effective is called the near point of accommodation. In very young people, the near point of accommodation is quite close to the eye, namely about 7 cm in front at 10 years old; at 40 years the distance has increased to about 16 cm, and at 60 years it is 100 cm or 1 m. Thus, a 60-year-old would not be able to read a book held at the convenient distance of about 40 cm, and the extra power required would have to be provided by convex lenses in front of the eye, an arrangement called the presbyopic correction.

#### **Mechanism of accommodation**

It is essentially an increase in curvature of the anterior surface of the lens that is responsible for the increase in power involved in the process of accommodation. A clue to the way in which this change in shape takes place is given by the observation that a lens that has been taken out of the eye is much rounder and fatter than one within the eye; thus, its attachments by the zonular fibres to the ciliary muscle within the eye preserve the unaccommodated or flattened state of the lens; and modern investigations leave little doubt that it is the pull of the zonular fibres on the elastic capsule of the lens that holds the anterior surface relatively flat. When these zonular fibres are loosened, the elastic tension in the capsule comes into play and remolds the lens, making it smaller and thicker. Thus, the physiological problem is to find what loosens the zonular fibres during accommodation. The ciliary muscle has been described earlier, and it has been shown that the effect of contracting its fibres is, in general, to pull the whole ciliary body forward and to move the anterior region toward the axis of the eye by virtue of the sphincter action of the circular fibres. Both of these actions will slacken the zonular fibres and therefore allow the change in shape. As to why it is the anterior surface that changes most is not absolutely clear, but it is probably a characteristic of the capsule rather than of the underlying lens tissue. Defective accommodation in presbyopia is not due to a failure of the ciliary muscle but rather to a hardening of the substance of the lens with age to the point that readjustments of its shape become ever more difficult.

### **Nerve action**

Accommodation is an involuntary reflex act, and the ciliary muscle belongs to the smooth involuntary class. Appropriate to this, the innervation is through the autonomic system, the parasympathetic nerve cells belonging to the oculomotor nerve (the third cranial nerve) occupying a special region of the nucleus in the midbrain called the Edinger-Westphal nucleus; the fibres have a relay point in the ciliary ganglion in the eye socket, and the postganglionic fibres enter the eye as the short ciliary nerves. The stimulus for accommodation is the nearness of the object, but the manner in which this nearness is translated into a stimulus is not clear. Thus, the fact that the image is blurred is not sufficient to induce accommodation; the eye has some power of discriminating whether the blurredness is due to an object being too far away or too close, so that something more than mere blurredness is required.

### **3.2.9 The work of the retina**

So far, attention has been directed to what are essentially the preliminaries to vision; it is now time to examine some of the elementary facts of vision and to relate them to the structure of the retina and, later, to chemically identifiable events.

An important means of measuring a sensation is to determine the threshold stimulus—*i.e.*, the minimum energy required to evoke the sensation. In the case of vision, this would be the minimum number of quanta of light entering the eye in unit time. If it is found that the threshold has altered because of a variation of some sort, then this change can be said to have altered the subject's sensitivity to light, and a numerical value can be assigned to the sensitivity by use of the reciprocal of the threshold energy. Practically, a subject may be placed in the dark in front of a white screen, and the screen may be illuminated by flashes of light; for any given intensity of illumination of the screen, it is not difficult to calculate the flow of light energy entering the eye. One may begin with a low intensity of flash and increase this successively until the subject reports that he can see the flash. In fact, at this threshold level, he will not see every flash presented, even though the intensity of the light is kept constant; for this reason, a certain frequency of seeing—*e.g.*, four times out of six—must be selected as the arbitrary point at which to fix the threshold.

When measurements of this sort are carried out, it is found that the threshold falls progressively as the subject is maintained in the dark room. This is not due to dilation of the pupil because the same phenomenon occurs if the subject is made to look through an

artificial pupil of fixed diameter. **The eye, after about 30 minutes in the dark, may become about 10,000 times more sensitive to light.** Vision under these conditions is, moreover, characteristically different from what it is under ordinary daylight conditions. Thus, in order to obtain best vision, the eye must look away from the screen so that the image of the screen does not fall on the fovea; if the screen is continuously illuminated at around this threshold level it will be found to disappear if its image is brought onto the fovea, and it will become immediately visible on looking away. The same phenomenon may be demonstrated on a moonless night if the gaze is fixed on a dim star; it disappears on fixation and reappears on looking away. This feature of vision under these near-threshold or scotopic conditions suggests that the cones are effectively blind to weak light stimuli, since they are the only receptors in the fovea. This is the basis of the duplicity theory of vision, which postulates that when the light stimulus is weak and the eye has been dark-adapted, it is the rods that are utilized because, under these conditions, their threshold is much lower than that of the cones. When the subject first enters the dark, the rods are the less sensitive type of receptor, and the threshold stimulus is the light energy required to stimulate the cones; during the first five or more minutes the threshold of the cones decreases; *i.e.*, they become more sensitive. The rods then increase their sensitivity to the point that they are the more sensitive, and it is they that now determine the sensitivity of the whole eye, the threshold stimuli obtained after 10 minutes in the dark, for example, being too weak to activate the cones.

### Scotopic sensitivity curve

When different wavelengths of light are employed for measuring the threshold, it is found, for example, that the eye is much more sensitive to blue-green light than to orange. The interesting feature of this kind of study is that the subject reports only that the light is light; he distinguishes no color. If the intensity of a given wavelength of light is increased step by step above the threshold, a point comes when the subject states that it is colored, and the difference between the threshold for light appreciation and this, the chromatic threshold, is called the photochromatic interval. This suggests that the rods give only achromatic, or colorless, vision, and that it is the cones that permit wavelength discrimination. The photochromatic interval for long wavelengths (red light) is about zero, which means that the intensity required to reach the sensation of light is the same as that to reach the sensation of color. This is because the rods are so insensitive to red

light; if the dark-adaptation curve is plotted for a red stimulus it is found that it follows the cone path, like that for foveal vision at all wavelengths.

### **Loss of dark adaptation**

If, when the subject has become completely dark-adapted, one eye is held shut and the other exposed to a bright light for a little while, it is found that, whereas the dark-adapted eye retains its high sensitivity, that of the light-exposed eye has decreased greatly; it requires another period of dark adaptation for the two eyes to become equally sensitive.

### **Bleaching of rhodopsin**

It may be assumed that a receptor is sensitive to light because it contains a substance that absorbs light and converts this vibrational type of energy into some other form that is eventually transmuted into electrical changes, and that these may be transmitted from the receptor to the bipolar cell with which it is immediately connected. When the retina of a dark-adapted animal is removed and submitted to extraction procedures, a pigment, originally called visual purple but now called rhodopsin, may be obtained. If the eye is exposed to a bright light for some time before extraction, little or no rhodopsin is obtained. When retinas from animals that had been progressively dark-adapted were studied, a gradual increase in the amount of rhodopsin that could be extracted was observed. Thus, rhodopsin, on absorption of light energy, is changed to some other compound, but new rhodopsin is formed, or rhodopsin is regenerated, during dark adaptation. The obvious inference is that rhodopsin is the visual pigment of the rods, and that when it is exposed to relatively intense lights it becomes useless for vision. When the eye is allowed to remain in the dark the rhodopsin regenerates and thus becomes available for vision. There is now conclusive proof that rhodopsin is, indeed, the visual pigment for the rods; it is obtained from retinas that have only rods and no cones—*e.g.*, the retinas of the rat or guinea pig, and it is not obtained from the pure cone retina of the chicken.

When the absorption spectrum is measured, it is found that its maximum absorption occurs at the point of maximum sensitivity of the dark-adapted eye. Similar measurements may be carried out on animals, but the threshold sensitivity must be determined by some objective means—*e.g.*, the response of the pupil, or, better still, the electrical changes occurring in the retina in response to light stimuli. Thus, the electroretinogram (ERG) is the record of changes in potential between an electrode

placed on the surface of the cornea and an electrode placed on another part of the body, caused by illumination of the eye.

The high sensitivity of the rods by comparison with the cones may be a reflection of the greater concentration in them of pigment that would permit them to catch light more efficiently, or it may depend on other factors—*e.g.*, the efficiency of transformation of the light energy into electrical energy. The pigments responsible for cone vision are not easily extracted or identified, and the problem will be considered in the material on color vision. An important factor, so far as sensitivity is concerned, is the actual organization of the receptors and neurons in the retina.

### **Synaptic organization of the retina**

The basic structure of the retina has been indicated earlier. As in other parts of the nervous system, the messages initiated in one element are transmitted, or relayed, to others. The regions of transmission from one cell to another are areas of intimate contact known as synapses. An impulse conveyed from one cell to another travels from the first cell body along a projection called an axon, to a synapse, where the impulse is received by a projection, called a dendrite, of the second cell. The impulse is then conveyed to the second cell body, to be transmitted further, along the second cell's axon.

It will be recalled that the functioning cells of the retina are the receptor cells—the rods and cones; the ganglion cells, the axons of which form the optic nerve; and cells that act in a variety of ways as intermediaries between the receptors and the ganglion cells. These intermediaries are named bipolar cells, horizontal cells, and amacrine cells.

### **Plexiform layers**

As was indicated earlier, the synapses occur in definite layers, the outer and inner plexiform layers. In the outer plexiform layer the bipolar cells make their contacts, by way of their dendrites, with the rods and cones, specifically the spherules of the rods and the pedicles of the cones. In this layer, too, the projections from horizontal cells make contacts with rods, cones, and bipolar cells, giving rise to a horizontal transmission and thereby allowing activity in one part of the retina to influence the behavior of a neighboring part. In the inner plexiform layer, the axons of the bipolar cells make connection with the dendrites of ganglion cells, once again at special synaptic regions. (The dendrites of a nerve cell carry impulses to the nerve cell; its

axon, away from the cell.) Here, too, a horizontal interconnection between bipolar cells is brought about, in this case by way of the axons and dendrites of amacrine cells.

The bipolar cells are of two main types: namely, those that apparently make connection with only one receptor—a cone—and those that connect to several receptors. The type of bipolar cell that connects to a single cone is called the midget bipolar. The other type of bipolar cell is called diffuse; varieties of these include the rod bipolar, the dendritic projections of which spread over an area wide enough to allow contacts with as many as 50 rods; and the flat cone bipolar, which collects messages from up to seven cones.

Ganglion cells are of two main types: namely, the midget ganglion cell, which apparently makes a unique connection with a midget bipolar cell, which in turn is directly connected to a single cone; and a diffuse type, which collects messages from groups of bipolar cells.

### **Convergence of the messages**

The presence of diffuse bipolar and ganglion cells collecting messages from groups of receptors and bipolar cells, and, what may be even more important, the presence of lateral connections of groups of receptors and bipolar cells through the horizontal and amacrine cells, means that messages from receptors over a rather large area of the retina may converge on a single ganglion cell. This convergence means that the effects of light falling on the receptive field may be cumulative, so that a weak light stimulus spread over about 1,000 rods is just as effective as a stronger stimulus spread over 100 or less; in other words, a large receptive field will have a lower threshold than a small one; and this is, in fact, the basis for the high sensitivity of the area immediately outside the fovea, where there is a high density of rods that converge on single bipolar cells. Thus, if it is postulated that the cones do not converge to anything like the same extent as the rods, the greater sensitivity of the latter may be explained; and the anatomical evidence favors this postulate.

It has been indicated above that the regeneration of visual pigment is a cause of the increased sensitivity of the rods that occurs during dark adaptation. This, apparently, is only part of the story. An important additional factor is the change in functional organization of the retina during adaptation. When the eye is light-adapted, functional convergence is small, and sensitivity of rods and cones is low; as dark adaptation proceeds, convergence of rods increases. The anatomical connections do not change, but the power of the bipolar cells and ganglion cells to collect impulses is increased,

perhaps by the removal of an inhibition that prevents this during high illumination of the retina.

### **Absolute threshold and minimum stimulus for vision**

As was indicated earlier, the threshold is best indicated in terms of frequency of seeing since, because of fluctuations in the threshold, there is no definite luminance of a test screen at which it is always seen by the observer, and there is no luminance just below this at which it is never seen. Experiments, in which 60 percent was arbitrarily taken as the frequency of seeing and in which the image of a patch of light covered an area of retina containing about 20,000,000 rods, led to the calculation that the mean threshold stimulus represents 2,500 quanta of light that is actually absorbed per square centimeter of retina. This calculation leads to two important conclusions: namely, that at the threshold only one rod out of thousands comes into operation, and that during the application of a short stimulus the chances are that no rod receives more than a single quantum. A quantum, defined as the product of Planck's constant ( $6.63 \times 10^{-27}$  erg-second) times the frequency of light, is the minimum amount of light energy that can be employed. A rod excited by a single quantum cannot excite a bipolar cell without the simultaneous assistance of one or more other rods. Experiments carried out in the 1940s indicated that a stimulus of about 11 quanta is required; thus it may require 11 excited rods, each receiving one quantum of light, to produce the sensation of light.

### **Quantum fluctuations**

With such small amounts of energy as those involved in the threshold stimulus, the uncertainty principle becomes important; according to this, there is no certainty that a given flash will have the expected number of quanta in it, but only a probability. Thus, one may speak of a certain average number of quanta and the actual number in any given flash, and one may compute on statistical grounds the shape of curve that is obtained by plotting frequency with which a flash contains, say, four quanta or more against the average number in the flash. One may also plot the frequency with which a flash is seen against the average number of quanta in the flash, and this frequency-of-seeing curve turns out to be similar to the frequency-of-containing-quanta curve when the number of quanta chosen is five to seven, depending on the observer. This congruence strongly suggests that the fluctuations in response to a flash of the same

average intensity are caused by fluctuations in the energy content of the stimulus, and not by fluctuations in the sensitivity of the retina.

### **Spatial summation**

In spatial summation two stimuli falling on nearby areas of the retina add their effects so that either alone may be inadequate to evoke the sensation of light, but, when presented simultaneously, they may do so. Thus, the threshold luminance of a test patch required to be just visible depends, within limits, on its size, a larger patch requiring a lower luminance, and vice versa. Within a small range of limiting area, namely that subtending about 10 to 15 minutes of arc, the relationship called Ricco's law holds; *i.e.*, threshold intensity multiplied by the area equals a constant. This means that over this area, which embraces several hundreds of rods, light falling on the individual rods summates, or accumulates, its effects completely so that 100 quanta falling on a single rod are as effective as one quantum falling simultaneously on 100 rods. The basis for this summation is clearly the convergence of receptors on ganglion cells, the chemical effects of the quanta of light falling on individual rods being converted into electrical changes that converge on a single bipolar cell through its branching dendritic processes. Again, the electrical effects induced in the bipolar cells may summate at the dendritic processes of a ganglion cell so that the receptive field of a ganglion cell may embrace many thousands of rods.

### **Temporal summation**

In temporal summation, two stimuli, each being too weak to excite, cause a sensation of light if presented in rapid succession on the same spot of the retina; thus, over a certain range of times, up to 0.1 second, the Bunsen-Roscoe law holds: namely, that the intensity of light multiplied by the time of exposure equals a constant. Thus it was found that within this time interval (up to 0.1 second), the total number of quanta required to excite vision was 130, irrespective of the manner in which these were supplied. Beyond this time, summation was still evident, but it was not perfect, so that if the duration was increased to one second the total number of quanta required was 220. Temporal summation is consistent with quantum theory; it has been shown that fluctuations in the number of quanta actually in a light flash are responsible for the variable responsiveness of the eye; increasing the duration of a light stimulus increases the probability that it will contain a given number of quanta, and that it will excite.

### **Inhibition**

In the central nervous system generally, the relay of impulses from one nerve cell or neuron to excite another is only one aspect of neuronal interaction. Just as important, if not more so, is the inhibition of one neuron by the discharge in another. So it is in the retina. Subjectively, the inhibitory activity is reflected in many of the phenomena associated with adaptation to light or its reverse. Thus, the decrease in sensitivity of the retina to light during exposure to light is only partially accounted for by bleaching of visual pigment, be it the pigment in rod or cone; an important factor is the onset of inhibitory processes that reduce the convergence of receptors on ganglion cells. Some of the rapidly occurring changes in sensitivity described as alpha adaptation are doubtless purely neural in origin.

Many so-called inductive phenomena indicate inhibitory processes; thus, the phenomenon of simultaneous contrast, whereby a patch of light appears much darker if surrounded by a bright background than by a black, is due to the inhibitory effect of the surrounding retina on the central region, induced by the bright surrounding. Many color-contrast phenomena are similarly caused; thus, if a blue light is projected onto a large white screen, the white screen rapidly appears yellow; the blue stimulus falling on the central retina causes inhibition of blue sensitivity in the periphery; hence, the white background will appear to be missing its blue light—white minus blue is a mixture of red and green—*i.e.*, yellow. Particularly interesting from this viewpoint are the phenomena of metacontrast; by this is meant the inductive effect of a primary light stimulus on the sensitivity of the eye to a previously presented light stimulus on an adjoining area of retina. It is a combination of temporal and spatial induction. The effect is produced by illuminating the two halves of a circular patch consecutively for a brief duration. If the left half only, for example, is illuminated for 10 milliseconds it produces a definite sensation of brightness. If, now, both halves are illuminated for the same period, but the right half from 20 to 50 milliseconds later, the left half of the field appears much darker than before and, near the centre, may be completely extinguished. The left field has thus been inhibited by the succeeding, nearby, stimulus. The right field, moreover, appears darker than when illuminated alone—it has been inhibited by the earlier stimulus (paracontrast).

**Flicker**

Another visual phenomenon that brings out the importance of inhibition is the sensation evoked when a visual stimulus is repeated rapidly; for example, one may view a screen that is illuminated by a source of light the rays from which may be intercepted at regular intervals by rotating a sector of a circular screen in front of it. If the sector rotates slowly, a sensation of black followed by white is aroused; as the speed increases the sensation becomes one of flicker—*i.e.*, rapid fluctuations in brightness; finally, at a certain speed, called the critical fusion frequency, the sensation becomes continuous and the subject is unaware of the alterations in the illumination of the screen.

At high levels of luminance, when cone vision is employed, the fusion frequency is high, increasing with increasing luminance in a logarithmic fashion—the Ferry-Porter law—so that at high levels it may require 60 flashes per second to reach a continuous sensation. Under conditions of night, or scotopic, vision, the frequencies may be as low as four per second. The difference between rod and cone vision in this respect probably resides in the power of the eye to inhibit activity in cones rapidly, so that the sensation evoked by a single flash is cut off immediately, and this leaves the eye ready to respond to the next stimulus. By contrast, the response in the rod lasts so much longer that, when a new stimulus falls even a quarter of a second later, the difference in the state of the rods is insufficient to evoke a change in intensity of sensation; it merely prolongs it. One interesting feature of an intermittent stimulus is that the intensity of the sensation of brightness, when fusion is achieved, is dependent on the relative periods of light and darkness in the cycle, and this gives one a method of grading the effective luminance of a screen; one may keep the intensity of the illuminating source constant and merely vary the period of blackness in a cycle of black and white. The effective luminance will be the average luminance during a cycle; this is known as the Talbot-Plateau law.

**Visual acuity**

As has been stated, the ability to perceive detail is restricted in the dark-adapted retina when the illumination is such as to excite only the scotopic type of vision; this is in spite of the high sensitivity of the retina to light under the same conditions. The power of distinguishing detail is essentially the power to resolve two stimuli separated in space, so that, if a grating of black lines on a white background is moved farther and farther away from an observer, a point is reached when he will be unable to distinguish this stimulus pattern from a uniformly gray sheet of paper. The angle subtended at the eye

by the spacing between the lines at the point where they are just resolvable is called the resolving power of the eye; the reciprocal of this angle, in minutes of arc, is called the visual acuity. Thus, a visual acuity of unity indicates a power of resolving detail subtending one minute of arc at the eye; a visual acuity of two indicates a resolution of one-half minute, or 30 seconds of arc. The visual acuity depends strongly on the illumination of the test target, and this is true of both daylight (photopic) and night (scotopic) vision; thus, with a brightly illuminated target, with the surroundings equally brightly illuminated (the ideal condition), the visual acuity may be as high as two. When the illumination is reduced, the acuity falls so that, under ordinary conditions of daylight viewing, visual acuity is not much better than unity. Under scotopic conditions, the visual acuity may be only 0.04 so that lines would have to subtend about 25 minutes at the eye to be resolvable; this corresponds to a thickness of 4.4 centimeters at a distance of six meters.

### **3.2.10 Electrophysiology of the retina**

#### **Neurological basis**

Subjective studies on human beings can traverse only a certain distance in the interpretation of visual phenomena; beyond this the standard electrophysiological techniques, which have been successful in unravelling the mechanisms of the central nervous system, must be applied to the eye; this, as repeatedly emphasized, is an outgrowth of the brain. Records from single optic nerve fibres of the frog and from the ganglion cell of the mammalian retina indicated three types of response. In the frog there were fibres that gave a discharge when a light was switched on the “on-fibres.” Another group, the “off-fibres,” remained inactive during illumination of the retina but gave a powerful discharge when the light was switched off. A third group, the “on-off fibres,” gave discharges at “on” and “off” but were inactive during the period of illumination. The responses in the mammal were similar, but more complex than in the frog. The mammalian retina shows a background of activity in the dark, so that on- and off-effects are manifest as accentuations or diminutions of this normal discharge. In general, on-elements gave an increased discharge when the light was switched on, and an inhibition of the background discharge when the light was switched off. An off-element showed inhibition of the background discharge during illumination and a powerful discharge at off; this off-discharge is thus a release of inhibition and reveals

unmistakably the inhibitory character of the response to illumination that takes place in some ganglion cells. Each ganglion cell or optic nerve fibre tested had a receptive field; and the area of frog's retina from which a single fibre could be activated varied with the intensity of the light stimulus. The largest field was obtained with the strongest stimulus, so that, in order that a light stimulus, falling at some distance away from the centre of the field, might affect this particular fibre it had to be much more intense than a light stimulus falling on the centre of the field. This means that some synaptic pathways are more favoured than others.

The mammalian receptive field is more complex, the more peripheral part of the field giving the opposite type of response to that given by the centre. Thus, if, at the centre of the field, the response was "on" (an on-centre field) the response to a stimulus farther away in the same fibre was at "off," and in an intermediate zone it was often mixed to give an on-off element. In order to characterize an element, therefore, it must be called on-centre or off-centre, with the meaning thereby that at the centre of its receptive field its response was at "on" or at "off," respectively, while in the periphery it was opposite. By studying the effects of small spot stimuli on centre and periphery separately and together, one investigator demonstrated a mutual inhibition between the two. A striking feature was the effect of adaptation; after dark adaptation the surrounding area of opposite activity became ineffective. In this sense, therefore, the receptive field shrinks, but, as it is a reduction in inhibitory activity between centre and periphery, it means, in fact, that the effective field can actually increase during dark adaptation—*i.e.*, the regions over which summation can occur—and this is exactly what is found in psychophysical experiments on dark adaptation.

### **Anatomical basis**

The receptive field is essentially a measure of the number of receptors—rods or cones or a mixture of these—that make nervous connections with a single ganglion cell. The organization of centre and periphery implies that the receptors in the periphery of an on-centre cell tend to inhibit it, while those in the centre of the field tend to excite it, so that the effects of a uniform illumination covering the whole field tend to cancel out. This has an important physiological value, as it means, in effect, that the brain is not bombarded with an enormous number of unnecessary messages, as would be the case were every ganglion cell to send discharges along its optic nerve fibre as long as it was illuminated. Instead, the cell tends to respond to change—*i.e.*, the movement of a light

or dark spot over the receptive field—and to give an especially prominent response, often when the spot passes from the periphery to the centre, or vice versa. Thus, the centre-periphery organization favours the detection of movement; in a similar way it favours the detection of contours because these give rise to differences in the illumination of the parts of the receptive fields. The anatomical basis of the arrangement presumably is given by the organization of the bipolar and amacrine cells in relation to the dendrites of the ganglion cell; it is interesting that the actual diameter of the centre of the receptive field of a ganglion cell is frequently equal to the area over which its dendrites spread; the periphery exerts its effects presumably by means of amacrine cells that are capable of connecting with bipolars over a wide area. These amacrine cells could exert an inhibitory action on the bipolar cells connected to the receptors of the central zone of the field, preventing them from responding to these receptors; in this case, the ganglion cell related to these bipolars would be of an on-centre and off-periphery type.

### **Direction-sensitive ganglion cells**

When examining the receptive fields of rabbit ganglion cells, investigators found some that gave a maximal response when a moving spot of light passed in a certain “preferred” direction, while they gave no response at all when the spot passed in the opposite direction; in fact, the spontaneous activity of the cell was usually inhibited by this movement in the “null” direction. It may be assumed that the receptors connected with this type of ganglion cell are organized in a linear fashion, so that the stimulation of one receptor causes inhibition of a receptor adjacent to it. This inhibition would prevent the excitatory effect of light on the adjacent receptor from having a response when the movement was in the null direction, but would arrive too late at the adjacent receptor if the light was moving in the preferred direction.

### **The electroretinogram**

If an electrode is placed on the cornea and another, indifferent electrode, placed, for example, in the mouth, illumination of the retina is followed by a succession of electrical changes; the record of these is the electroretinogram or ERG. Modern analysis has shown that the electrode on the cornea picks up changes in potential occurring successively at different levels of the retina, so that it is now possible to recognize, for example, the electrical changes occurring in the rods and cones (the receptor potentials)

those occurring in the horizontal cells, and so on. In general, the electrical changes caused by the different types of cell tend to overlap in time, so that the record in the electroretinogram is only a faint and attenuated index to the actual changes; nevertheless, it has, in the past, been a most valuable tool for the analysis of retinal mechanisms. Thus, the most prominent wave—called the *b*-wave—is closely associated with discharge in the optic nerve, so that in animals, or man, the height of the *b*-wave can be used as an objective measure of the response to light. Hence, the sensitivity of the dark-adapted frog's retina to different wavelengths, as indicated by the heights of the *b*-waves, can be plotted against wavelength to give a typical scotopic sensitivity curve with a maximum at 5000 angstroms (one angstrom =  $1 \times 10^{-4}$  micron) corresponding to the maximum for absorption of rhodopsin.

### **Flicker**

Electrophysiology has been used as a tool for the examination of the basic mechanism of flicker and fusion. The classical studies based on the electroretinogram indicated that the important feature that determines fusion in the cone-dominated retina is the inhibition of the retina caused by each successive light flash, inhibition being indicated by the *a*-wave of the electroretinogram. In the rod-dominated retina—*e.g.*, in man under scotopic conditions—the *a*-wave is not prominent, and fusion depends simply on the tendency for the excitatory response to a flash to persist, the inhibitory effects of a succeeding stimulus being small. More modern methods of analysis, in which the discharges in single ganglion cells in response to repeated flashes are measured, have defined fairly precisely the nature of fusion, which, so far as the retinal message is concerned, is a condition in which the record from the ganglion cell becomes identical with the record observed in the ganglion cell during spontaneous discharge during constant illumination.

### **Visual acuity**

Although the resolving power of the retina depends, in the last analysis, on the size and density of packing of the receptors in the retina, it is the neural organization of the receptors that determines whether the brain will be able to make use of this theoretical resolving power. It is therefore of interest to examine the responses of retinal ganglion cells to gratings, either projected as stationary images on to the receptive field or moved slowly across it. One group of investigators showed that ganglion cells of the cat

differed in sensitivity to a given grating when the sensitivity was measured by the degree of contrast between the black and white lines of the grating necessary to evoke a measurable response in the ganglion cell. When the lines were made very fine (*i.e.*, the “grating-frequency” was high), a point was reached at which the ganglion cell failed to respond, however great the contrast; this measured the resolving power of the particular cell being investigated. The interesting feature of this work is that individual ganglion cells had a special sensitivity to particular grating-frequencies, as if the ganglion cells were “tuned” to particular frequencies, the frequencies being measured by the number of black and white lines in a given area of retina. When the same technique was applied to human subjects, the electrical changes recorded from the scalp being taken as a measure of the response, the same results were obtained.

### 3.2.11 Color vision

The spectrum, obtained by refracting light through a prism, shows a number of characteristic regions of color—red, orange, yellow, green, blue, indigo, and violet. These regions represent large numbers of individual wavelengths; thus, the red extends roughly from 760 nm to 650 nm; the yellow from 630 to 560 nm; green from 540 to 500 nm; blue from 500 to 420 nm; and violet from 420 to 400 nm. Thus, the limits of the visual spectrum are commonly given as 760 to 400 nm. In fact, however, the retina is sensitive to ultraviolet light to 350 nm, the failure of the short wavelengths to stimulate vision being due to absorption by the ocular media. Again, if the infrared radiation is strong enough, wavelengths as long as 1000–1050 nm evoke a sensation of light.

Within the bands of the spectrum, subtle distinctions in hue may be appreciated. The power of the eye to discriminate light on the basis of its wavelength can be measured by projecting onto the two halves of a screen lights of different wavelengths. When the difference is very small—*e.g.*, five angstroms—no difference can be appreciated. As the difference is increased, a point is reached when the two halves of the screen appear differently colored. The hue discrimination (hue is the quality of color that is determined by wavelength) measured in this way varies with the region of the spectrum examined; thus, in the blue-green and yellow it is as low as 1 nm, but in the deep red and violet it may be 10 nm or more. Thus, the eye can discriminate several hundreds of different spectral bands, but the capacity is limited. If it is appreciated that there are a large number of nonspectral colors that may be made up by mixing the spectral

wavelengths, and by diluting these with white light, the number of different colors that may be distinguished is high indeed.

### **Spectral sensitivity curve**

At extremely low intensities of stimuli, when only rods are stimulated, the retina shows a variable sensitivity to light according to its wavelength, being most sensitive at about 500 nanometers, the absorption maximum of the rod visual pigment, rhodopsin. In the light-adapted retina one may plot a similar type of curve, obtained by measuring the relative amounts of light energy of different wavelengths required to produce the same sensation of brightness; now the different stimuli appear colored, but the subject is asked to ignore the colors and match them on the basis of their luminosity (brightness). This is carried out with a special instrument called the flicker-photometer. There is a characteristic shift in the maximum sensitivity from 500 nanometers for scotopic (night) vision to 555 nanometers for photopic (day) vision as shown in figure 3.5.

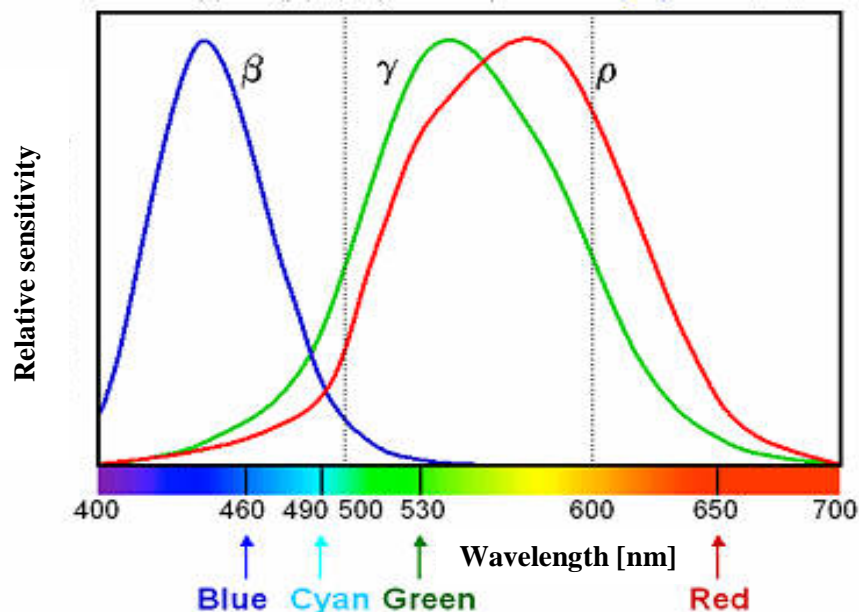


**Figure 3.5** Human Spectral Sensitivity to color (three cone types –  $\rho$ ,  $\gamma$ ,  $\beta$  – correspond roughly to R, G, B).

It has been suggested that the cones have a pigment that shows a maximum of absorption at 555 nanometers, but the phenomena of color vision demand that there be three types of cone, with three separate pigments having maximum absorption in the red, green, and blue, so that it is more probable that the photopic luminosity curve is a reflection of the summated behavior of the three types of cone rather than of one.

It may be observed, as evening draws on, that the luminosities of different colors of flowers in a garden change; the reds become much darker or black, while the blues become much brighter. What is happening is that, in this range of luminosities, called mesopic, both rods and cones are responding, and, as the rod responses become more pronounced—*i.e.*, as darkness increases—the rod luminosity scale prevails over that of the cones.

It may be assumed that the sensation of luminosity under any given condition is determined by certain ganglion cells that make connections to all three types of cone and also to rods; at extremely low levels of illumination their responses are determined by the activity aroused in the rods. As the luminance is increased, the ganglion cell is activated by both rods and cones, and so its luminosity curve is governed by both rod and cone activity. Finally, at extremely high luminance, when the rods are “saturated” and ceasing to respond, the luminosity curve is, in effect, compounded of the responses of all three types of cone.

### **Color mixing**

The fundamental principle of color mixing was discovered by Isaac Newton when he found that white light separates spatially into its different component colors on passing through a prism. When the same light is passed through another prism, so that the individual bands of the spectrum are superimposed on each other, the sensation becomes one of white light. Thus, the retina, when white light falls on it, is really being exposed to all the wavelengths that make up the spectrum. Because these wavelengths fall simultaneously on the same receptors, the evoked sensation is one of white. If the wavelengths are spread out spatially, they evoke separate sensations, such as red or yellow, according to which receptors receive which bands of wavelengths. In fact, the sensation of white may be evoked by employing much fewer wavelengths than those in the spectrum: namely, by mixing three primary hues: red, green, and blue.

Furthermore, any color, be it a spectral hue or not, may be matched by a mixture of these three primaries, red, green, and blue, if their relative intensities are varied. Many of the colors of the spectrum can be matched by mixtures of only two of the primary colors, red and green; thus the sensations of red, orange, yellow, and green may be obtained by adding more and more green light to a red one.

To one accustomed to mixing pigments, and to mixing a blue pigment, for example, with yellow to obtain green, the statement that red plus green can give yellow or orange,

or that blue plus yellow can give white, may sound strange. The mixing of pigments is essentially a subtractive process, however, as opposed to the additive process of throwing differently colored lights on a white screen. Thus, a blue pigment is blue because it reflects mainly blue (and some green) light and absorbs red and yellow; and a yellow pigment reflects mainly yellow and some green and absorbs blue and red. When blue and yellow pigments are mixed, and white light falls on the mixture, all bands of color are absorbed except for the green color band.

### **Responses of uniform population of receptors**

The scotopic (night) visual system, mediated by rods, is unable to discriminate between different wavelengths; thus, a threshold stimulus of light with a wavelength of 480 nm gives a sensation of light that is indistinguishable from that evoked by a wavelength of 530 nm. If the intensities are increased, however, the lights evoke sensations of blue and green, respectively. Rods are unable to mediate wavelength, or color, discrimination while the cones can because the rods form a homogeneous population, all containing the same photopigment, rhodopsin. Thus, the response of a nerve cell connected with a rod or group of rods will vary with the wavelength of light. When the response, measured in frequency of discharge in the bipolar or ganglion cell, is plotted against the wavelength of the stimulating light, the curve is essentially similar to the absorption spectrum of rhodopsin when the same amount of energy is in each stimulus; thus, blue-green of 500 nm has the most powerful effect because it is absorbed most efficiently, while violet and red have the smallest effects. In this sense, the rods behave as wavelength discriminators, but it is to be noted that there are pairs of wavelengths on each side of the peak to which the same response is obtained; thus, a blue of 480 nm and a yellow of 600 nm give the same discharge. Moreover, if the intensity of the stimulus is varied, a new curve is obtained, and now the same response is obtained with a high intensity of violet at 400 nm as with blue at the lower intensity. In general, it is easy to show that, by varying the intensity of the stimulus of a single wavelength, all types of response may be obtained, so that the brain would never receive a message indicating, in a unique fashion, that the retina was stimulated with, say, green light of 530 nm; the same message could be given by blue light of 480 nm, red light of 650 nm, and so on.

Ideally, color discrimination would require a large number of receptors specifically sensitive to small bands of the spectrum, but the number would have to be extremely

large because the capacity for hue discrimination is extremely great, as has been indicated. In fact, however, the phenomena of color mixing suggest that the number of receptors may be limited.

### **The nervous messages**

If the three types of cones respond differently to light stimuli, one may expect to find evidence for this difference in type of response by examining the electrophysiological changes taking place in the retina; ideally, one should like to place a microelectrode in or on a cone, then in or on its associated bipolar cell, and so on up the visual pathway. In the earliest studies, the optic nerve fibres of the frog were examined—*i.e.*, the axons of ganglion cells. The light-adapted retina was stimulated with wavelengths of light stretching across the spectrum, and the responses in arbitrarily selected single fibres were examined. The responses to stimuli of the same energy but different wavelengths were plotted as frequency of discharge against wavelength, and the fibres fell into several categories, some giving what the investigator called a dominator response, the fiber responding to all wavelengths and giving a maximum response in the yellow-green at 560 nm. Other fibres gave responses only over limited ranges of wavelengths, and their wavelengths of maximum response tended to be clustered in the red, green, and blue regions. The investigator called these modulators, and considered that the message in the dominator indicated to the brain the intensity of the stimulus—*i.e.*, it determined the sensation of brightness—while the modulators indicated the spectral composition of the stimulus, the combined messages in all the modulators resulting in a specific color sensation. In the dark-adapted retina, when only rods were being stimulated, the response was of the dominator type, but this time the maximum response occurred with a wavelength of 500 nm, the absorption maximum of rhodopsin.

A more careful examination of the responses in single fibres, especially in the fish, which has good color vision, showed that things were not quite as simple as the original investigator had thought because, as has been seen, the response of a ganglion cell, when light falls on its receptive field in the retina, is not just a discharge of action potentials that ceases when the light is switched off. This type of response is rare; the most usual ganglion cell or optic nerve fiber has a receptive field organized in a concentric manner, so that a spot of light falling in the central part of the field produces a discharge, while a ring of light falling on the surrounding area has the opposite effect,

giving an off-response—*i.e.*, giving a discharge only when the light is switched off. Such a ganglion cell would be called an on-centre-off-periphery unit; others behaved in the opposite way, being off-centre-on-periphery.

When these units are examined with colored lights, and when care is taken to stimulate the centers and surrounding areas separately, an interesting feature emerges; the centre and surrounding areas usually have opposite or opponent responses. Thus, some may be found giving an on-response to red in the centre of the field and an off-response to green in the surrounding area, so that simultaneous stimulation of centre with red and surrounding area with green gives no response, the inhibitory effect of the off-type of response cancelling the excitatory effect of the on-type. With many other units the effects were more complex, the centre giving an on-response to red and an off-response to green, while the surrounding area gave an off-response to red and an on-response to green, and vice versa. This opponent organization probably subserves several functions. First, it enables the retina to emphasize differences of color in adjacent parts of the field, especially when the boundary between them moves, as indeed it is continually doing in normal vision because of the small involuntary movements of the eyes. Second, it is useful in “keeping the retina quiet”; there are about one million optic nerve fibres, and if all these were discharging at once the problem of sorting out their messages, and making meaning of them, would be enormous; by this “opponence,” diffuse white light falling on many of these chromatic units would have no effect because the inhibitory surrounding area cancelled the excitatory centre, or vice versa. When the light became colored, however, the previously inactive units could come into activity.

These responses show that by the time the effect of light has passed out of the eye in the optic nerve the message is well color-coded.

The three types of receptor, responding to different regions of the spectrum in specific manners, transmit their effects to bipolar and horizontal cells. The latter neurons have been studied from the point of view of their color-coding. The potentials recorded from them were called *S*-potentials; these were of two types, which classified them as responding to color (*C*-units) and luminosity (*L*-units).

The *C*-type of cell gave an opponent type of response, in the sense that the electrical sign varied with the wavelength band, red and green having opponent effects on some cells, and blue and yellow on others. These responses reflect the connections of the horizontal cells to groups of different cones, the blue-yellow type, for example, having

connections with blue and red and green cones, while the red-green would have connections only with red and green cones.

**References**

- [1] <http://www.britannica.com/EBchecked/topic/1688997/human-eye>
- [2] [http://en.wikipedia.org/wiki/Iris\\_%28anatomy%29](http://en.wikipedia.org/wiki/Iris_%28anatomy%29)
- [3] <http://en.wikipedia.org/wiki/Pupil>
- [4] <http://en.wikipedia.org/wiki/Cornea>
- [5] <http://en.wikipedia.org/wiki/Sclera>
- [6] <http://www.daviddarling.info/encyclopedia/C/choroid.html>

## 4. Flicker and Flickermeter

### 4.1 Flicker phenomena and terminology

Rapidly varying loads such as electric furnaces, arc welders, large motors, etc. cause disturbances during power generation, transmission or distribution, that are the origin of supply voltage fluctuation. This is a power quality problem which generated engineering concern since the onset of electrical illumination technology.

The term “flicker” is strongly associated with the operation of varying loads. Flicker involves voltage fluctuation and its effect on the lighting system resulting in changes in luminance and consequent irritation of human vision.

The type of voltage fluctuation, caused by subharmonics and interharmonics of voltage, associated with lighting is commonly called “voltage flicker” which can be divided into two general categories: cyclic and non-cyclic. The first one results from periodic loads such as welders as in the given system. The second, on the other hand, may be caused by a motor starting or breaking on a random schedule. The operation of an arc furnace is commonly followed by a mixture of both cyclic and non-cyclic voltage flicker.

Considering the filament incandescent lamp in the light system, cyclic voltage flicker can be conveniently expressed as the RMS value of the modulating waveform divided by the RMS value of the fundamental voltage. For a non-cyclic case, it also can be expressed as the change in voltage divided by the average voltage, multiplied by 100, to obtain, in this way, a percent of change.

The measurement of the voltage flicker involves the determination of the system RMS voltage variation and the frequency at which it occurs. The maximum permissible voltage disturbances that the system can tolerate without complaints about light flicker and annoyance is termed “*Light Flicker Voltage Requirements*”.

The International Electrotechnical Vocabulary [1] defines Flicker as the “*impression of unsteadiness of visual sensation induced by a light stimulus whose luminance or spectral distribution fluctuates with time*”. So, “Light Flicker” is a subjective impression of luminance fluctuation of light emanation or gleams from a lamp.

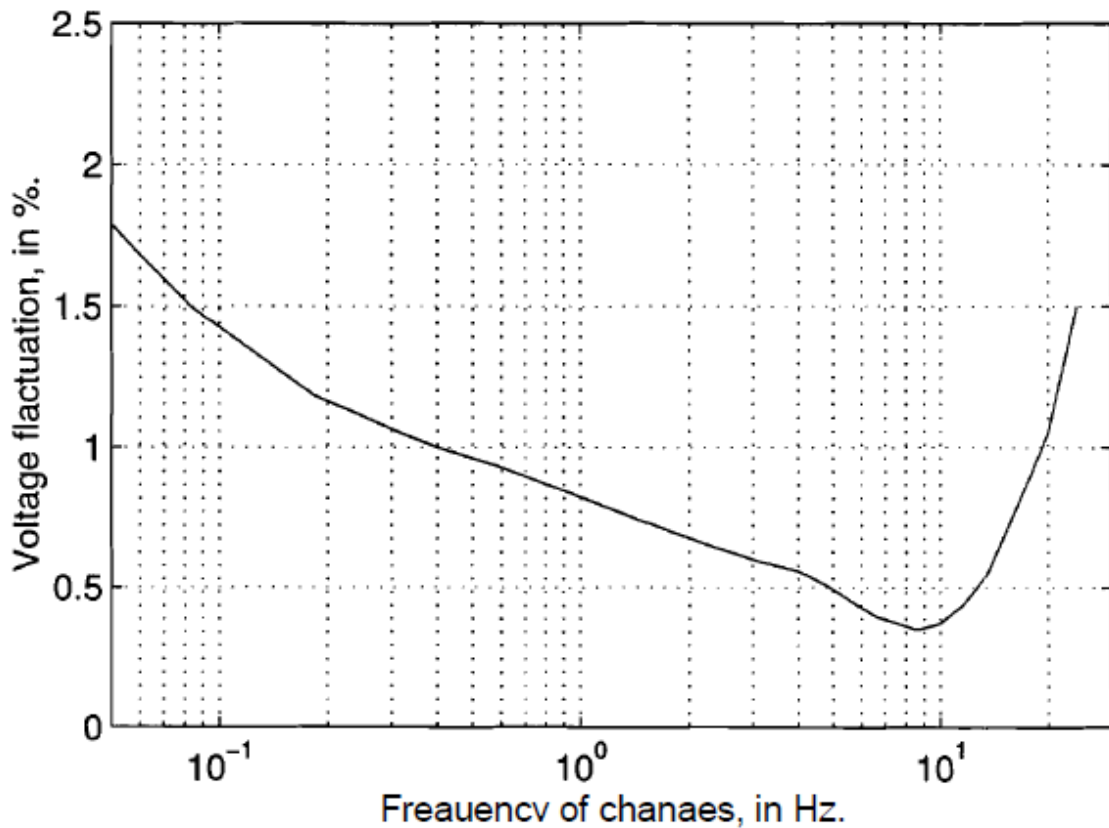


**Figure 4.1** Borderline of irritation for rectangular voltage fluctuation

The fluctuations qualities resulting from changes brightness, modulation of intensity, or variation in color may be sufficient to be perceptible to the human eye which is able to perceives light fluctuations with frequency not over 30 Hz. As described in Chapter 3, the human vision, in turn, is a very complex system consisting of optical, neurological and cognitive elements, which provide the eye with the ability to adapt to illumination over a big range of intensities. The smallest stimulus able to producing a recognizable sensation with 50% probability of detecting the presence of this stimulus is called the *Visual Threshold*.

Tests have shown that the human eye is most sensitive to light modulating frequencies in the range of 8-10 Hz. In this band, even a very slight voltage flicker of about 0.3-0.4% (as shown in figure 4.1) in a system with incandescent lamps is noticeable and can be even annoying to certain individuals. The permissible amount of voltage fluctuation to avoid complaints about the light flicker is very difficult to determine succinctly or precisely for many reasons. The light fluctuations depends to a great extent on the type of lamps used, their wattage, design, etc. The method used to predict light flicker from an incandescent lamp may not be the same as it would be for a fluorescent lamp, which

in turn, depends on the type of ballast circuit. Finally the reaction of human observers is a subjective matter, and varies quite widely from person to person.

The disturbances caused by flicker are dependant not only on the endurance extent of the human subject or on the exposition time, but also on the flicker severity. The International Electrotechnical Commission (IEC) and the Union International for Electroheat (UIE) have developed both a flicker standard and a precise technique for flicker evaluation presented in IEC Publication 868 and its amendment [2-5]. So, for several years, statistical investigations have been conducted to know with a satisfactory approximation the relationships between the luminous flux modulation and the annoyance provoked by it on human body. In this connection, before to start measurements on volunteers, it was necessary to define how to perform the tests. A 60W- 50 Hz - 230 V incandescent filament lamp was selected, because it was the most commonly used type of lamp in Europe. People were subjected to several flicker stimuli, i.e. characterized by particular combinations of magnitude (changeable from zero to some percent of the fundamental) and low frequency (0 ÷ 30 Hz). By statically analyzing the test results, the maximum annoyance was verified when a 8.8 Hz-frequency modulation was applied.

In some cases, observable flicker may be very irregular with vast deviation of its peaks over long periods. Depending on the type of loads and their mutual work schedule, the flicker will vary in its level over a wide range of time. However, a unique method equally applicable to any fluctuating load was proposed by UIE in which the flicker sensation is statistically evaluated over some representative observation period as a measure of its severity. In this connection, the observation period of 10 minutes and two hours are recommended for the short- and long-term ( $P_{st}$  and  $P_{lt}$  respectively) evaluation.

The instantaneous flicker is discretized so that a particular flicker level is assigned to each of the evenly spaced moments in time. A sampling of the flicker signal at a fixed rate, usually more frequent than the fundamental frequency of the source, would provide sufficient input data for the statistical evaluation.

The flicker severity over the short-term can be expressed as:

$$P_{st} = \sqrt{\sum_{i=1}^n k_i P_i} \quad (4.1)$$

where  $P_i$  is the flicker level exceeded during a particular percent of the time 10 minutes of the observation period,  $k_i$  is the corresponding weighting coefficient.

The long-term flicker severity can be derived from consequentially measured  $P_{st}$ , as:

$$P_{lt} = \sqrt[3]{\frac{\sum_{i=1}^N P_{st}^3}{N}} \quad (4.2)$$

where  $N$  denotes the number of short-term measurements in the corresponding long-term observation period. The cubic law is recommended for cases with relatively small chance of coincidence in load operations [5].

The Standard EN 50160 [6] establishes that under normal operating conditions, in any period of one week the long term flicker severity caused by voltage fluctuation should be  $P_{lt} \leq 1$  for 95 % of the time. Reaction to flicker is subjective and can vary depending on the perceived cause of the flicker and the period over which it persists. In some cases  $P_{lt} = 1$  gives rise to annoyance, whereas in other cases higher levels of  $P_{lt}$  are found without annoyance.

## 4.2 Flickermeter UIE

### 4.2.1 Blocks

The Flickermeter architecture is described by the block diagram of figure 4.2, and can be divided into two parts, each performing one of the following tasks:

- Simulation of the response of the lamp-eye-brain chain;
- On-line statistical analysis of the flicker signal and presentation of the results.

The first task is performed by blocks 2,3 and 4 of figure 4.2, while the second task is accomplished by block 5.

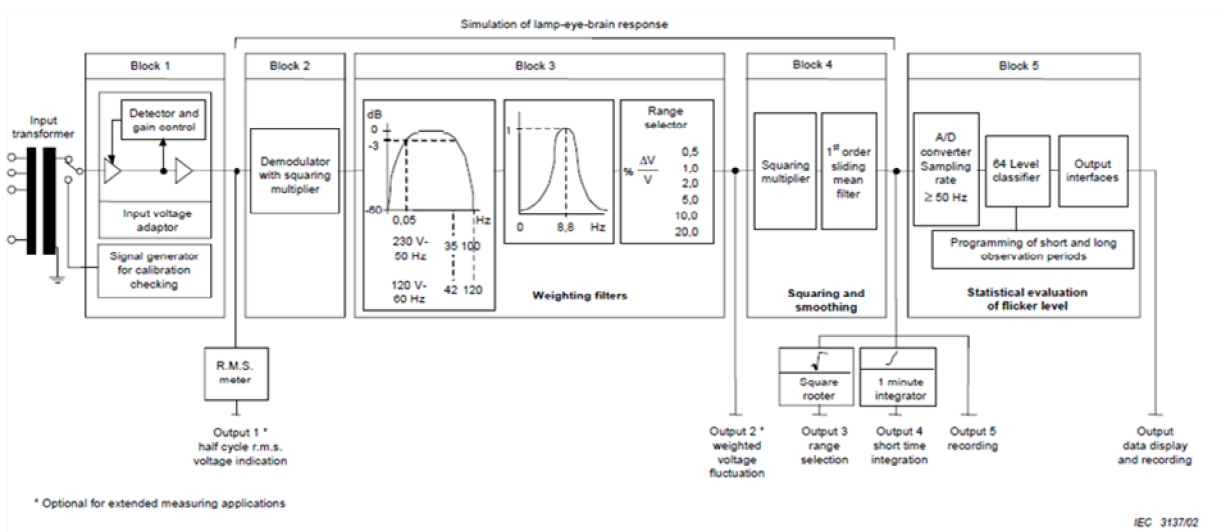


Figure 4.2 Functional diagram of IEC Flickermeter.

### **Block 1- Input voltage adaptor and calibration checking circuit**

The block contains a signal generator to check the calibration of the Flickermeter on site and a voltage adapting circuit that scales the mean rms value of the input mains frequency voltage down to an internal reference level. In this way flicker measurements can be made independently of the actual input carrier voltage level and expressed as a per cent ratio. Taps on the input transformer establish suitable input voltage ranges to keep the input signal to the voltage adaptor within its permissible range.

The internal generator shall provide a sine wave at mains frequency modulated by a  $(50/17)$  Hz = 2,94 Hz, rectangular voltage fluctuation for 50 Hz systems, and by a  $(60/17)$  Hz = 3,53 Hz, rectangular voltage fluctuation for 60 Hz systems.

Checking shall be made by providing an indication that shows alignment with a reference mark or value. The significant characteristics of this circuit are the following:

- carrier phase-locked to the mains;
- $\Delta V/V$  modulation 1 %;
- carrier level suitable for all measuring ranges;
- accuracy of modulating frequency 1 %.
- 

### **Block 2- Square law demodulator**

The purpose of this block is to recover the voltage fluctuation by squaring the input voltage scaled to the reference level, thus simulating the behavior of a lamp.

The circuit included on this block shall give as a component of its output a voltage linearity related to the amplitude of the fluctuation modulating the input. The input operating range of the demodulator shall be capable of accepting up to 150 % of the reference value  $V_R$ .

### **Blocks 3 and 4- Weighting filters, squaring and smooting**

*Block 3* is composed of a cascade of two filters and a measuring range selector, which can precede or follow the selective filter circuit.

These filters are used to:

- eliminate the d.c component and the component at twice the mains frequency present at the output of the demodulator (the amplitude of higher components is negligible);
- weight the voltage fluctuation according to the lamp-eye-brain sensitivity.

The filter for the suppression of the unwanted components incorporates a first order high-pass (suggested 3 dB cut-off frequency at about 0,05 Hz) and a low-pass section, for which a Butterworth filter of 6<sup>th</sup> order with a 3 dB cut-off frequency of 35 Hz for 230V/50 Hz system is suggested. This suggestion takes into account the fact that the component at twice the mains frequency is also attenuated by the weighting filter block 3. A band stop or notch filter tuned at this frequency may also be added to increase the resolution, but it shall not significantly affect the response of the instrument frequencies within the measurement bandwidth.

A suitable transfer function for block 3, assuming that the carrier suppression filter defined above has negligible influence inside the frequency bandwidth associated to voltage fluctuation signals, is of the following type:

$$F(s) = \frac{k\omega_1 s}{s^2 + 2\lambda s + \omega_1^2} * \frac{1 + s/\omega_2}{\left(1 + \frac{s}{\omega_3}\right) * \left(1 + \frac{s}{\omega_4}\right)} \quad (4.3)$$

where  $s$  is the Laplace complex variable and the values of the parameters are the following:

$$k=1.74802, \lambda=2\pi 4.05981, \omega_1=2\pi 9.1549, \omega_2=2\pi 2.27979, \omega_3=2\pi 1.22535, \omega_4=2\pi 21.9.$$

The range selector determines the instrument sensitivity, varying the gain according to the amplitude of the voltage fluctuation to be measured.

The measuring ranges expressed as relative voltage change  $\Delta V/V$  for an 8,8 Hz sine wave modulation are 0,5; 1; 2; 5; 10; 20 % . The range 20 % is optional as at large depths of modulation, non-linearity of the demodulator may introduce significant errors. Block 3 alone is based on the borderline perceptibility curve for sinusoidal voltage fluctuations; the correct weighting of non-sinusoidal and stochastic fluctuations is achieved by an appropriate choice of the complex transfer function for blocks 3 and 4. Accordingly the correct performance of the model has also been checked with periodic rectangular signals as well as with transient signals.

The output of block 4 represents the *instantaneous flicker sensation*.

**Block 4** is composed of a squaring multiplier and a first order low-pass filter. The human flicker sensation via lamp, eye and brain is simulated by the combined non-linear response of blocks 2,3, and 4.

It performs two functions:

- squaring of the weighted flicker signal to simulate the non-linear eye-brain perception;
- sliding mean averaging of the signal to simulate the storage effect in the brain.

The squaring operator shall have input and output operating ranges sufficient to accommodate the admissible flicker level at 8,8 Hz.

The sliding mean operator shall have the transfer function of a first order low-pass resistance/capacitance filter with a time constant of 300 ms.

### **Blocks 5 – On-line statistical analysis**

Block 5 incorporates a microprocessor that performs an on-line analysis of the flicker level, thus allowing direct calculation of significant evaluation parameters.

A suitable interface allows data presentation and recording. The use of this block is related to methods of deriving measurements of flicker severity by statistical analysis.

The statistical analysis shall be made by subdividing the amplitude of the flicker level signal into a suitable number of classes. The flicker level signal is sampled at a constant rate. Every time that the appropriate value occurs, the counter of the corresponding class is incremented by one. In this way, the frequency of at least twice the maximum flicker frequency, the final result at the end of the measuring interval represents the distribution of flicker level duration in each class. Adding the content of the counters of all classes and expressing the count of each class relative to the total gives the probability density function of the flicker levels. From this function is obtained the cumulative probability function used in the time-at-level statistical method. Figure 4.3 schematically represents the statistical analysis method, limited for simplicity of presentation to 10 classes.

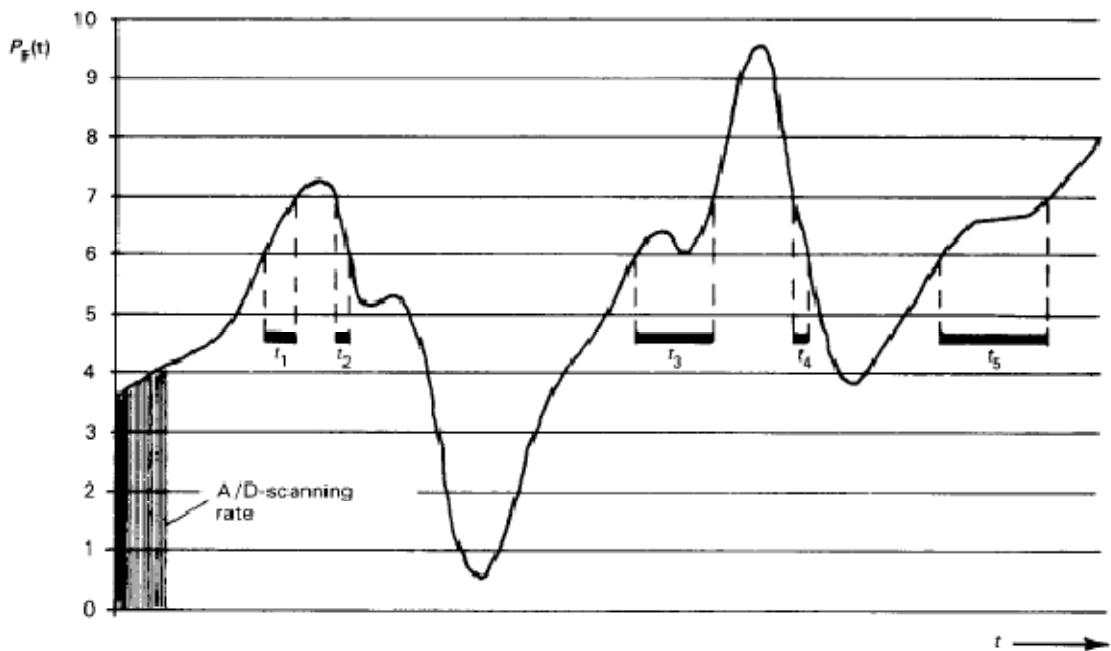


**Figure 4.3a** Flicker level as a time-varying function. Signal permanence in class no.7 is indicated as an example:

$$T_7 = \sum_{i=1}^{i=5} t_i$$

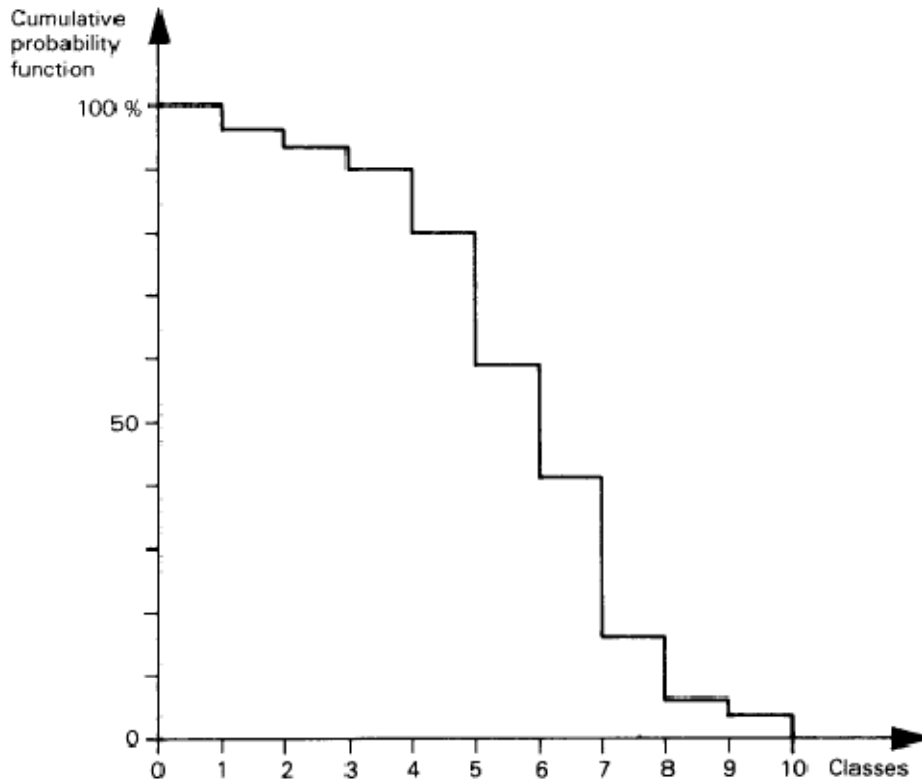


**Figure 4.3b** Cumulative probability function of the time-at-level method.

For the cumulative probability function, significant statistical values can be obtained such as mean, standard deviation, flicker level being exceeded for a given percentage of time or, alternatively, the percentage of time that assigned flicker level has been exceeded. The observation period is defined by two adjustable time intervals:  $T_{\text{short}}$  and  $T_{\text{long}}$ . The long interval defines the total observation time and is always a multiple of the short interval ( $T_{\text{long}} = n * T_{\text{short}}$ ). For on line processing, immediately after conclusion of each short time interval, the statistical analysis of the next interval is started and the results for the expired interval are made accessible for output. In this way,  $n$  short time analyses will be available for a given observation period  $T_{\text{long}}$  together the results for the total interval. Cumulative probability function plots should preferably be made by using a Gaussian normal distribution scale.

### 4.2.2 Analysis procedure

The analysis expressing the output of block 4 in digital form with at least 6 bits resolution and using at least 64 classes. Minimum sampling rate is 50 samples per second. The relationship between the range selector and the level corresponding to the

highest class of the cumulative probability function resulting from the classification is indicated in the following table:

**Table 4.1** Relationship between the range selector values and sensation levels

$\frac{\Delta v}{v} \%$	Sensation levels in units of perceptibility threshold
0,5	4
1	16
2	64
5	400
10	1 600
20	6 400

$T_{\text{short}}$  can be selected between 1 min, 5 min and 15 min.

$T_{\text{long}}$  shall be an integer multiple of the selected  $T_{\text{short}}$  up to at least 1008, corresponding to seven days with a  $T_{\text{short}}$  of 10 min.

### 4.2.3 Short-term flicker evaluation

The measure of severity based on an observation period  $T_{\text{st}} = 10$  min is designated  $P_{\text{st}}$  and is derived from the time-at-level statistics obtained from the level classifier in block 5 of the Flickermeter. The following formula is used:

$$P_{\text{st}} = \sqrt{0.0314P_{0.1} + 0.0525P_{1s} + 0.0657P_{3s} + 0.28P_{10s} + 0.08P_{50s}} \quad (4.4)$$

Where the percentiles  $P_{0.1}$ ,  $P_1$ ,  $P_{10}$ , and  $P_{50}$  are the flicker levels exceeded for 0.1, 1, 3, 10 and 50 % of the time during the observation period. The suffix s in the formula indicates that the smoothed value should be used; these are obtained using the following equations:

$$P_{50} = (P_{30} + P_{50} + P_{80})/3$$

$$P_{10} = (P_6 + P_8 + P_{10} + P_{13} + P_{17})/5$$

$$P_{3s} = (P_{2.2} + P_3 + P_4)/3$$

$$P_{1s} = (P_{0.7} + P_1 + P_{1.5})/3$$

The 0.3 s memory time-constant in the Flickermeter ensures that  $P_{0.1}$  cannot change abruptly and no smoothing is needed for this percentile.

### 4.2.4 Long-term flicker evaluation

The 10 min period on which the short-term flicker severity evaluation is based is suitable for assessing the disturbance caused by individual sources with a short-cycle.

Where the combined effect of several disturbing loads operating randomly (e.g. welders, motors) has to be taken into account or when flicker sources with long and variable duty cycle (e.g. arc furnaces) have to be considered, it is necessary to provide a criterion for the long-term assessment of the flicker severity. For this purpose, the long-term flicker severity  $P_{lt}$ , shall be derived from the short-term severity values,  $P_{sti}$ , over an appropriate period related to the duty cycle of the load or a period over which an observer may react to flicker, e.g. a few hours, using formula:

$$P_{lt} = \sqrt[3]{\frac{\sum_{i=1}^N P_{sti}^3}{N}} \quad (4.5)$$

Where  $P_{sti}$  ( $i = 1, 2, 3, \dots$ ) are consecutive readings of the short-term severity  $P_{st}$ .

### 4.2.5 Outputs

The Flickermeter diagram of figure 4.8 shows a number of outputs between blocks 1 and 5. The outputs marked with an asterisk are not essential, but may allow a full exploitation of the instrumental potential for the investigation of voltage fluctuations. Further optional outputs may be considered.

#### **Output 1**

The aim of optional output 1 and its associated rms voltmeter is to display the voltage fluctuation waveform in terms of changes in rms value of the input voltage. This can be achieved by squaring, integrating between zero crossing on each half-cycle and square-rooting the signal.

Un order to observe small voltage changes with good resolution, an adjustable dc offset and rectification should be provided.

#### **Output 2**

Output 2 is optional and mainly intended for checking the response of block3 and making adjustments.

#### **Output 3**

Output 3 is optional and gives an instantaneous linear indication of the relative voltage change  $\Delta V/V$  expressed as per cent equivalent of an 8.8 Hz sinusoidal wave modulation. This output is useful when selecting the proper measuring range.

#### **Output 4**

Output 4 is optional and gives the 1 min integral of the instantaneous flicker sensation.

#### **Output 5**

Output 5 is mandatory; it represents the instantaneous flicker sensation and can be recorded on a strip-chart recorder for a quick on-site evaluation, or on magnetic tape for long-duration measurements and for later processing.

#### **Output 6**

Output 6 in block 5 is mandatory and is connected to a serial digital interface suitable for a printer and magnetic tape recorder. Analogue plots of the cumulative probability function can be obtained directly from this block by using another digital-to-analogue converting interface.

### **4.2.6 Performance testing**

Each Flickermeter, with its classifier, shall be subjected to regular series of rectangular voltage changes given in the table below.

**Table 4.2** Test specification for flicker classifier

Rectangular changes per minute	Voltage changes $\frac{\Delta V}{V}$ %	
	120 V lamp 60 Hz system	230 V lamp 50 Hz system
1	3,166	2,724
2	2,568	2,211
7	1,695	1,459
39	1,044	0,906
110	0,841	0,725
1 620	0,547	0,402
4 000	Test not required	2,40
4 800	4,834	Test not required
NOTE 1 620 rectangular changes per minute corresponds to 13,5 Hz.		

In each case, the flicker severity,  $P_{st}$ , shall be  $1,00 \pm 0,05$  (see 4.10.1).

In addition, the manufacturer shall determine the range of the magnitude of voltage changes for which the corresponding  $P_{st}$  values are given with an accuracy of 5 % or better. To make these tests, the magnitude of  $\Delta V/V$  (%) given in the table shall be increased and decreased while keeping the repetition rate constant, and the value of  $P_{st}$  shall be obtained. If, for instance, at a repetition rate of seven changes per minute the input voltage changes are increased by a factor of 3 from 1.46 % to 4.38 % then  $P_{st}$  should increase from  $1.0 \pm 5$  % to  $3.0 \pm 5$  %.

The range over which the accuracy of 5 % is maintained is the working range of the classifier. If selectable sensitivity ranges are employed in the Flickermeter, then similar tests should be performed for each range.

**References**

- [1] E. L. Owen, "power disturbance and quality: light flicker voltage requirements," *Ind. Appl. Magazine*, vol. 2, no. 1, pp. 20-27, Jan. 1996.
- [2] IEC publication 868 "Flickermeter, functional and design specification," 1986.
- [3] IEC International Standard. Amendment 1 to publication 868 (1986) "Flickermeter, functional and design specification," 1990.
- [4] IEC Technical report 868-0, Part 0, "Evaluation of flicker severity," 1991.
- [5] International Union for Electroheat (UIE), C. Mirra, P.G. Kendall, "An international study of flicker," Cired 1989.
- [6] EN 50160 "Voltage characteristics of electricity supplied by public distribution systems", Geneva, CH, 2004.

## 5. Toward an innovative Flickermeter

### 5.1 Introduction

As described in the previous chapter, among the several parameters defined by the European Standard EN-50160 [1] for evaluating the voltage characteristics, flicker severity is probably the most particular one. Usually, flicker applies to cycle instability of light intensity resulting from supply voltage fluctuation, which, in turn, can be caused by disturbances, subharmonics and interharmonics of voltage, introduced during power generation, transmission or distribution. In particular, cycloconverters, welders and arc furnaces, eccentrically operating tools and integral cycle controlled power equipment are notorious for producing voltage flicker.

Nevertheless, the luminous variation may be caused by how a certain light source reacts to non-sinusoidal voltages and hence, from this point of view, flicker is also a power quality phenomenon.

It is clear that the relationship between voltages and luminous fluctuation is closely dependent on the kind of source and that how the human eye perceives light variation is the results of complex neuro-physiological and psychological mechanisms which may change among people. Therefore, the evaluation of flicker severity shall theoretically require information on the light source, the voltage supplying it and, obviously, the response of the human visual system to the produced luminous radiation, pending such a model holds for all the people.

The instrument defined by the standard EN 61000-4-15 [3] and described in chapter 4, which has been adopted by the IEEE as IEEE Std 1453 [4], processes the voltage and compute an index representing the flicker severity that must be compared with the limit in [1] to verify if the voltage is compliance or not. Such an instrument assumes that the light source is a 60 W – 230 V – 50 Hz incandescent filament lamp and implements a model of the eye-brain system. The reason for which an incandescent lamp is considered is very simple: when the Standard was written, such kind of light was the most commonly light source used. As far as the visual system model is concerned, it was obtained starting from the studies carried out by Rashbass [5] and by Koenderink – Van Doorn [6, 7] in the 1970s. It consists in a statistically-based psychometric curve that defines, for fluctuation frequencies up to some tens of hertz and for a given

fluctuation amplitude, the irritability threshold. Roughly speaking, it provides a sort of frequency response of the human visual system.

Over the years, technical, economical and environmental motivations have led to its replacement first in the industry and then, even if the process is still in progress, in household use. Moreover a recent directive of the European Commission [8] has agreed on their removing from the market on September 2011.

As a consequence, the use of the standard flickermeter leads to results that, of course, allow checking the compliance of the voltage with [1], but, probably, are not related to the actual annoyance caused to a person. This is not a comfort problem only. In fact, for example, it is common experience that the fluorescent lamps (most likely the most used in non-domestic environments) are generally less sensitive than incandescent ones to voltage fluctuations. It means that if the flicker severity was correctly measured, voltages featuring higher variations might be accepted.

For these reasons, in the last two decades, many scientific contributions have faced these issues [9-17]. For example, the adoption of suitable “gain factor” [9] or the implementation of novel model of the eye brain response to flicker [14-17] have been suggested to overcome the strict dependence of the standard [1] on the kind of light source. In particular, the model proposed in [14] and modified in [15] has shown quite interesting results when applied to different light sources [16]. Such a model relies on the analysis of the physiological mechanism of pupillary light reflex. As known, the pupil size can vary for two main reasons: i) changes in the ambient illumination and ii) changes in the distance between the eye and the object to be focused. The response of the human visual system is usually referred to as *pupillary light reflex* in the former case and *pupillary accommodation reflex* in the latter one.

The light first enters the eye through the cornea and then through the pupil, which is a circular aperture in the iris. The crystalline lens converges the light rays into a focal point; namely the light progresses through the vitreous humour and it is focused on the

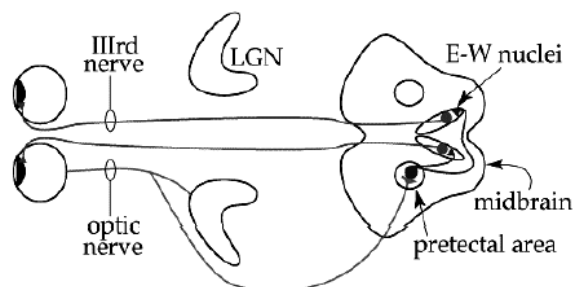


**Figure 5.1.** Signal pathways in the pupillary light reflex

central fovea and the macula which are the light-sensitive elements in the retina. In this tissue, a chemical reaction (photoreceptors) transforms the light impulse into electrical signals, which are then sent to

the brain by the optic nerve. The region of the brain devoted to interpret such electrical signals is located in the occipital lobe: the signal bypasses the LGN (Lateral Geniculate Nucleus), which helps the visual system to focus its attention on the most important information, and arrives to pretectal nucleus that communicates with a suitable midbrain element (named Edinger-Westphal nuclei) aimed at managing the size of the pupillary aperture by driving the sympathetic and parasympathetic pathways. Such nerves, which are referred to as “3rd nerve” in Figure 5.1, control the movements of two opposing smooth muscles: the dilator and the sphincter (iris muscle). The flicker phenomena causes a continuous action of the dilator and the sphincter muscles, since the Edinger-Westphal (E-W) nuclei try to keep constant the amount of luminous intensity which reaches the central fovea and the macula. As a consequence, an annoyance sensation arises. This last effect must be ascribed to the energy spent for the iris muscles for forth and back motions.

Starting from some basic physiological information, an analytical model describing the lamp-eye-brain system has been developed in [14].

On the basis of the above described physiological mechanism and under the assumption of small signals (i.e. small variations  $\Delta\ell$  of luminance with respect to a bias value  $\bar{\ell}$ ) the dynamic analytical model depicted in figure 5.2 has been derived in [14, 15]. In figure 5.2,  $A$  is the pupil area, the finite delay  $D(s)$  models the behaviour of both the optic and IIIrd nerve, the motor  $M(s)$  is used for describing the action of the iris muscles to vary the size of the pupil area, and finally the integrator  $I(s)$  takes into account the mechanical inertia of the masses in motion. The output  $p$  is the instantaneous flicker sensation.

The transfer function  $H(s)$  of the network is:

$$H(s) = \frac{p(s)}{A(s) \cdot \Delta\ell} = \frac{p_2 s^2 + p_0}{q_8 s^8 + q_6 s^6 + q_4 s^4 + q_2 s^2 + q_0} \quad (5.1)$$

where the parameters  $p_i$  and  $q_i$  take proper values [16]. However, it must be kept in

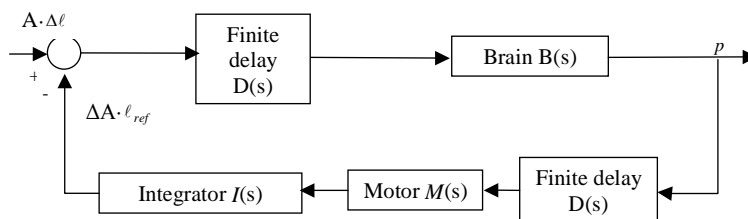


**Figure 5.2** Schematic block diagram of the pupillary light reflex - based model of the eye-brain system

mind that the only real data available to test any new model are those which the Standard [1] is based on.

On the other hand, it should be underlined that the eye-brain model included in the standard Flickermeter derives from psychometric studies and then it essentially features “subjective” characteristics. In this connection, the research activity carried out for this thesis, could be a significant step in the direction of a new Flickermeter. In fact, the intent has been to find different methods for implementing a new instrument, getting through the evident limits and problems concerning the Standard [3].

Principally, the intent has been the development of an improvement of a visual system model starting from information obtained by measuring a physiological parameter, thus allowing to get a more “objective” representation of the human eye response to flicker.

The idea to consider the pupil size as a potential index to provide the annoyance caused by flickering lights, has been suggested by previous studies [18, 19] on the physiological behaviour of the photoreceptors. In particular, some researchers have studied the electroretinograms evoked by excitation of human cones when subjected to a different flickering lights. They understand that the photoreceptors are similar to band-pass filters (i.e. a device which passes frequencies within a certain range and rejects (attenuates) those outside that range). According to experimental findings, correspondingly to particular frequency, there is a sort of anti-resonance and the photoreceptors send to the brain, via the optic nerve, electrical signals containing not real information about a more intense light. In this way, as known, the brain controls the iris muscles to contract the pupil.

This means that the pupil size is the response of complex chain mainly managed by the light source, the photoreceptors and the brain. So, it is fair to suppose that the pupil diameter can contain helpful information to allow an “objective” representation of the human eye response to flicker, and improve the Standard [3].

In this respect, the use of the mean value of the pupil diameter has been taken as parameter for investigating the reaction of the brain to flickered light and developed a system for its measure [20, 21]. In the following section, two measurements setup and their characterization will be presented.

## 5.2 First system setup “A”

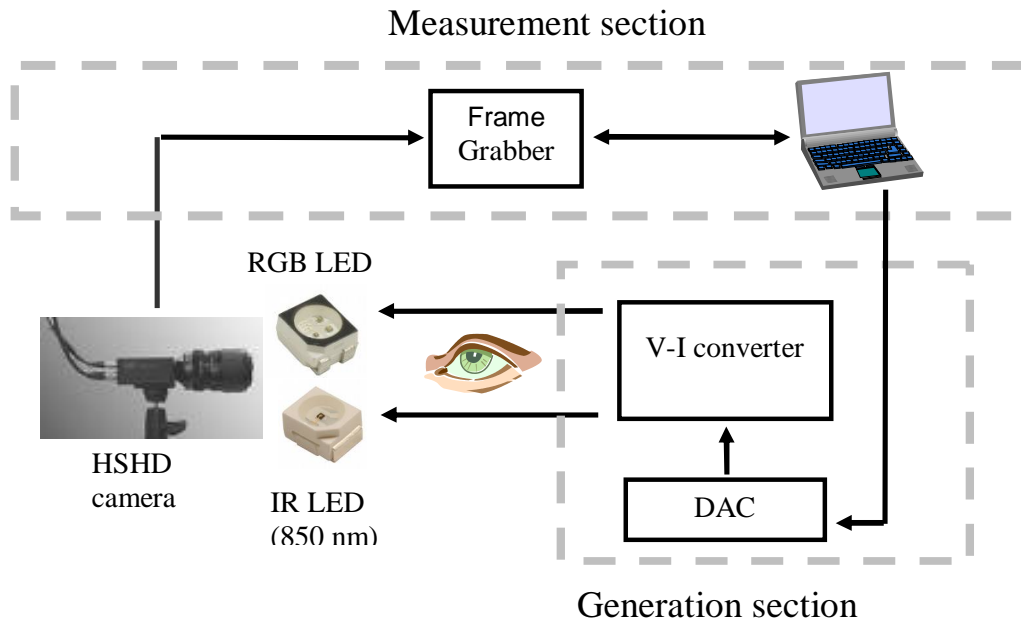


**Figure 5.3** Schematically representation of the system.

Basically, it allows stimulating the eye through different types of light stimuli with given amplitude, frequency and colour, acquiring eye images with a certain rate and, lastly, processing them to get the pupil diameter. Therefore, as shown in figure 5.3, it consists of two main blocks: i) the generation section and ii) the measurement section.

The generation section comprises an RGB LED, two infrared (IR) LEDs (figure 5.4), a voltage-to-current converter and a 16 bit Digital-to-Analogue Converter (DAC) controlled by personal computer. The RGB LED is positioned near the eye of subject under test and generates the flicker. The two IR LEDs illuminate the eye without varying the pupil size given that the human vision system is not sensitive to these wavelengths. Frequency and magnitude of the flicker are set, for each colour, via personal computer by acting on the output voltage of the DAC.

The measurement section is implemented by a high-speed high-definition (HSHD) camera, a frame grabber and a personal computer. The camera (CM140MCL, Jai, Denmark), equipped with a 50-mm focal length objective, is a digital monochrome progressive scan one that features up to 1380 x 1040 pixels, 31 frames-per-second (fps). Its CCD sensor has a spectral response that includes the infrared region (400 nm to 1000 nm) [22].

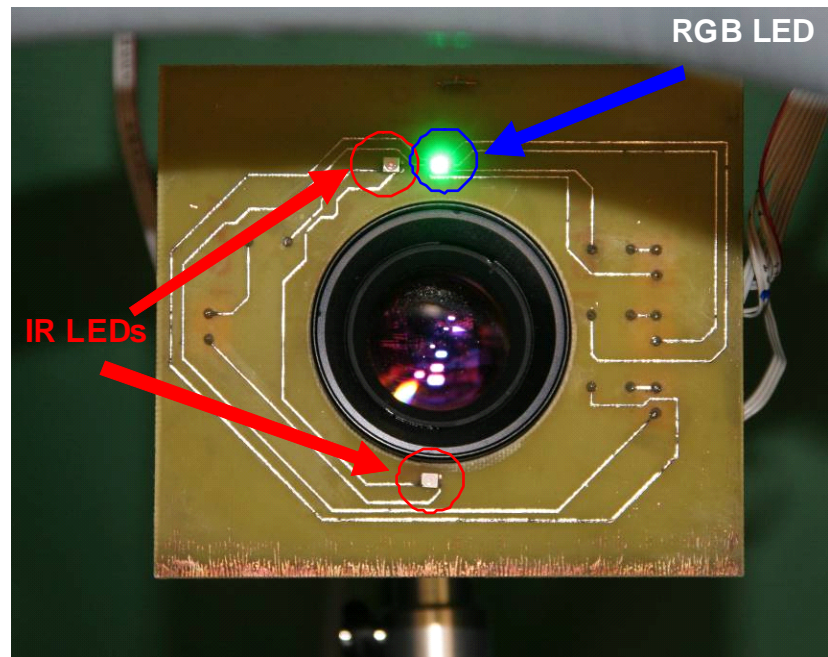


**Figure 5.4** LED board mounted on the camera lens.

The frame grabber, made by National Instruments, manages the connections with a personal computer that stores the acquired images and runs an algorithm, developed in Labview environment, which measures, frame by frame, the pupil diameter. First of all, the image is binarized by applying a threshold computed by statistically analyzing the picture itself. In practice, it is chosen by multiplying the darker tones with a suitable coefficient. Then, particles having area lower than 20% of the one of the whole image are removed: this way reflected light spot are deleted; a further refinement is obtained by filling the convex hulls that may appear in the image after the particle deleting process. The so achieved binary picture is finally processed by a function that separates the pupil (approximated by a circle) from the background and computes its diameter (figure 5.5). This analysis procedure essentially relies on the use of the Danielsson coefficient [23] to reconstitute the circular form and on a weighted least square circular fitting to get the diameter. The proposed system is completed by a chin rest used by the subject under test to keep a comfortable and stable position during the measurements. Both the equipment and the volunteer are covered by a heavy sheet to ensure that no different lights than the LED ones stimulate the eye, as shown in figure 5.6.

After the first measurement campaigns executed thanks to this system, the improvement of some structural details became necessary.

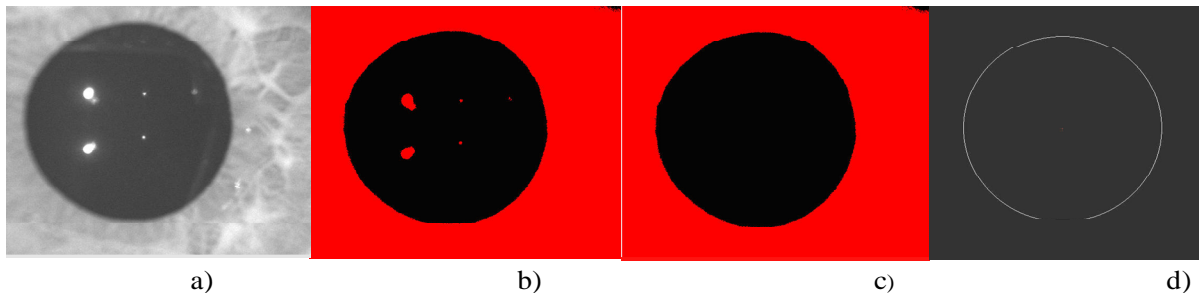


**Figure 5.5** a) pupil image b) c) d) images obtained by the analysis software for the computation of the pupil diameter.



**Figure 5.6** The proposed system.

The use of a chin rest assures to keep fixed the distance between the source and the eye under test, which is a necessary requirement for a better reliability of the results. In the next section, a second system setup will be presented.

### 5.3 Second system setup “B”

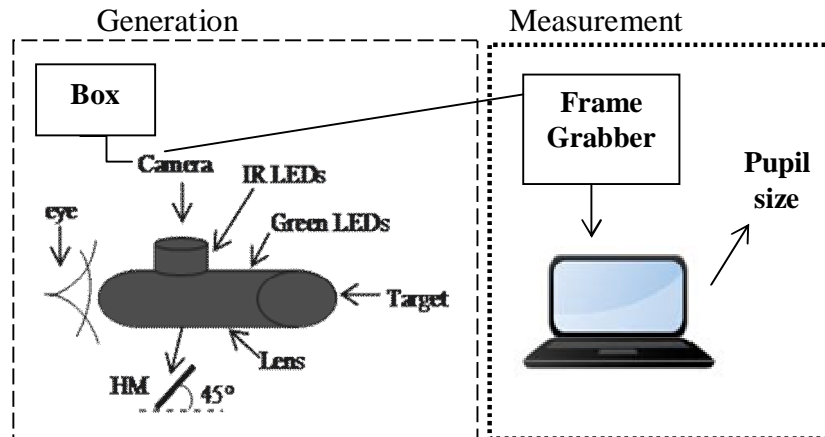


Figure 5.7 Schematic block diagram of the second experimental setup.

Essentially, the measurement system, schematically shown in figure 5.7 and photographed in figure 5.8, has been designed to perform the same actions of the first one: the generation of different flicker stimuli, the acquisition of the pupil images and the measurement of the pupil diameters. It consists in two blocks: a) the measurement section and b) the generation section. As for the measurement section a), it includes a black and white miniature camera, a frame grabber and a personal computer. The camera, (XC-EI50CE, Sony, South Korea), equipped with a 25-mm focal length objective (HF25HA-1B), is an high resolution (752(H) x 582 (V) pixels) camera provided with a 1/3” enhanced super sensitive ex-view Sony CCD sensor with a spectral response which includes the infrared region (400 nm to 870 nm).

The frame grabber, made by Sensory, connects the camera to a personal computer that stores the images and controls a specific algorithm, developed under Labview environment, which computes the diameter of each acquired pupil. All the pictures are firstly binarized by applying a threshold computed on the basis of a statistical analysis of the picture itself. Then, particles (reflected light spots) having area lower than 20% of the entire image are deleted. Finally, a function identifies the circle that best approximates the pupil and estimates the diameter. In this way, the mean values and standard deviations, for each specific flickering light condition, are computed.

The generation section b) is mainly a black tube where all the components are located in. As shown in figure 5.7, in front of the only one open extreme, the eye of the subject under test is leant. Around the camera, on the top of the tube, four infrared (IR) LEDs



**Figure 5.8** The test system.

(850 nm) on a circular support have been fixed; in this way the IR light is reflected by the hot mirror HM (NT55-233, Edmund scientific), 45° angled and positioned 4 cm away from the eye and 1,5 cm from the camera. Essentially, this is a dichroic filter that allows visible light to pass, while reflects wavelengths in the range 750 ÷ 1250 nm (IR region). Then, the camera works fine with the right illumination and the eye is safe.

To obtain a good distribution of the flickering light, six green LEDs (525 nm) are placed equidistant from each other on a second ring that is mounted almost in the end of the tube (~ 17 cm away from the eye). They light the target thus allowing to obtain a uniform flickering surface. Between the HM and the green LEDs ring, a bi-convex lens (LB1723-N-BK7,  $\varnothing 2''$ ,  $f = 60$  mm, Uncoated, Thorlabs) has been located to grant more visibility also for myopic people. Given that the pupil diameter may vary also for the so-called pupillary accommodation reflex (i.e. for the attempt of the visual system to focus a certain object) and this may significantly affect the correctness of our measurements, the subject under test is asked to focus his attention on the target.

An external box (the white box in figure 5.8) supplies both the camera and the light sources (IR and green LEDs) and allows to select between six singular different frequencies (1, 5, 10, 15, 20, 25 Hz) in addition to a green fixed light.

## 5.4 Characterization of the system “A”

The experimental tests have three main purposes: a) evaluation of the pupil-diameter measurement algorithm behaviour in presence of different kind of images; b) measurement of the dominant wavelength of each colour of the RGB LED as well as of the power radiated by both RGB and IR LEDs that hit the eye; c) characterization of the whole system in order to estimate the uncertainty that can affect measurements that will be performed with the proposed equipment.

### 5.4.1 Test of the algorithm for pupil diameter measurement

The correct behaviour of the developed software has been first evaluated by processing a set of images (600 x 600 pixels, greyscale bitmap) drawn by using a commercial graphics editing program. Each of them represents a black circle with known diameter and prearranged background colour. Diameter ranging from 108 to 442 pixels has been considered given that their dimensions are similar to those of actual human pupil in our system. As for background colours (in 8 bit representation) values of 128, 192 and 255 has been chosen, thus considering different colours of the iris. Figure 5.9 shows some samples of the test images. The analysis software has provided correct results for the whole set of images. In addition, an image with a white circle simulating an hypothetical reflection in the pupil caused by the IR LED (see the right figure at the second row in figure 5.9) has been used to further test the software. Also in this case the algorithm has provided the expected diameter. After that, the presence of noise has been simulated. Gaussian noise with suitable variance has been added to the above test images to get pictures with unitary SNR, that is the standard deviation of the noise equals the one of the test image. By way of example, figure 5.10 shows a test image (diameter 162 pixel, background colour 128) with noise superposed. A Monte Carlo Method (MCM) procedure [24] with  $M = 10,000$  trials has been run to determine mean value and standard deviation. Table I reports the obtained results. It can be noted that the behaviour of the developed algorithm is substantially independent of noise. The most significant effect is a bias of 2 pixels that, of course, may be unpleasant for the shorter diameters.

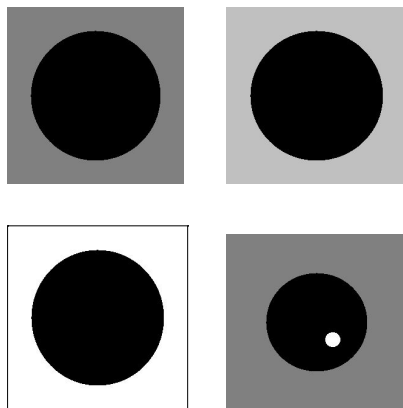


**Figure 5.9** Samples of test pictures

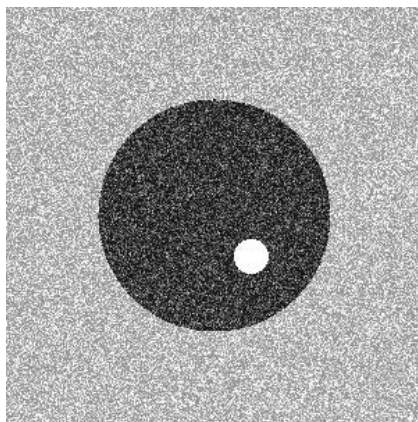


**Figure 5.10** Test image (SNR= 1) corrupted by adding Gaussian noise.

**TABLE 5.1** MEAN VALUES AND STANDARD DEVIATION PROVIDED BY RUNNING A MONTE CARLO METHOD PROCEDURE WITH 10,000 TRIALS ON DIFFERENT REFERENCE IMAGES CORRUPTED WITH GAUSSIAN NOISE (SNR = 1)

Reference diameter (pixels)	Monte Carlo Method (10,000 trials)	
	Mean value (pixels)	Standard deviation (pixels)
108	105.9	1.6
162	160.0	0.89
220	218.0	0.85
320	318.0	0.53
440	438.0	0.72

However, it should be kept in mind that the simulations have been performed by considering pictures having an high SNR and that, according to Table 5.1, the bias does not depend on the diameter value. Therefore, given that it is interesting the study of the

diameter variation, such a little bias can be considered as not affecting the characterization results.

### 5.4.2 Radiated power

The proposed equipment is used to perform measurements on human beings and hence it is necessary to verify if some important requirements of the IEC 60825 standard [25] are fulfilled. In particular it defines the maximum permissible exposure (MPE) as the highest power or energy density of a light source that is considered safe, i.e. that has negligible probability for creating damage. Figure 5.11 shows, according to [25], the relationship between the MPE (in  $\text{W}/\text{cm}^2$ ) and the exposure time (in seconds) for different wavelengths. In this connection, the dominant wavelength, that is the spectral component having the maximum amplitude, have to be first determined for each colour of the RGB LED. To this purpose, the optical head of a spectrometer sensor is positioned instead of the human eye, at about 170 mm from the source. The spectrometer (32-channel photosensor module, H8353, Hamamatsu) allows to measure wavelengths in the range 400 nm - 710 nm with steps of 10 nm. A sampling frequency of 500 Sa/s (10,000 samples acquired) was set and 20 acquisitions were performed for each colour. The measured spectra of the red, green and blue colours lights are shown in figure 5.12. It can be stated that they feature dominant wavelengths equal to 640 nm, 520 nm and 460 nm, respectively. As for the IR LED, its actual wavelength cannot be measured given that its nominal value is outside the spectrometer range. Therefore, its nominal wavelength (850 nm) is assumed as dominant one.

The power emitted by both the RGB and IR LEDs has been measured by positioning a powermeter (Lasercheck Handheld) instead of the human eye, 170 mm away from the

**TABLE 5.2** MEASURED VALUES OF POWER  $P$  AND RELEVANT COMPUTED POWER DENSITY  $P$  ALONG WITH THE ASSOCIATED STANDARD UNCERTAINTY.

Colour	$P$ ( $\mu\text{W}$ )	$u(P)$ ( $\mu\text{W}$ )	$P$ ( $\text{W}/\text{cm}^2$ )	$u(p)$ ( $\text{W}/\text{cm}^2$ )
<b>Red</b>	4.20	0.21	$3.3 \cdot 10^{-5}$	$0.2 \cdot 10^{-5}$
<b>Green</b>	4.25	0.21	$3.3 \cdot 10^{-5}$	$0.2 \cdot 10^{-5}$
<b>Blue</b>	4.18	0.21	$3.3 \cdot 10^{-5}$	$0.2 \cdot 10^{-5}$
<b>IR</b>	70.0	3.5	$5.6 \cdot 10^{-4}$	$0.6 \cdot 10^{-4}$

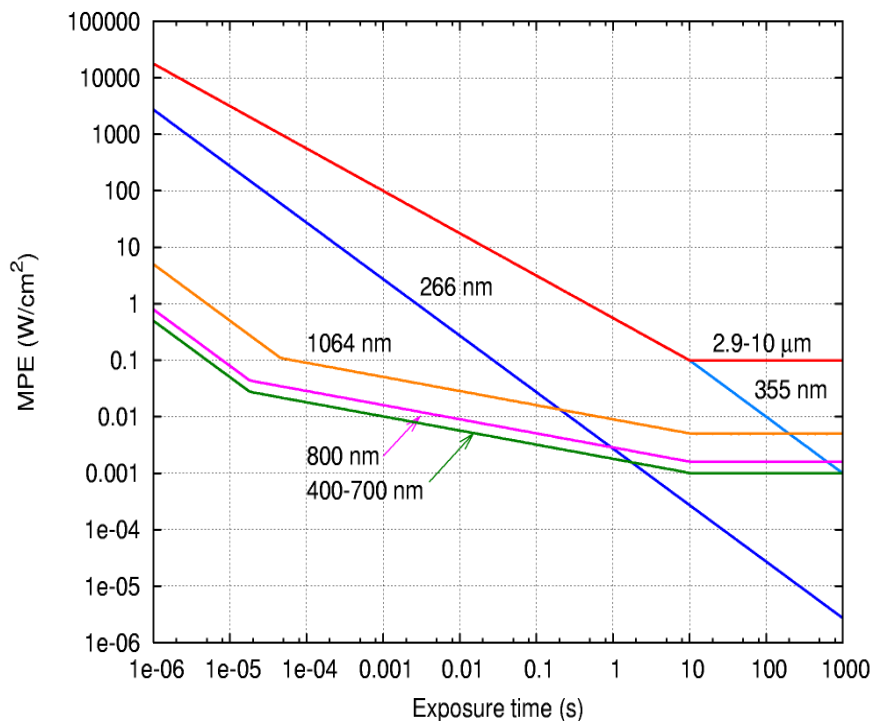


**Figure 5.11** MPE vs. exposure time (picture made by *Han-Kwang Nienhuy* on the basis of IEC 60825 values, published under GNU Free Documentation License).

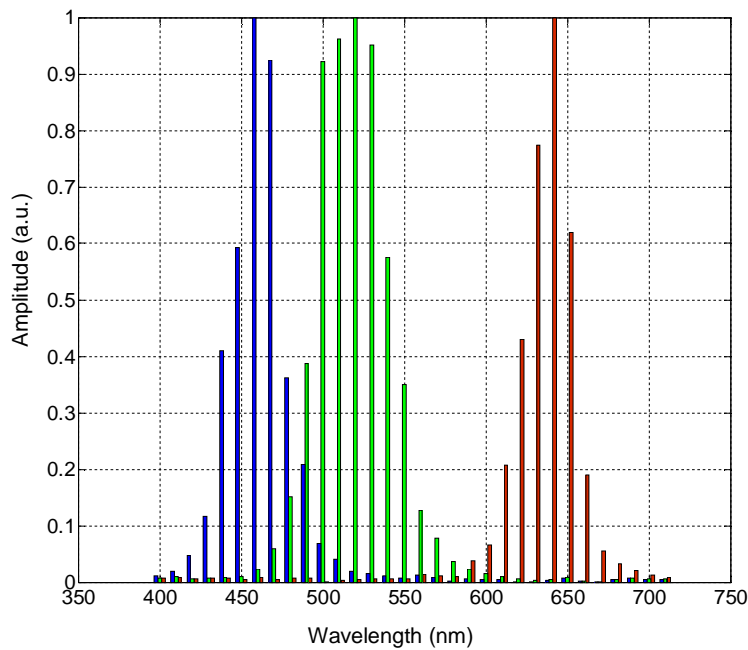


**Figure 5.12** Measured spectra of the colors provided by the RGB LED. The amplitude are normalized to the maximum value of each spectrum.

source. The powermeter features 5%-accuracy in the range 400 nm -1064 nm and can measure powers from 0.5 μW up to 10 mW by setting the wavelength to be checked.

As for the supply voltages of the V-I converter (and hence the currents feeding the LEDs), they were chosen, according to the LEDs datasheets, to get, for each colour, the same luminous intensity and for the IR the maximum illumination of the eye. Table 5.2 shows the powers  $P$ , measured according to the above described procedure, and the power density  $p$  impinging the cornea, computed by assuming a pupil diameter of 4 mm, which is a typical value. The uncertainty  $u(P)$  and  $u(p)$  are also reported. It can be learned that: i) the three components of the RGB LED irradiate, within the  $1\sigma$  - confidence interval defined by the standard uncertainty, the same power; ii) the requirements of the standard IEC 60825-1 [25] are fulfilled given that all the power densities  $p$  are lower than the MPE values for the considered wavelength and for exposure time greater than 1000 s ( $1 \text{ mW/cm}^2$ , see figure 5.11).

### 5.4.3 System accuracy

The main goal of this characterization is to verify whether the diameter estimation is affected by the pupil size itself and, mainly, by the relative position between eye and camera. Indeed, even if at the beginning of the test the camera is locked and focused on the subject eye, unpredictable iris movement may occur thus leading to different apparent diameter for the same pupil size. To investigate on the above topics, properly designed targets with pictures representing pupils with different diameters (2, 3, 4, 5 mm) have been placed in front of the camera instead of the human eye and fixed on a metallic frame (see figure 5.13).



**Figure 5.13** Frame used for the system characterization

1L	1C	1R
2L	2C	2R
3L	3C	3R

**Figure 5.14** Ideal division of the camera shot and positions where the targets were located for evaluating the system accuracy

**TABLE 5.3** GREEN LIGHT: MEAN VALUES AND STANDARD DEVIATIONS OF MEASURED TARGET DIAMETERS (10 s ACQUISITION TIME) FOR DIFFERENT DIAMETER VALUES AND DIFFERENT POSITIONS. POSITIONS ARE LABELLED ACCORDING TO FIGURE 5.12.

Diameter (mm)	2		3		4		5	
	Mean (pixels)	Std. Dev. (pixels)						
1L	115.1	1.4	213.7	1.3	284.7	1.5	349.3	1.3
2L	114.8	1.6	210.4	1.4	285.7	1.3	348.0	1.7
3L	110.8	1.6	206.4	1.4	286.3	1.5	344.1	1.4
1C	121.4	1.4	215.7	0.9	279.7	1.0	352.1	1.4
2C	119.6	1.6	215.6	0.8	284.9	1.1	352.2	1.3
3C	116.3	2.4	215.4	1.0	281.8	1.1	351.1	1.3
1R	119.2	1.5	217.6	1.4	277.3	1.6	349.6	1.3
2R	118.8	1.3	218.0	1.6	276.2	1.3	349.5	1.3
3R	117.8	1.6	220.3	1.7	275.2	1.5	346.4	1.7

Under the highly reasonable assumption that, during the measurements on volunteers, the pupil always remain inside the camera shot, useful information on the effect of different relative position between camera and eye can be obtained by moving the targets inside the frame and, hence, inside the shot. In particular, the shot has been ideally divided into nine equal squares, as shown in figure 5.14, and acquisitions were performed by placing the targets inside them. Ten seconds of camerawork were taken for each target diameter and for each colour. This allows taking into account also the effect of the illuminating colour. Of course, to better simulate measurements in actual conditions, the camera was focused only one time, at the beginning of the test, on the target having 3-mm diameter and placed in position 2C (see figure 5.14) with green colour turned on. Tables 5.3 to 5.5 report, for different test positions, the mean values and the standard deviations of measured diameters relevant to green, red and blue colour, respectively. Positions are labelled according to figure 5.14. The effect of the various uncertainty sources can be better highlighted by summarizing the huge amount of data shown in Table 5.3-5.6 with the mean values and the standard deviations, computed for each colour and for each target size over the all nine different test positions and reported in Table 5.6. On the basis this outcomes, it can be stated that the colour used to illuminate the target does not affect the measurement result: if the uncertainty on the mean value, in term of its standard deviation, is considered, it is

**TABLE 5.4 RED LIGHT: MEAN VALUES AND STANDARD DEVIATIONS OF MEASURED TARGET DIAMETERS (10 S ACQUISITION TIME) FOR DIFFERENT DIAMETER VALUES AND DIFFERENT POSITIONS. POSITIONS ARE LABELLED ACCORDING TO FIGURE 5.12**

Diameter (mm)	2		3		4		5	
	Mean (pixels)	Std. Dev. (pixels)	Mean (pixels)	Std. Dev. (pixels)	Mean (pixels)	Std. Dev. (pixels)	Mean (pixels)	Std. Dev. (pixels)
1L	111.8	1.2	202.3	1.2	275.4	1.2	341.3	1.6
2L	111.8	1.2	203.6	1.2	277.4	1.5	341.5	0.9
3L	108.3	1.5	201.1	1.4	277.7	1.3	338.8	1.0
1C	120.4	1.2	210.8	1.0	279.7	0.9	347.1	1.3
2C	118.4	1.4	209.4	1.0	278.3	1.0	346.9	1.3
3C	115.9	1.6	209.1	1.2	276.7	1.2	344.9	1.2
1R	115.0	1.3	207.4	1.1	271.2	1.7	340.8	1.3
2R	115.1	1.3	207.7	1.3	270.3	1.2	341.7	1.3
3R	113.8	1.5	209.4	1.4	270.7	1.6	340.0	1.4

**TABLE 5.5** BLUE LIGHT: MEAN VALUES AND STANDARD DEVIATIONS OF MEASURED TARGET DIAMETERS (10 S ACQUISITION TIME) FOR DIFFERENT DIAMETER VALUES AND DIFFERENT POSITIONS. POSITIONS ARE LABELLED ACCORDING TO FIGURE 5.12

Diameter (mm)	2		3		4		5	
Position	Mean (pixels)	Std. Dev. (pixels)						
1L	114.7	1.7	211.6	1.3	281.8	2.0	348.7	1.2
2L	114.4	1.6	209.0	1.3	276.3	0.7	347.1	1.4
3L	111.3	1.5	205.2	1.3	275.1	1.0	343.6	1.7
1C	122.2	2.0	214.6	0.9	283.9	1.1	350.9	1.4
2C	120.8	1.7	213.5	0.9	283.7	1.3	351.4	1.3
3C	119.0	2.2	211.8	0.9	281.4	1.1	350.7	1.3
1R	119.1	1.2	215.2	1.4	273.4	1.8	348.8	1.2
2R	118.9	1.3	215.9	1.6	275.4	1.5	343.3	1.5
3R	117.7	1.3	218.2	1.6	275.3	1.4	345.3	1.5

**TABLE 5.6** MEAN VALUES AND STANDARD DEVIATIONS FOR EACH COLOUR AND FOR EACH TARGET DIAMETER EVALUATED OVER THE 9 TEST POSITIONS

Target diameter	2 mm		3 mm		4 mm		5 mm	
	Mean (pixels)	Std. Dev. (pixels)						
Red	115	4	207	4	275	4	343	3
Green	117	3	215	4	281	4	349	3
Blue	118	4	213	4	278	4	348	3

trivial to verify that measurements performed under different light colours provide the same diameter estimate. This holds for all the considered targets. Moreover, it can be stated that the standard deviation does not significantly vary with diameter as well as colour: in any situation, it is 3 or 4 pixels.

According to the ISO GUM [26], the standard deviation is the standard uncertainty and then, on the basis of the previous observation, it can be concluded that the diameter measurements performed by the developed instrument are affected by a standard uncertainty equal to 4 pixels. Such a value is completely acceptable for our application.

## 5.5 Characterization of the system “B”

Three characterization procedures have been carried out.

The first one was aimed at evaluating the accuracy of the whole pupil size measurement system. In the second procedure, the purpose was to get the relationship between the

**TABLE 5.7** MEAN VALUES ( $\mu$ ) AND STANDARD DEVIATION OF THE MEAN ( $s$ ) OF THE TARGET DIAMETERS

Frequency	8 mm		9 mm		10 mm		11 mm		12 mm	
	$\mu$ [pixel]	$s$ [pixel]								
1	316	0.81	348	0.44	391	0.97	418	0.60	459	0.54
5	317	1.00	348	0.83	391	1.05	418	0.56	460	0.15
10	317	1.00	348	0.63	391	0.98	418	0.65	460	0.09
15	317	1.05	348	0.45	391	1.01	418	0.69	460	0.25
20	317	1.00	348	0.29	391	1.00	419	0.93	460	0.18
25	317	0.99	348	0.42	391	0.93	418	0.20	460	0.09

supply voltage and the optical power emitted by the green LEDs. Instead, the last step was to verify the optical power steadiness emitted by the green source.

### 5.5.1 Accuracy of the measurement system

To evaluate the accuracy of the pupil size measurement system, an properly designed set of targets representing a human eye with different pupil diameters has been used. Diameters from 8 to 12 mm with step of 1 mm have been considered and the chosen six frequencies were 1 Hz, 5 Hz, 10 Hz, 15 Hz, 20 Hz, 25 Hz. The targets have been placed in the same position of the human eye to simulate real condition. Twenty seconds of camera work were taken for each selected frequency and target diameter. Finally, the mean values and standard deviations have been computed.

Table 5.7 reports the mean values and the standard deviations of the measurements described. It can be highlight that the mean diameter estimation is not dependant on the flicker frequency: the “pupil size” is the same (the maximum noted difference is just 1 pixel) for each frequency; in addition, the relationship between the reference (mm) and the estimated diameter (pixel) shows a very good linearity, no matter the frequency. The correlation coefficient is 0.99 in all the case. By way of example, figure 5.15 depicts the case of 1-Hz stimulus.

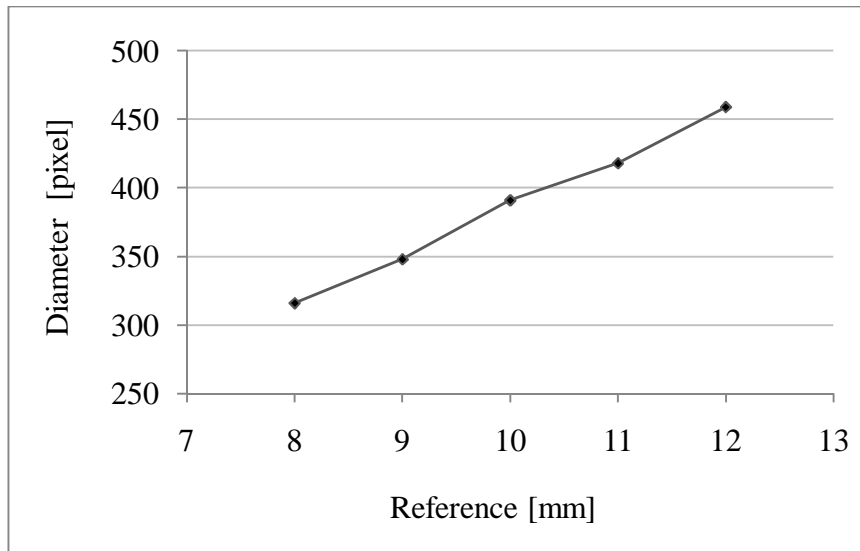


**Figure 5.15** Relationship between reference (mm) and estimated diameter at 1-Hz frequency.

### 5.5.2 Optical power stability

Aim of this test was to verify the optical power stability emitted by the six green LEDs over a period of time considerably longer than the usual duration of the experiments on the human subjects. To this purpose, a Fast Optical Power Meter (OE-200-SI/FEMTO), a Digital Oscilloscope (DSO 6052 A/Agilent), a collimating lens (74-VIS/Ocean Optics, USA) and an Optical Fiber have been used.

The first step has been to align the optical power meter with the system, in the same position of the human eye, to maximize the optical coupling between the source (six green LEDs) and the detector. The tests have been executed in two different days using first all the selected frequencies starting from 1 Hz to 25 Hz and then considering the reverse sequence.

One hour before the beginning of the test, the FEMTO and the oscilloscope were turned on to ensure their warm-up. With regard to the Fast Optical Power Meter, a gain equal to  $10^8$ , a bandwidth FBW (200 kHz upper-cut-off frequency (-3 dB) relevant to that gain) and a DC coupling were chosen. After the instrument settings, the green LEDs have been switched on and, in dark condition, 500-s optical power measurements (2 kSa sampling frequency,  $10^6$  samples) have been performed for each frequency.

For each frequency  $f$ , the  $10^6$  values of optical power have been linearly interpolated according to a least square method. The differences  $\Delta_{f,i}$  ( $i=1,2$ ) between the extreme of the best fitting straight lines, normalized to the mean values of the corresponding set of

powers, have been used as index of the optical power stability. Table 5.8 shows, for each frequency, the index  $\Delta\% = 100 \cdot (\Delta_{f,1} + \Delta_{f,2})/2$ : the lower is  $\Delta\%$ , the higher is stability, in time, of the emitted power. It can be easily verified that the variation of the power is absolutely negligible and independent of the frequency.

To verify if the radiated power does not depend on the frequency, the following index has been computed for each frequency:

$$\Delta P = \frac{P_f}{\frac{1}{N} \sum_f P_f}, \quad (5.1)$$

where  $P_f$  is the mean value of the power at frequency  $f$  and  $N$  is the number of frequency. It can be observed that the amount of power emitted by the system used to generate flickering light is the same for all frequency given that a maximum difference of only 0.27% holds (Table 5.9).

**TABLE 5.8** OPTICAL POWER STABILITY AT DIFFERENT FREQUENCY: THE LOWER IS  $\Delta\%$ , THE HIGHER IS THE STABILITY

Frequency (Hz)	$\Delta\%$
1	-0.24
5	-0.36
10	-0.34
15	-0.30
20	-0.34
25	-0.34

**TABLE 5.9** POWER  $P$  AND RELEVANT COMPUTED POWER DENSITY  $p$  ALONG WITH THE ASSOCIATED STANDARD UNCERTAINTY

Wavelength [nm]	$P$ ( $\mu\text{W}$ )	$u(P)$ ( $\mu\text{W}$ )	$p$ ( $\text{W}/\text{cm}^2$ )	$u(p)$ ( $\text{W}/\text{cm}^2$ )
525	270	13.5	$0.95 \cdot 10^{-3}$	$4.8 \cdot 10^{-5}$

### 5.5.3 Radiated power

The proposed equipment will be used to perform measurements on human beings, so it has been necessary to verify if the limits of the Standard IEC 60825-1 [25] were satisfied. Specifically, this standard defines the maximum permissible exposure (MPE) as the greatest power of energy density of a light source that isn't considered unsafe.

In this connection, once the source dominant wavelength is known (available in the LED datasheet), the power emitted by the six green LEDs has been measured by a calibrated dc power meter (Lasercheck Handheld) placed instead of the human eye (~17 cm away from the source). The used instrument features 5%-accuracy in the range 400 nm – 1064 nm and can measure power from 0.5  $\mu\text{W}$  to 10 mW. By considering a typical pupil size equal to 6 mm and the green fixed light, the power density impinging the cornea can be evaluated starting from the measured values.

The measured power  $P$  (dominant wavelength 525 nm) and the relevant power density  $p$  evaluated by assuming the diameter of 6 mm are reported in Table 5.9. The uncertainty  $u(P)$  and  $u(p)$  are also shown.

It's possible to conclude that the requirements of the Standard are respected, because the power density  $p$  is lower than the MPE values ( $1 \text{ mW}/\text{cm}^2$ ) imposed for the considered wavelength and for exposure time greater than 10 s [25].

The system characterization has highlighted satisfactory behavior, in terms of both accuracy of the diameter estimation and stability of the radiated power. This last feature is very important because it implies the repeatability, pending the physiological variability between human subjects, of the measurements.

In the next chapter the results of all the executed measurement campaigns on human volunteers will be described with final observations and comments.

**References**

- [1] EN 50160, “Voltage characteristics of electricity supplied by public distribution systems”, Geneva, CH, 2004
- [2] IEC 60050-161, “International Electrotechnical Vocabulary – Electromagnetic Compatibility,” Geneva, Switzerland, 1997.
- [3] EN 61000-4-15, “Testing and measurement techniques: flickermeter-functional and design specification”, Geneva, CH, 1997
- [4] IEEE Std. 1453, “IEEE recommended practice for measurement and limits of voltage fluctuations and associated light flicker on AC power systems”, New York, USA, 2005.
- [5] C. Rashbass, “The visibility of transient changes of luminance”, *Journal of Physiology*, no. 210, pp. 165-186, 1970.
- [6] J. J. Koenderink, A. J. Van Doorn, “Visibility of unpredictability flickering lights” , *Journal of the Optical Society of America*, vol. 64, no. 11, pp. 1517-1522, 1974
- [7] J. J. Koenderink, A. J. Van Doorn, “Detectability of power fluctuations of temporal visual noise”, *Vision Research*, vol. 18, pp. 191-195, 1978.
- [8] European Commission, “Commission Regulation (EC) No 244/2009 of 18 March 2009 implementing Directive 2005/32/EC of the European Parliament and of the Council with regard to ecodesign requirements for non-directional household lamps”, *Official Journal of the European Union*, n.76, March, 24<sup>th</sup>, 2009, pp. 3-16.
- [9] EPRI Power Electronics Applications Center, “Lamp Flicker Predicted by Gain-Factor Measurements”, Brief n. 36, July 1996
- [10] A. E. Emanuel, L. Peretto, “The response of fluorescent lamp with magnetic ballast to voltage distortion”, *IEEE Trans. on Power Delivery*, vol. 12, n. 1, pp.289-294, January 1997.
- [11] D. Gallo, R. Langella, A. Testa, “Light flicker prediction based on voltage spectral analysis”, *Proc. of 2001 IEEE Porto Power Tech*, Porto (Portugal), September 2001.
- [12] G. Diez, L.I. Eguiluz, M. Manana, J.C Lavandero, A Ortiz, “Instrumentation and methodology for revision of European flicker threshold”, *10th International Conference on Harmonics and Quality of Power*, vol. 1, pp. 262 – 265, 2002

- [13] M. Szlosek, B. Swiqtek, Z. Hanzelka, and A. Bien, "Application of neural networks to voltage fluctuations measurement-a proposal for a new flickermeter", *11th International Conference on Harmonics and Quality of Power, 2004*, Lake Placid, USA, September 2004, pp. 403-407.
- [14] A.E. Emanuel, and L. Peretto, "A simple lamp-eye-brain model for flicker observation," *IEEE Trans. on Power Delivery*, vol. 19, n. 3, pp. 1308-1313, 2004.
- [15] L. Peretto, E. Pivello, R. Tinarelli, and A.E. Emanuel, "Theoretical analysis of the physiologic mechanism of luminous variation in eye-brain system," *IEEE Trans. on Instrumentation and Measurement*, vol. 56, n. 1, pp. 164-170, 2007
- [16] L. Peretto, L. Rovati, G. Salvatori, R. Tinarelli, and A.E. Emanuel, "Investigation on the response of the human eye to light flicker produced by different lamps," *IEEE Trans. on Instrumentation and Measurement*, vol. 56, n. 4, pp. 1384-1390, 2007
- [17] D. Gallo, C. Landi, and N. Pasquino, "Design and Calibration of an Objective Flickermeter," *IEEE Trans. on Instrumentation and Measurement*, Vol. 55, n. 6, pp. 2118-2125, 2006.
- [18] A. Fadda, B. Falsini, "Precision LED-based stimulator for focal electroretinography", *Med. Biol. Eng. Comput.*, 1997, 35, 441-444.
- [19] B. Falsini, C. E. Riva, E. Logean, "Flicker-Evoked Changes in Human Optic Nerve Blood Flow: Relationship with retinal neural activity", *Investigative Ophthalmology & Visual Science*, July 2002, Vol. 43, no. 7.
- [20] M.G.Masi, L.Peretto, R.Tinarelli, L. Rovati, "A Pupil Size Measurement System for the Analysis of the Impact of Flicker on Human Being", *Proc. of the 16th IMEKO TC-4 Symposium*, Florence, Italy, September, 22-24, 2008, pp.419-424.
- [21] M.G.Masi, L.Peretto, R.Tinarelli, L. Rovati, "Measurement of the pupil diameter under flicker light stimula ", *Proc. of the 26th IEEE I2MTC/09*, Singapore, May 2009, pp. 1652-1656.
- [22] Jai, "CM-140 MCL / CB-140 MCL User Manual", Denmark, 2007.
- [23] P.E. Danielsson, "Euclidean Distance Mapping", *Computer Graphics and Image Processing*, Vol. 14, 1980, pp. 227-248.

- [24] JCGM, “Evaluation of measurement data — Supplement 1 to the Guide to the expression of uncertainty in measurement — Propagation of distribution using a Monte Carlo method”, JCGM, Paris, 2008.
- [25] IEC 60825-1, “Safety of laser products – Part 1: Equipment classification and requirements”, *International Electrotechnical Commission*, Geneva, CH, 2007, 2<sup>nd</sup> edition.
- [26] ISO “Guide to the expression of uncertainty in measurement”, *International Standardization Organization*, Geneva (Switzerland), 1995.

## 6. Experimental activities

### 6.1 Introduction

The systems described in the previous chapter, in different measurement campaigns have been used. In the next section, all the tests and relative results will be presented and commented. For each experimental activity, a specific protocol has been used and many people have been chosen to have a significant data collection.

Each selected volunteer gave informed consent to participate in the study and was adequately informed on the protocol details. Moreover all the protocols implemented have been designed in accordance with inputs come from different ophthalmologists.

### 6.2 System “A”: results

#### 6.2.1 First measurement campaign

##### A) Protocol #1

Nine adult subjects with normal vision and different iris colours were selected for the first study. Their ages ranged from 20 to 40 years. All measurements were performed while subjects were lying in a quiet room with dimmed light.

To avoid variation of the pupil size due to the so-called pupillary accommodation reflex (chapter 5), the subject under test might focus on a target located behind the camera. This is the reason for which, at this step of the research, only volunteers without visual defects have been chosen. In fact, for example, a myopic eye changes its pupil size when trying to focus on the target, thus clearly inducing artefacts in the pupil diameter computation.

There are many parameters that can affect the response of the complex human eye system to light and the wavelength of the incident radiation is one of the most important. Therefore, to simplify the study, only the green colour light of the RGB LED has been used in the following experiments. As shown in the section 5.6.2, it features a dominant wavelength of 540 nm.

Measurements of the pupil diameter were performed, as said before, according to a specific protocol#1 that can be divided into four epochs:

- 1) rest condition;

- 2) eye is subjected to an impulse stimulus;
- 3) eye under flicker stimulus;
- 4) rest condition;

Thus way, a possible effect due to the tiredness caused by the stimuli can be highlighted.

Figure 6.1 schematically shows the time sequence of the measurement protocol.

During the rest epoch, first the eye of the subject under test was taken for 5 minutes under dark condition where only the IR LEDs, with specific characteristics (power density  $10 \text{ mW/m}^2$ , in accordance with the IEC 60825 [1]), were on allowing the camera works. Then, an acquisition of 60 s was performed followed by a rest time of 10 minutes; this procedure is aimed at estimating the initial pupil diameter before the visual annoyance.

After an adaptation of 10 minutes in dark condition, the eye response to a light impulse was recorded. This stimulus has been generated by a voltage pulse having 800-mV max value and duration 0.5 s. Further 10 minutes of rest time forewent the application of flicker. To this purpose the V-I amplifier was fed by a 1-Hz sinusoidal voltage having 800-mV amplitude and 400-mV offset. This way a flickering light ( $1 \text{ mW/m}^2$  power density) was obtained.

Before performing the 60s-acquisition, 5 minutes of adaptation time was waited. Once the camera work has been completed, the same flicker stimulus was applied for 15 minutes. Then a further record of 60 s was taken. Finally, dark condition was set for 15 minutes and a last 60-s acquisition was performed. This epoch is aimed at measuring the pupil diameter after a quite long period of light stimulus condition.

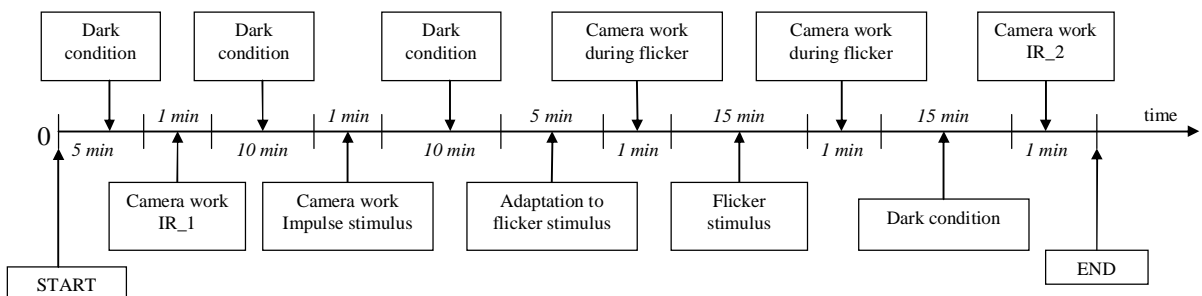
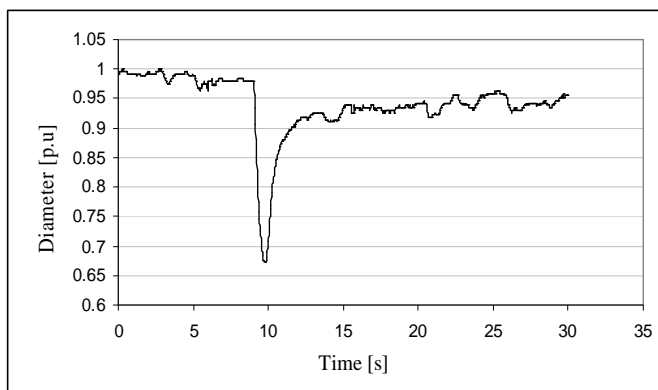
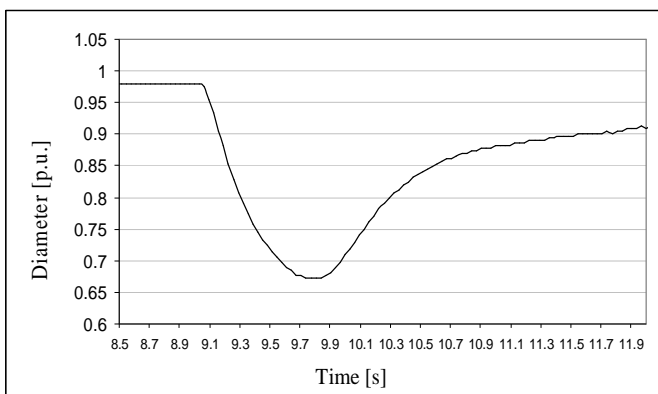


Figure 6.1 Time sequence of the protocol#1.

The eye response to the impulse stimulus, for a 25 y.o. male with brown iris, is reported in figure 6.2 where the diameter is normalized to its maximum value.



**Figure 6.2** Eye response to impulse stimulus.



**Figure 6.3** Particular of the eye response to impulse stimulus.

To better highlight both the falling and the rising front of the response, its shape in the time interval between 8.5 s and 12 s is shown in figure 6.3. By analysing such figure, it can be drawn that the diameter takes the minimum value after 0.7 s from the beginning of the event; then the 90% of the pre-impulse diameter is reached after further 1.7 s. The obtained shape is in good agreement with the one shown in the literature (e.g. [2]), even if the amplitude of the light pulse is different.

Similar results were obtained for all volunteers.

Moreover, the duration of the falling front suggests that the pupillary light reflex mechanism is not able to follow luminous flux variation with frequencies greater than about 4 Hz. As for the test under flicker condition, the chart in figure 6.4 shows the eye

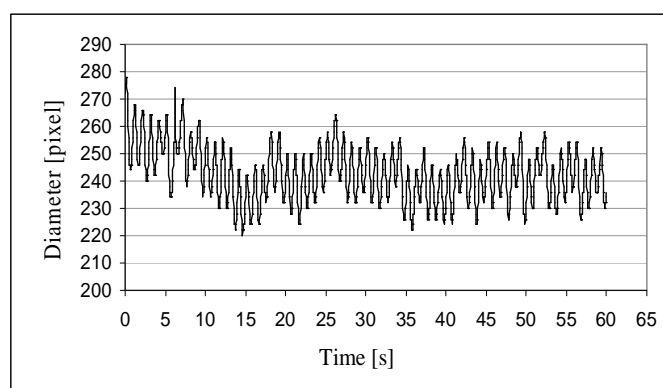


**Figure 6.4** Eye pulse response to 1-Hz flicker stimulus.

response to 1-Hz frequency whereas a 5-s zoom (from 20 s to 25 s) is reported in figure 6.5. This highlights that, according to the previous consideration the eye is able to follow the light variation a 1-Hz light variation.

Figure 6.6 is the magnitude

spectrum of the signal in figure 6.4.

It is well evident the presence of 1-Hz component (about 10 pixel) and a DC term (representing the mean pupil diameter related to the environmental illumination).

To investigate on the possibility to get useful information on the state of the tiredness of an eye subjected to flicker by measuring the pupil diameter, let us consider the result in Table 6.1. It shows, for all the volunteers, the diameter's mean values at the beginning (B) and in the end (A) of the flicker stimulus application. Moreover the ratio B/A is also reported: it is always lower than one, varying from 0.893 and 0.976 if subject #9 is discarded.

This means that the 15-minutes application of flicker has been caused a decrease of diameter mean value. Such consideration is confirmed by figure 6.7 where the pupil size trend vs time, before (thin line) and after (bold line) the application of the light stimuli as described before is shown for person #5. The mean values at the beginning and in the end of the measurement protocol are 441 and 322 pixels, respectively. It represents the trend vs time of the mean values of the ratio between the diameters computed for all subject after and before the application of the light stimuli (pulse light and flicker).

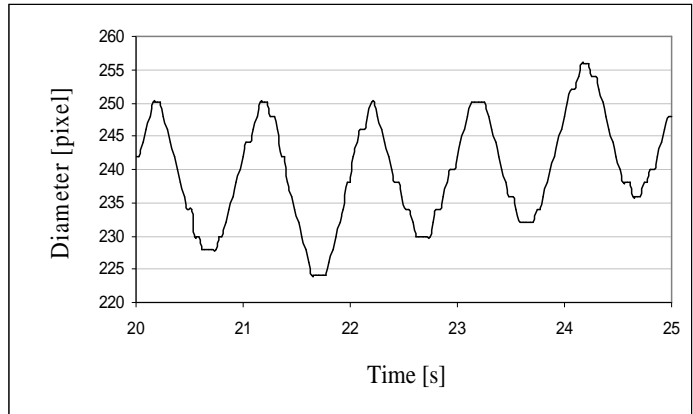


Figure 6.5 Particular of eye pulse response to 1-Hz flicker stimulus.

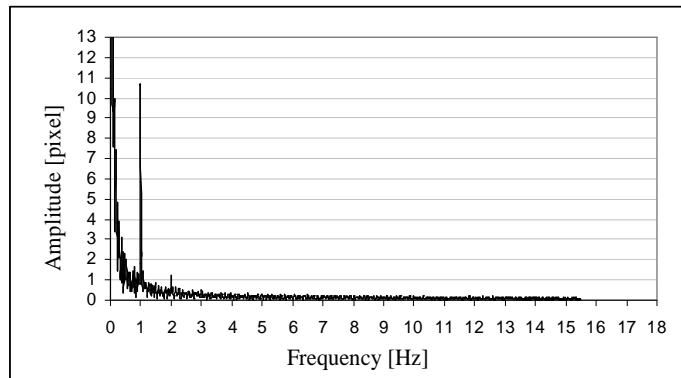


Figure 6.6 Magnitude spectrum of the signal in Figure 6.4.

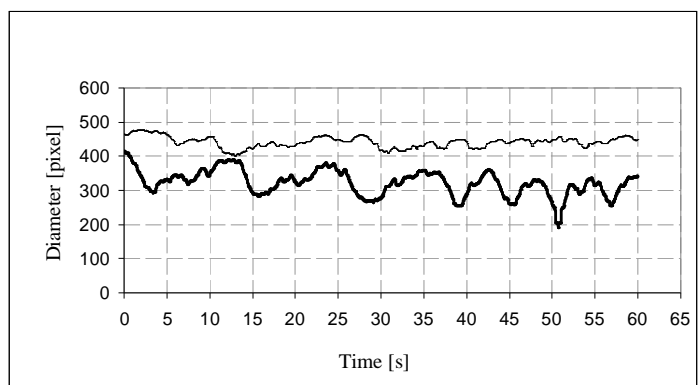
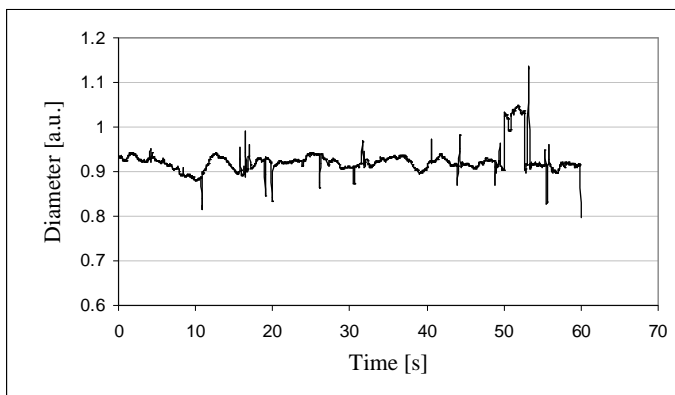


Figure 6.7 Pupil size trend vs. time, before (IR\_1) and after (IR\_2) the application of the light stimuli.

**TABLE 6.1** DIAMETER'S MEAN VALUES AT THE BEGINNING (B) AND IN THE END (A) OF THE FLICKER STIMULUS APPLICATION

Volunteer	Diameter [pixel]		Diameter ratio
	B	A	A/B
1	475	433	0.912
2	355	317	0.893
3	327	311	0.951
4	557	540	0.969
5	245	239	0.976
6	395	363	0.919
7	454	410	0.903
8	350	320	0.914
9	357	356	0.997

**Figure 6.8** Trend vs time of the ratio between the pupil diameter measured after and before the application of light stimuli.

learned that, on the average, the pupil stay contracted: in fact the normalized diameter “d” results to be less than one, almost in the whole period. It is reasonable to suppose that the iris muscles, after a prolonged annoyance caused by several minutes of exposition to light stimuli, stay contracted, thus resulting in a smaller pupil size than the initial one. This phenomena has occurred in all tested subjects as proved by the plot in figure 6.8.

These achievements can be considered to be meritorious of further investigations. Indeed establishing a relationship between pupil-size mean value and the stress condition of a human being due to light flicker could represent a first-attempt-response to the important target pointed to investigate on a methodology which allows gathering objective information regarding the annoyance condition of a human being due to light flicker [3].

This first measurement campaign, on human subjects, has represented the beginning of a research activity aimed at finding a different approach to determine the annoyance due to flicker. It was clear that those results cannot be used to provide a reliable model

In other words, each value  $d_k$  of figure 6.8 is evaluated as follow:

$$d_k = \frac{1}{N} \sum_{i=1}^N \frac{D_{A,i}}{D_{B,i}} \quad (6.1),$$

Where  $N(=9)$  is the number of tested subjects,  $D_{A,i}$  is the diameter of the  $i$ -th volunteer in the end of the measurement protocol while  $D_{B,i}$  is the diameter of the  $i$ -th subject at the beginning of the test.

Of course is  $1 \leq k \leq 1860$  given that  $31 \times 60 = 1860$  frames have been acquired over 60 s at 31 fps.

From figure 6.7 it can be

of the human eye response to flicker by means of an objective parameter. However they put in evidence that the mean value of the pupil diameter can contain information useful for the purposes given that its decreasing seems to be related to an increase of the eye tiredness.

### **6.2.2 Second measurement campaign**

After the first measurement campaign, it was verified that the pupil follows the 1-Hz flickering light (figure 6.5). Moreover it was found that the pupil diameter measured before applying the light stimulus is greater than the one evaluated at the end of the experiment (figure 6.7). In fact, the estimated mean values of diameters are: equal to 441 pixels at the beginning of the measurement protocol and 322 pixels at the end. So it was reasonable to suppose that the iris muscles, after a prolonged annoyance caused by several minutes of exposition to light stimuli, stay contracted, thus resulting in a smaller pupil size than the initial one.

Thanks to these conclusions, the next step has been to find the eventual relationship between the pupil size and the frequency. A second measurement campaign started. Three different protocols have been adopted aimed at verifying if there is a relationship between flicker frequency and decrease of the pupil diameter. The following arrangements hold for all of them:

- six volunteers tested and asked to sit in front of the camera;
- flicker generated by supplying the LED with sinusoidal input voltage having 800 mV peak value and 400-mV offset;
- green light used as in the preliminary investigation.

#### **B) Protocol #2**

This sequence of flicker frequency was used: 1Hz-5Hz-10Hz-15Hz-20Hz-15Hz-10Hz-5Hz-1Hz. Each of them was applied for 10 minutes, to allow the eye adaptation to the light, plus one of camera work (data acquisition).

The above frequencies sequence was chosen to highlight the effects of a long exposition to flicker. Of course the frequencies ranged in the well known interval where the human eye is sensitive to flicker. Figure 6.9 schematically represents the protocol#2.

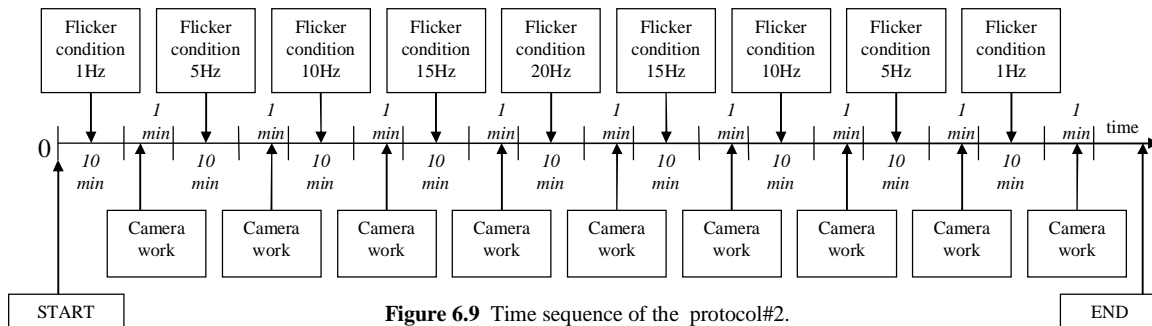


Figure 6.9 Time sequence of the protocol#2.

### C) Protocol #3

The third protocol is schematically presented in figure 6.10 and differs from the first one only for the frequencies sequence order: 20Hz-15Hz-10Hz-5Hz-1Hz-5Hz-10Hz-15Hz-20Hz.

This helps in understanding if the effects to flicker frequency are correlated to the time of exposition.

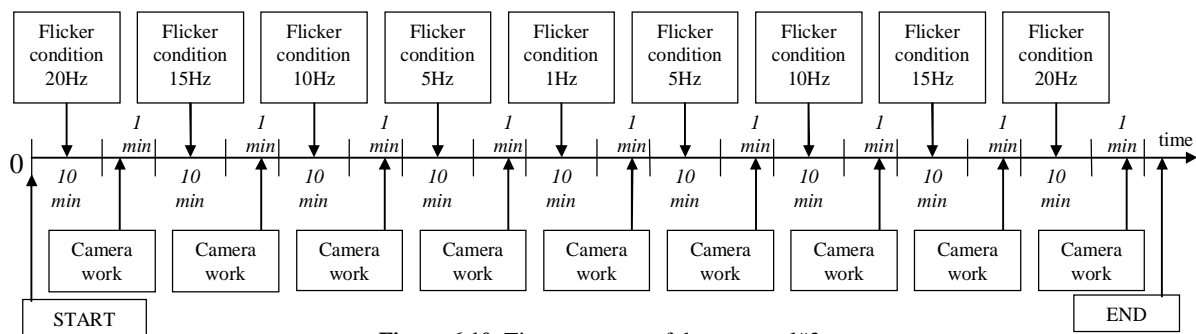


Figure 6.10 Time sequence of the protocol#3.

### D) Protocol #4

This procedure, schematically shown in figure 6.11, mainly differs from the protocols previously described because:

- there is a 10 minutes of rest time between two consecutive test. This way each result should not be affected by the possible tiredness caused by the previous experiment.
- a preliminary diameter measurement is performed with no light flickering conditions to get a value used as reference for the pupil size evaluated under flicker conditions. This allows to compare measurements that can be carried out in slightly different relative position between the eye and the camera. As a matter of fact it should be kept in mind that during the rest time people move from the chin rest.

The flicker frequencies were: 3Hz - 8Hz - 11Hz - 13Hz - 18Hz.

The reference diameter is measured by processing 10 s of camera work taken after a 1-min adaptation time where the eye was subjected to a fixed light having a luminous flux equal to the mean value of the one irradiated during flicker time.

Then the flicker was applied for 6 minutes including a final 60 s of camera work.

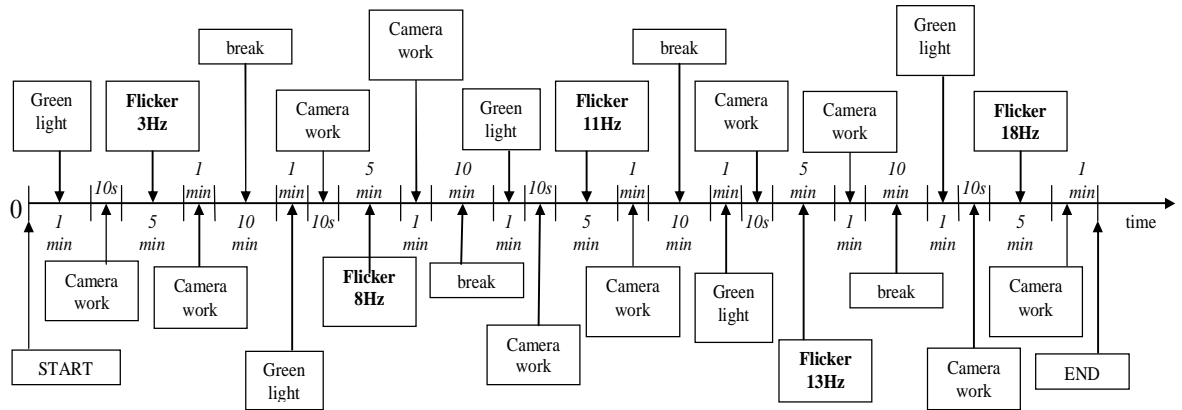


Figure 6.11 Time sequence of the protocol#4.

In all previously described protocols the flicker frequencies ranged between 1 and 20 Hz.

It is well known that the pupil size is able to follow light variation up to about 4 Hz. Therefore, even if the camera works at 31 fps, no aliasing occurs. To confirm the above statements let us compare figure 6.6 and figure 6.12. As described in section 6.2.1, figure 6.6 shows that when a 1-Hz flicker is applied the signal representing the pupil diameter vs time has

1Hz component.

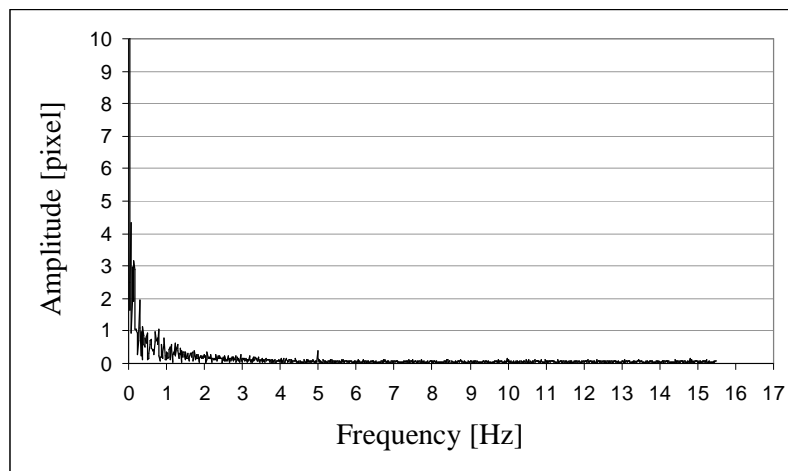


Figure 6.12 Magnitude spectrum of the signal of the diameter vs time signal in the case of a 5-Hz flicker.

Figure 6.12 reports the magnitude spectrum of the diameter vs time signal in the case of a 5-Hz flicker. Contrary to figure 6.6 a spectral component located at the flicker frequency does not appear. In all the used protocols the

diameter mean value computed, at each frequency, over the 60 s of acquisition is taken as parameter representing the flicker effect.

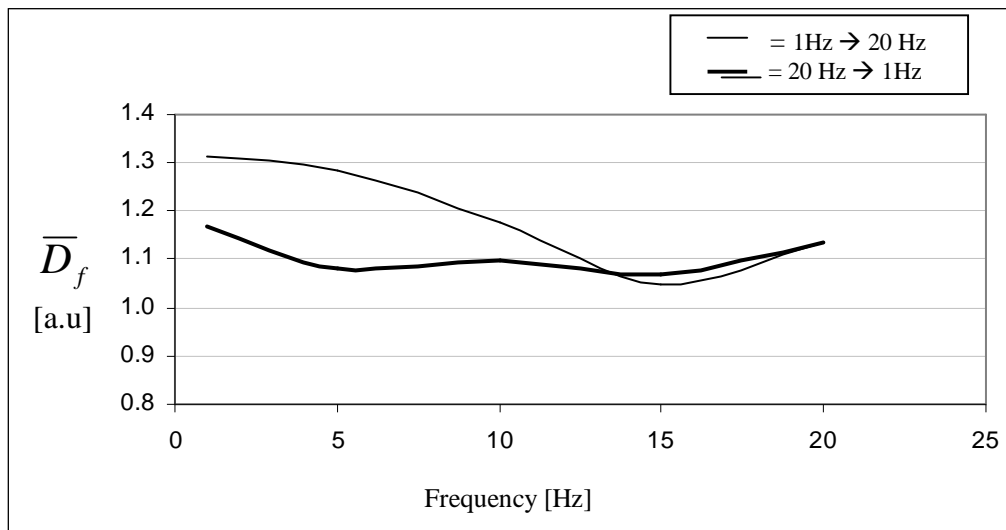


Figure 6.13 Summarizing chart of the protocol #2.

As far as protocols #2 and #3 are concerned, they differ for the order of flicker frequency sequences only.

Figure 6.13 and figure 6.14 are the summarizing chart of the protocol #2 and #3, respectively. They have been plotted by considering all the results obtained: for each frequency  $f$ , the average  $\bar{D}_f$  of the six normalized mean  $\bar{d}_k$  ( $k = 1, \dots, 6$ ) pupil diameter has been calculated. Each  $\bar{d}_k$  is a value normalized to the minimum value computed for the  $k$ -th person by considering all the frequencies sequence. In figure 6.13 and figure 6.14, the thin and the bold line refer to the results of tests carried out with frequencies varying from 1Hz to 20Hz and 20Hz to 1Hz respectively. The shape of the curves in figure 6.13 and 6.14 is similar. In both cases, the minimum value is about 15 Hz; in addition, when the frequency goes from 20Hz to 1Hz, the diameter mean values are smaller than those calculated for frequencies ranging from 1Hz to 20Hz, if figure 6.13 is considered. On the contrary as for figure 6.14, the opposite occurs. According to protocols #2 and #3, this means that a decrease of the pupil size occurs after a long exposition to flicker. This outcome is in a good agreement with the one obtained in the preliminary test.

So, also in these circumstances, iris muscles stay contracted and the mean value of the diameter results lower. Moreover, it must be noted that the diameter also depends on the frequency and hence two superposed effects are present: annoyance, due to the different flicker response with frequency, and tiredness caused by an extended exposition to luminous stimuli.

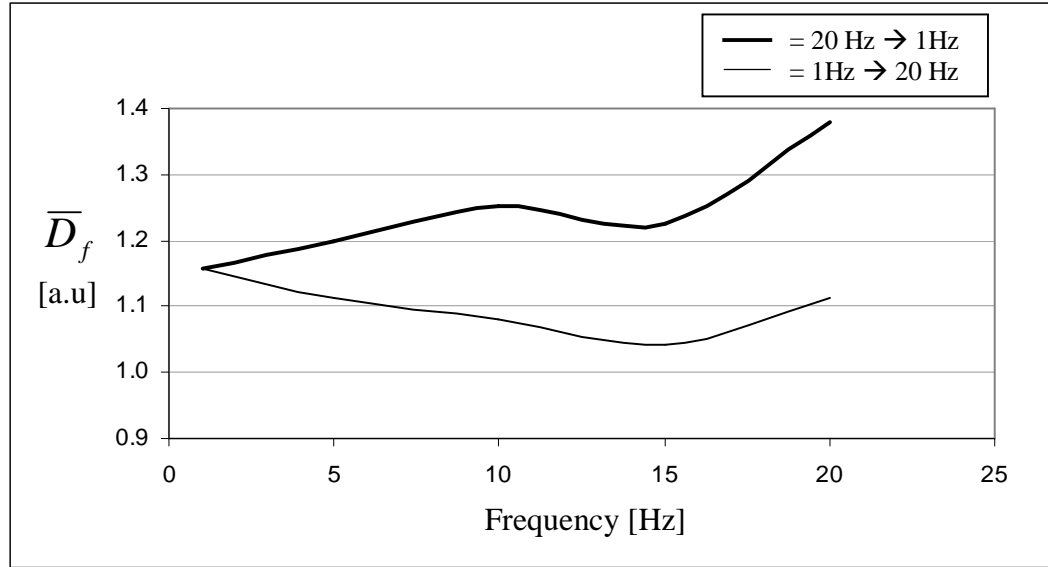


Figure 6.14 Summarizing chart of the protocol #3.

Given that our purpose is to evaluate the behaviour of the eye under flicker condition, protocol #4 is aimed at considering the annoyance only. This is the reason for which 10 minutes of rest time are scheduled between tests at different frequencies. This way tiredness caused by prolonged exposition to light can be considered negligible.

In figure 6.15 the eye response, in term of mean diameter, to a sequence of five different flickering lights is reported. Each value  $\bar{\Phi}_f$  ( $f = 3\text{Hz}, 8\text{Hz}, 11\text{Hz}, 13\text{Hz}, 18\text{Hz}$ ) has been calculated as follows:

$$\bar{\Phi}_f = \frac{1}{N} \sum_{k=1}^N \frac{d_{k,f}}{dref_{k,f}}, \quad (6.2)$$

where  $N = 6$  is the number of volunteers;  $\bar{d}_{k,f}$  the mean diameter computed for the  $k$ -th person over the last 60 s of 6-min exposition to flicker with frequency  $f$ ;  $dref_{k,f}$  is the mean value of the diameter computed for the  $k$ -th person over the last 10 s of 70-s exposition to a fixed light just before the flicker test at frequency  $f$ .

To verify that this response depends on the frequency only and not on the order of the test are performed, measurement were carried out by randomly arranging the frequencies.

Figure 6.16 compares results of the above described test (bold line) with the once obtained for the same person (thin line) subjected to the protocol #4.

It can be concluded that the variation of the mean diameter due to different flickering light depends on the frequencies only.

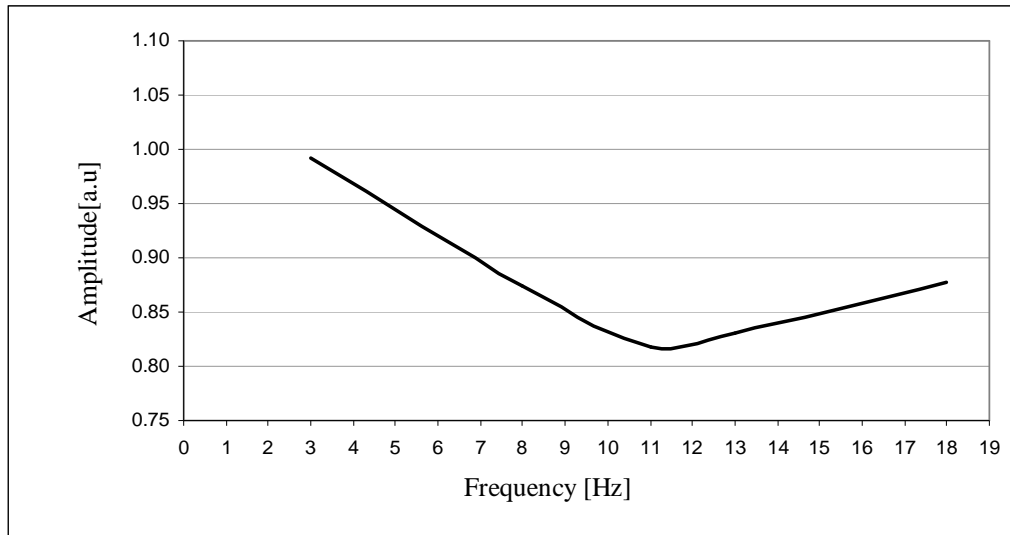


Figure 6.15 Summarizing chart of the protocol #4.

Table 6.2 shows the  $\bar{\Phi}_f$  values along with the relevant standard deviations  $\sigma(\bar{\Phi}_f)$  that ranges from about 2% to 10% of  $\bar{\Phi}_f$ . In [4] it has been demonstrated that measurements performed by the proposed system are affected by a standard uncertainty lower than 4 pixels that, in this case, turns into about 1.5% of  $\bar{\Phi}_f$ . Therefore the expanded uncertainty  $U(\bar{\Phi}_f)$  on  $\bar{\Phi}_f$  goes from 3% to 10% depending on the values of  $\bar{\Phi}_f$ , as shown in Table 6.2.

On the basis of these considerations, the plot in figure 6.15 can be taken as a trustworthy representation of the annoyance caused by a green light flicker, even if it is clear that more and more tests need to be performed in order to develop an exhaustive model. Essentially, it can be stated that the greater annoyance occurs at 11Hz and at 3Hz it is lower than the one at 18Hz.

This outcome is in good agreement with the model endorsed by [5] even if it refers to a light (incandescent-filament lamp) featuring a different spectrum.

TABLE 6.2 DIAMETER'S MEAN VALUES AND STANDARD DEVIATION S

Frequency [Hz]	Mean Value $\bar{\Phi}_f$	Standard Deviation $\sigma(\bar{\Phi}_f)$
3	1.0	0.11
8	0.87	0.09
11	0.82	0.04
13	0.83	0.05
18	0.88	0.02

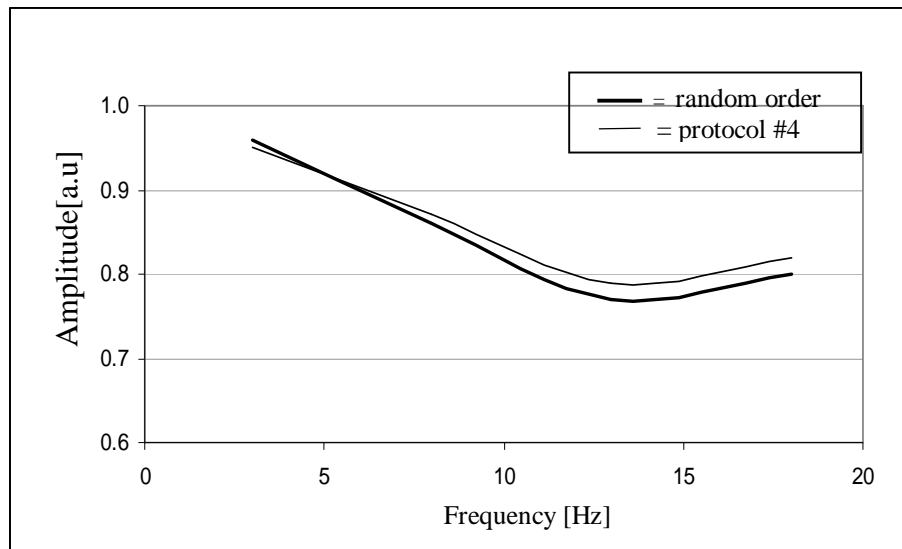


**Figure 6.16** Comparison between results of protocol #3 (thin line) with the once obtained using the same frequency but in a random order (bold line).

This second measurement campaign has presented the most recent developments of the research activity aimed at finding a different approach to determine the annoyance due to flicker. In this respect, it has been shown the procedure and the results obtained by subjecting some people to three different kinds of test.

Obviously, given the limited number of considered people, these results cannot be intended as useful to provide a full and reliable model of the human eye response to flicker by means of an objective parameter (the pupil diameter mean value). However, they have allowed to gather some very interesting information about the behavior of the pupil diameter in presence of flicker produced by a green light.

First of all, protocol #2 and #3 have put in evidence that the mean value of the pupil diameter can contain information useful for our purposes given that its decreasing seems to be related to an increase of both the eye tiredness and annoyance.

Protocol #4 has been developed to avoid the tiredness of the subject eye due to a prolonged exposition to light flicker and the results have shown that an evident relationship between the mean value of the pupil diameter and the flicker frequency holds [3]. In particular, the pupil diameter takes the minimum value at a frequency consistent with what is reported in previous literature about flicker annoyance.

## 6.3 System “B”: results

### 6.3.1 Third measurement campaign

#### E) Protocol #5

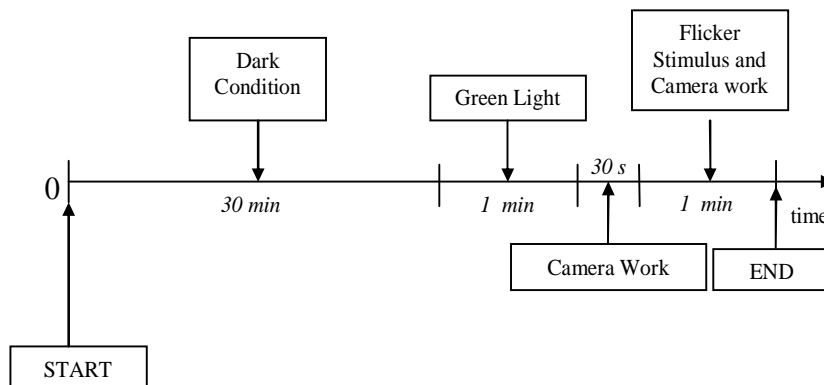


Figure 6.17 Time sequence of the protocol#5.

As highlighted in section 5.4, some structural details of the first measurement setup have been improved. The good results obtained during the system characterization (section 5.7) allowed to start the third measurement campaign on human subjects. The purpose has been to evaluate a more reliable behaviour of the eye under flicker conditions. Four adults subjects with different iris colours were selected for the third measurement campaign and a new protocol, schematically shown in figure 6.17, has been used.

The test starts with a 30 min-dark condition, in fact, as described in Chapter 3 (section 3.2.9) the eye may become about 10.000 times more sensitive to light.

The reference diameter is measured by processing 30 s of camera work, after 1 min-adaptation time where the eye was subjected to green fixed light having a luminous flux equal to the mean value of the one irradiated during flicker time. In this way, all the measurements can be compared. After, the flicker has been applied and, at the same time, a final 60 s of camera work was taken. This procedure, for each volunteer, has been used six times, in different days, with six frequencies; 1Hz, 5 Hz, 10 Hz, 15 Hz, 20 Hz, 25 Hz.

In this way, for each volunteer, six references  $R_{k,f}$  and pupil sizes,  $M_{k,f}$ , under flicker condition, with the relevant standard deviations, have been obtained. The relevant normalized mean value have been computed as follow:

$$V_{k,f} = \frac{M_{k,f}}{R_{k,f}} \tag{6.3}$$

$M_{k,f}$  is the mean diameter computed for the k-th person during the 60-s exposition to flicker with frequency  $f$  ( $f = 1\text{Hz}, 5\text{Hz}, 10\text{Hz}, 15\text{Hz}, 20\text{Hz}, 25\text{Hz}$ );  $R_{k,f}$  is the mean value of the diameter computed for the k-th person over the last 30 s of 90 s exposition to a fixed light just before the flicker test at frequency  $f$ . Tables 6.3-6.6 show all the obtained values.

TABLE 6.3  $R_{k,f}, M_{k,f}, V_{k,f}$  of volunteer#1

Frequency [Hz]	Reference [Pixel]		Diameter [Pixel]		$V_{k,f}$ [a.u]
	$R_{k,f}$	Std. Dev	$M_{k,f}$	Std. Dev	
1	100	4.93	110	10.9	1.10
5	101	3.63	95.9	4.50	0.95
10	86.4	3.61	85.4	3.97	0.99
15	90.3	4.44	90.8	3.80	1.01
20	92.5	3.23	97.4	3.61	1.05
25	95.1	3.48	98.1	6.72	1.03

TABLE 6.4  $R_{k,f}, M_{k,f}, V_{k,f}$  of volunteer#2

Frequency [Hz]	Reference [Pixel]		Diameter [Pixel]		$V_{k,f}$ [a.u]
	$R_{k,f}$	Std. Dev	$M_{k,f}$	Std. Dev	
1	107	11	109	10	1.01
5	113	8.5	109	7.4	0.96
10	114	10	110	9.7	0.96
15	131	9.5	137	12	1.04
20	125	13	128	11	1.03
25	123	12	144	15.6	1.17

TABLE 6.5  $R_{k,f}$ ,  $M_{k,f}$ ,  $V_{k,f}$  of volunteer#3

Frequency [Hz]	Reference [Pixel]		Diameter [Pixel]		$V_{k,f}$ [a.u.]
	$R_{k,f}$	Std. Dev	$M_{k,f}$	Std. Dev	
1	166	13	150	12	0.90
5	184	15	144	9.8	0.78
10	166	12	134	20	0.81
15	152	12	152	12	1.00
20	158	13	188	16	1.2
25	168	10	171	15	1.02

TABLE 6.6  $R_{k,f}$ ,  $M_{k,f}$ ,  $V_{k,f}$  of volunteer#4

Frequency [Hz]	Reference [Pixel]		Diameter [Pixel]		$V_{k,f}$ [a.u.]
	$R_{k,f}$	Std. Dev	$M_{k,f}$	Std. Dev	
1	190	6.7	134	10	0.71
5	214	12	137	7.0	0.64
10	179	7.9	164	6.6	0.92
15	193	4.3	198	7.9	1.03
20	172	7.1	204	9.9	1.2
25	179	9.9	207	17	1.2

The eye response, in term of mean diameter, to the selected sequence of six different flickering lights is reported in figure 6.18. Each value  $Q_{k,f}$  has been calculated as follows:

$$Q_{k,f} = \frac{1}{N} \sum_{k=1}^N V_{k,f}, \quad (6.4)$$

where  $N=4$ . Table 6.7 shows the  $Q_k$  values along with the relevant standard deviations  $\sigma(Q_k)$  that ranges from about 1% to 17% of  $Q_k$ .

An important observation can be highlight. In this case, the minimum mean diameter has been obtained for frequency equal to 5 Hz, while with the protocol#4, is correspondingly 11 Hz.

The different eye response to flicker could be explained considering that the light source weren't the same. In fact, in the first measurement system a punctiform source (one

TABLE 6.7 DIAMETER'S MEAN VALUES AND STANDARD DEVIATION S

Frequency [Hz]	$Q_{k,f}$ [a.u]	$\sigma (Q_{k,f})$
1	0.93	0.17
5	0.83	0.15
10	0.92	0.08
15	1.02	0.01
20	1.11	0.09
25	1.09	0.08

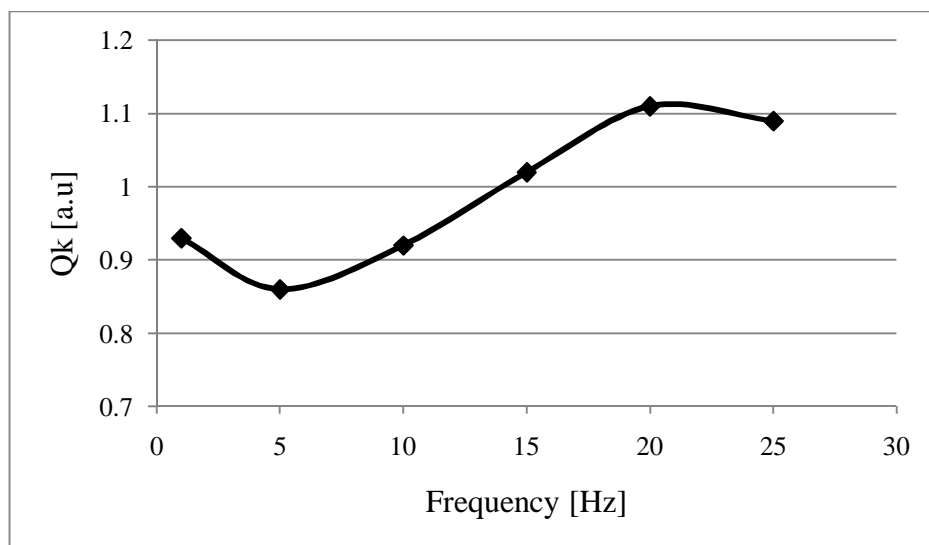


Figure 6.18 Summarizing chart of the protocol #5.

RGB LED) has been used (as shown in chapter 5, figure 5.10) and it was positioned towards the eye under test. For the second system, six green LEDs have been positioned on a ring, equidistant from each other, to light the target (and not directly the human eye) thus allowing to obtain a uniform flickering surface. It's easy to suppose that in this two cases, the eyes have been stimulated in a different manner, so, it's not wrong to expect a different eye response to flicker, highlighted, in this case, by a diverse minimum mean pupil size.

### 6.3.2 Fourth measurement campaign

#### F) Protocol #6

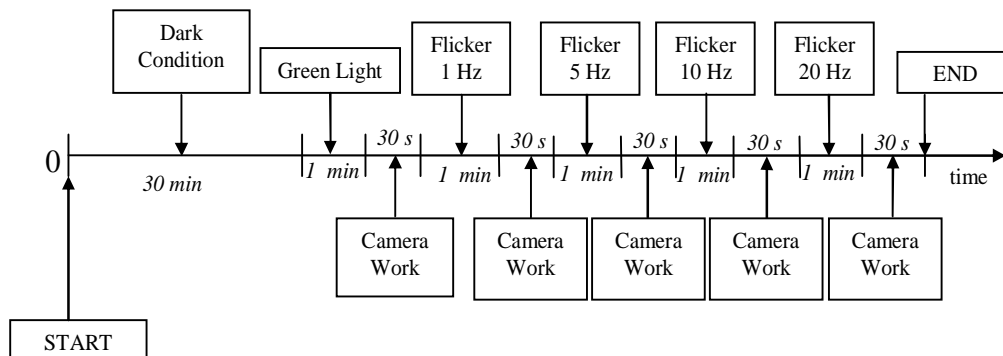


Figure 6.19 Time sequence of the protocol#6.

For the fourth measurement campaign, eight adult subjects with different iris colours and no significant sight defects have been selected.

The new protocol is slightly different from the last one, because a smaller light intensity has been used and a shorter camera work under flicker condition have been executed. So, the time of exposition to flicker is the same of the previous protocol (for 1 minute) but just the last 30-s have been stored, as presented in the figure 6.19.

That is a significant variation of this procedure, in fact it's important to highlight that the initial 30-s during flickering light haven't stored and then the transitory of the eye adaptation to flicker have not taken in account. In this way, the possibility to consider a wrong answer of the eye is avoided.

Aim of this measurement campaign was to evaluate the eye response to a diverse stimulus in terms of light intensity. For this reason, another set of six green LEDs has been chosen. Also in this case, as described in section 5.7.3, the power emitted by the new source has been measured by a calibrated dc power meter (Lasercheck Handheld) placed instead of the human eye (~17 cm away from the source). The measured power  $P$  (dominant wavelength 570 nm) and the relevant power density  $p$  evaluated by assuming the diameter of 6 mm are reported in Table 6.8. The uncertainty  $u(P)$  and  $u(p)$  are also shown.

In this measurement campaign, all the stimuli have been used during the same test, not in different days as in the previous protocol. In this way a minus number of frequencies has been necessary to not annoy excessively the eye and compromise the

**TABLE 6.8** POWER  $P$  AND RELEVANT COMPUTED POWER DENSITY  $p$  ALONG WITH THE ASSOCIATED STANDARD UNCERTAINTY

Wavelength [nm]	$P$ ( $\mu\text{W}$ )	$u(P)$ ( $\mu\text{W}$ )	$p$ ( $\text{W}/\text{cm}^2$ )	$u(p)$ ( $\text{W}/\text{cm}^2$ )
570	175	8.8	$0.62 \cdot 10^{-3}$	$3.1 \cdot 10^{-5}$

results. The reference diameter has been measured by processing 30 s of camera work, after 30 min of dark condition and 1 min-adaptation time where the eyes have been subjected to the green fixed light. After, the flickering lights have been applied for 60 s and the last 30s were acquired with the camera. As shown in figure 6.19, the selected frequencies are: 1Hz, 5 Hz, 10 Hz, 20 Hz. This procedure, for each volunteer, four times, in different days, has been repeated.

The eye response of this procedure in term of mean diameters is shown in figure 6.20 .

Each value  $Q_{k,f}$  has been calculated as follows:

$$Q_{k,f} = \frac{1}{n} \sum_{k=1}^N \overline{V}_{k,f}, \tag{6.5}$$

where  $n=8$  is the numbers of volunteers and

$$\overline{V}_{k,f} = \frac{1}{N} \sum_{k=1}^N \frac{M_{k,f}}{R_k} \tag{6.6}$$

is the expression to evaluate the normalized mean of the mean pupil sizes;  $N=4$  is the number of tests per person,  $M_{k,f}$  is the  $k$ -th mean pupil size evaluated under a specific flickering light during the  $k$ -th test, while  $R_k$  is the reference of the  $k$ -th test. Tables 6.9 and 6.10 summarize the computed results. The standard deviations  $\sigma(Q_k)$  ranges from 5% to 6% of  $Q_k$ . Figure 6.20 shows the final eye response of the protocol #6.

Also in this case, the minimum value has been evaluated next to a different frequency (1 Hz) by comparison to protocol#4 (11 Hz) and protocol#5 (5 Hz).

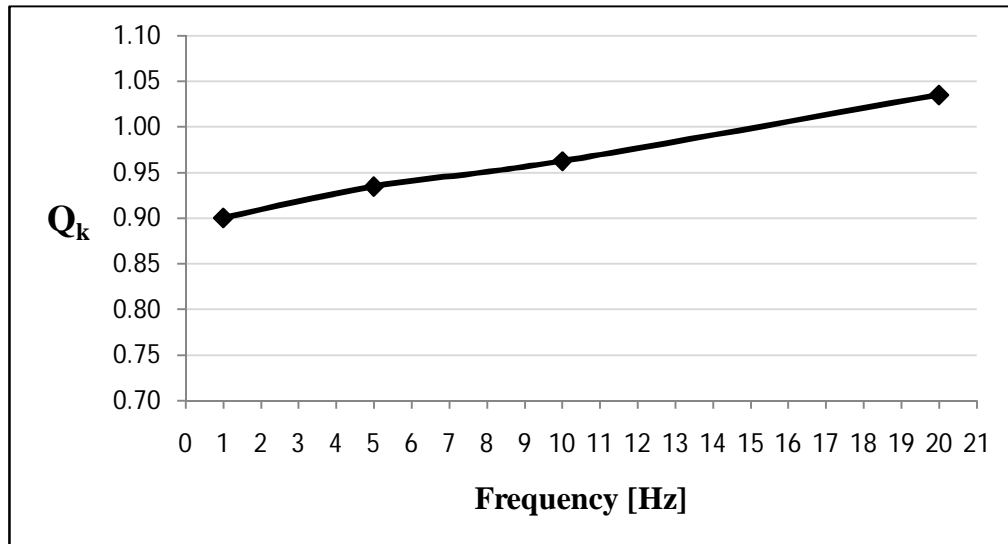


Figure 6.20 Summarizing chart of the protocol #6.

TABLE 6.9 DIAMETER'S MEAN VALUES AND STANDARD DEVIATION S

Frequency $f$ [Hz]	$\bar{V}_{1,f}$	$\bar{V}_{2,f}$	$\bar{V}_{2,f}$	$\bar{V}_{4,f}$	$\bar{V}_{5,f}$	$\bar{V}_{6,f}$	$\bar{V}_{7,f}$	$\bar{V}_{8,f}$
1	0.89	0.93	0.92	0.98	0.83	0.88	0.95	0.83
5	0.88	0.91	0.98	0.97	0.89	0.90	1.00	0.96
10	0.89	0.97	1.00	1.01	0.99	0.86	1.01	0.98
20	1.02	0.95	1.04	1.09	1.11	0.99	1.01	1.09

TABLE 6.10 DIAMETER'S MEAN VALUES AND STANDARD DEVIATION S

Frequency [Hz]	$Q_{k,f}$ [a.u]	$\sigma(Q_{k,f})$
1	0.90	0.055
5	0.93	0.047
10	0.96	0.058
20	1.04	0.056

A possible explanation of the reason the minimum value has moved towards lower frequencies is the different light power. In this last case it was the smallest one with respect to that of other measurements. In this particular case both cones and rods are working together for transmitting information to the brain. In the former cases, being the light power well higher than in this last case, only the cone could have provided the information to the brain. These measurement campaigns have been conducted to verify if a physiological phenomenon, that is the pupil diameter, is a valid index to get an objective and more reliable evaluation of the human annoyance caused by flicker.

The results demonstrate that there is an evident relationship between this geometrical parameter and the flicker frequency. In addition, the mean value of the pupil diameter

can contain useful information for our purposes. In fact, it seems that a decrease of the diameters is related to an increase of the human tiredness, a conclusion in good agreement with the model endorsed by the standard even if it refers to an incandescent filament lamp.

Even if the presented outcomes are very encouraging, it's clear that some issues must be tackled before a novel instrument for flicker measurement can be built up.

Essentially, it must investigate on the pupil response to different colours (red and blue) and on how these responses have to combine to get the annoyance caused by commercial lamps that features a spectrum containing several wavelengths.

In addition, if we consider the gain factor of a lamp, expressed as follow:

$$K(f) = \frac{\frac{\Delta\Phi}{\Phi}(f)}{\frac{\Delta V}{V}(f)} \tag{6.7}$$

where  $\Delta\Phi/\Phi$  is the relative variation of the luminous flux and  $\Delta V/V$  is the relative variation of the voltage rms that supplies the lamp.

All the parameters are known and we can obtain  $\Delta\Phi$  thanks to (6.7):

$$\Delta\phi = \phi * K * \frac{\Delta V}{V} \tag{6.8}$$

Once the different stimuli, for each frequency and fundamental colour, have been applied on human volunteers and the response in terms of pupil diameter are known, the model for a new flickermeter could be implemented.

An achievable new Flickermeter can be therefore designed by implementing three simple main blocks, as shown in figure 6. 21. Once the voltage  $u(t)$  is properly conditioned and digitized, it is processed to get, by means of a proper lamp model, a

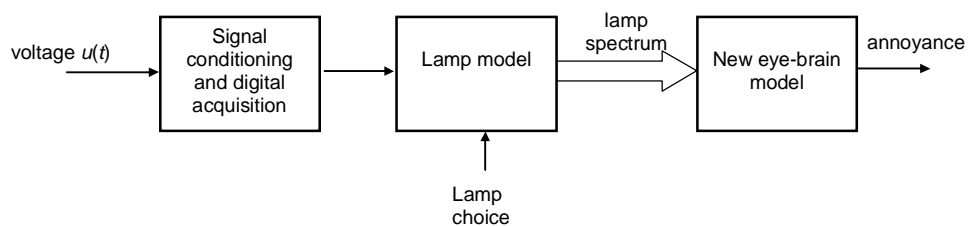


**Figure 6.21** Schematic block of a possible new Flickermeter.

signal representing the spectrum of the light radiation. The objective eye-brain model elaborates it to provide an index representing the annoyance of the human eye. As for the lamp, the operator can choose between the different ones whose well-known models are implemented in the instrument, thus allowing the device to be used in all practical situations.

---

## References

- [1] IEC 60825-1, “Safety of laser products – Part 1: Equipment classification and requirements”, *International Electrotechnical Commission*, Geneva, CH, 2007, 2<sup>nd</sup> edition.
- [2] J. L. Barbur., N. B. Prescott., R. H. Douglas, J. R. Jarvis., C. M. Wathes, “A Comparative Study of Stimulus-Specific Pupil Responses in the Domestic Fowl (*Gallus gallus domesticus*) and the human”, *Vision Research*, 2002.
- [3] Patent pending n. BO2009A000128, “A method and an apparatus for evaluating the psychophysical condition of human beings and/or animals by measuring geometrical characteristics of the pupil” (in Italian).
- [4] M.G. Masi, L. Peretto, R. Tinarelli, L. Rovati, “Study of flicker on the pupil diameter: design and characterization of the measurement system”, companion paper, submitted to *IEEE Transactions on Instrumentation and Measurement*
- [5] EN 61000-4-15 “Testing and measurement techniques: flickermeter – functional and design specification,” Geneva, CH, 1997.

## 7. Medical Studies

### 7.1 Introduction

The model presented in Chapter 5, first proposed in [1] and then improved [2,3] to take into account the different lamp spectra, can reasonably be considered as a correct representation of the human-eye response to light flicker. However, it must be kept in mind that the above model is a simplified representation of a high complex phenomenon that occurs when the modulated light strikes the human eye. Fundamentally, it provides a mathematical description of the variations of the pupil area size as a consequence of changes in the level of ambient retinal illumination. The flicker phenomenon causes a continuous action of the dilator and the sphincter muscles, since the brain tries to keep constant the amount of luminous intensity, which reaches the central fovea and the macula. As a consequence, a well-known annoyance sensation arises. The results provided by this model in the case of 60 W incandescent lamp are in accordance with the measurements given by the standard flickermeter.

As highlighted in chapter 5, the main goal of this thesis is to exceed one of the standard Flickermeter limit with the intent to find an “objective” response to flicker. In the last decade, in addition to the proposed system described in chapter 5, other studies have been conducted considering physiological parameter.

### 7.2 Laser Doppler Flowmetry

#### 7.2.1 First activity

One of the first activity [4] had the aim to study the relationship, in human being, between the fluctuations of the light emitted by a certain source and the variations of the blood flow at optic nerve head. This way, an “objective” evaluation of the annoyance due to flicker can be gauged, given that the above variations can reasonably be associated to an increasing activity of the eye-brain system. The “objective” evaluation of the flicker effects allows performing two key actions:

- (i) checking the correctness of previous developed models;
- (ii) developing a new model based on more reliable experimental data.

The optical setup adopted for the experimental activity is shown in figure 7.1.

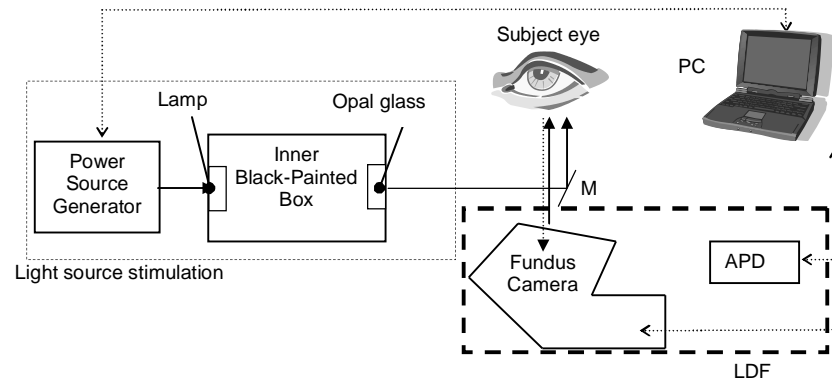


**Figure 7.1** Measurement system setup.

It consists of four main blocks: (i) the light source stimulation, (ii) a fundus camera, (iii) an Avalanche PhotoDiode (APD) and (iv) a Personal Computer (PC). Blocks (ii) and (iii) implement an apparatus for the Laser Doppler Flowmetry (LDF). The stimulus considered was the light flicker obtained by properly supplying a 100 W - 230 V incandescent lamp. This lamp was chosen to obtain a sufficient illumination of the retinal area. It was inserted in an inner black-painted box and supplied by a programmable power source generator (able to provide up to 400 V and 13 A) controlled by a PC. The black box was used to create a reference environment where the spectrum of incident light can be measured and repeatable. To this purpose, an acquisition system, the same used in [3], based on a spectrometer (32-channel photosensor module, H8353, Hamamatsu), was located at the box output; for the sake of simplicity, this system is omitted in figure 7.1. The light flicker generated by the lamp is diffused by means of an opal glass (50 mm diameter, NT46-106, Edmund Optics) and then it is reflected by a dicroic mirror (M) into the eye (figure 7.1) illuminating a 30° field centred at the optic disc.

A LDF for non-invasively measuring the optic nerve blood flow changes in response to diffuse flicker stimulation was simultaneously adopted [5]. The operating principle of such an instrument can be summarized as follows [5]. A laser beam (670 nm wavelength), whose power is in compliance with standard [6] in terms of maximum permissible exposure, illuminates red blood cells (RBCs) moving through a network of capillaries at various velocities and in different directions. The light scattered by the RBCs consists of a summation of waves with various Doppler shifts. The back-scattered light is collected by an optical fiber (200  $\mu\text{m}$  diameter at the fundus), converted in electric current by an avalanche photodiode APD (C30902, EG&G, USA) and then further processed by electronic filtering and amplification. The so-called “Doppler

signal” contains the sum of the Doppler shift components from all moving RBCs. These signal components are separated from each other by using fast Fourier analysis followed by power spectrum estimation. The resulting Doppler Shift Power Spectrum (DSPS) is essentially the histogram (distribution) of signal power as a function of Doppler shift frequency. According to the theory proposed in [7], the LDF [5] processes the DSPS to estimate the mean speed ( $Vel$ ) of the RBCs moving in the sampling volume (proportional to the mean Doppler frequency shift), the number of moving RBCs ( $Vol$ ) in the sampling volume (proportional to the area under the DSPS curve) and the total RBC flux  $F$  in the sampling volume:  $F = Vel \cdot Vol$ , where  $Vel$  is expressed in Hertz and  $F$  and  $Vol$  in arbitrary unit. The quantity  $F$  is usually referred to as “blood flow” even if it is the RCBs flux. Both are proportional only if the hematocrit remains constant during an experiment. A fixation target for the subject, which is aimed at reducing the eye movements during the measurement, completed the instrument.

These measurements were useful to determine a relationship between the light inside the box (measured by the spectrometer as described in the previous Section) and the light reflected by the dichroic mirror  $M$  and striking the subject eye. This way, we are able to relate the eye-brain response with the incident light. To this purpose, the lamp was supplied with a 230 V sinusoidal voltage and the emitted light was measured by the spectrometer. Then, the spectrometer sensor was located in front of the dichroic mirror ( $M$ ), in place of the subject eye, and the incident light was measured. Figure 7.2 depicts the spectrum of the light emitted by the lamp and measured inside the box. It shows the typical shape of an incandescent lamp. Figure 7.3 illustrates the normalized ratio between the spectrum of the light reflected by  $M$  and the spectrum in figure 7.2. Hence, it represents the transmittance

function of the opal glass – dichroic mirror optical system. It can be concluded that the optical system used to transmit the light from the source to subject eye behaves as a filter cutting the colors close to the orange – red ones, given

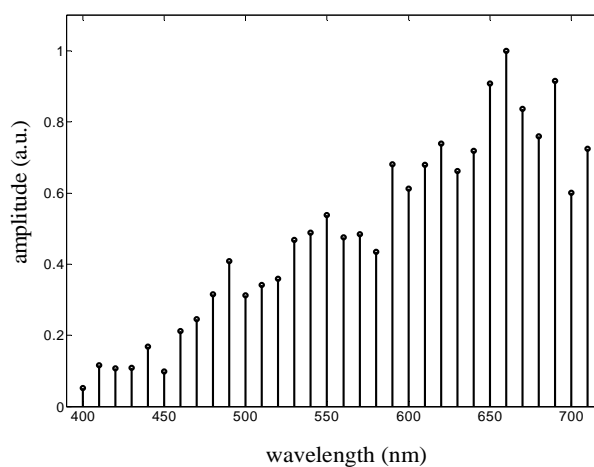


**Figure 7.2** Spectrum of the light inside the box

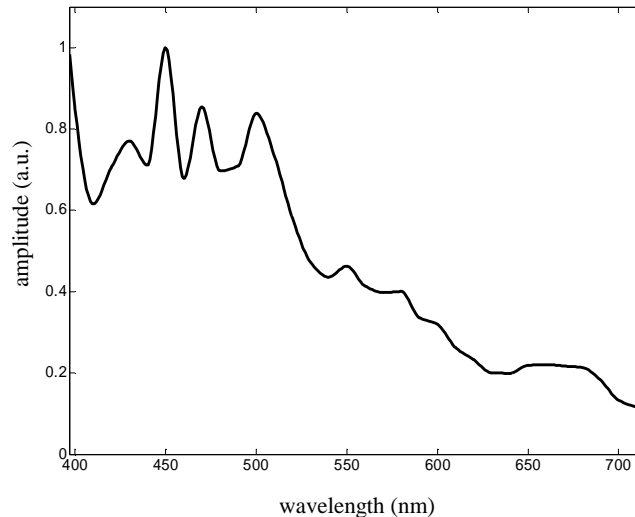


**Figure 7.3** Transmittance function of the opal glass – dichroic mirror optical system.

that they are attenuated till the 20% of their original amplitude. Of course, this means that the light striking the subject eye differs from the one emitted by the incandescent lamp.

## Tests

Experiments were performed by supplying the lamp with sinusoidal modulated

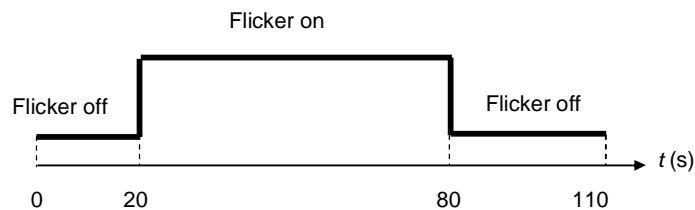


**Figure 7.4** Schematic representation of the measurement protocol.

voltages. The modulating frequency was varied in the range between 2 Hz and 24 Hz with steps of 2 Hz. As for the modulation depth  $m$ , it was kept constant (10 %) during all the measurements in order to get the frequency response of the human eye system to this kind of light fluctuation. The  $m$  value is higher than the ones usually considered for flicker evaluation to obtain a not negligible variation of the blood flow.

Measurements were performed according to a specific protocol that, as schematically shown in figure 7.4, can be divided in three periods. Firstly, the eye of the subject under test was exposed to 20 s of non-modulated light. Then, the flicker was applied for 60 s and, finally 30 s of rest period with non-modulated light complete the protocol. Because

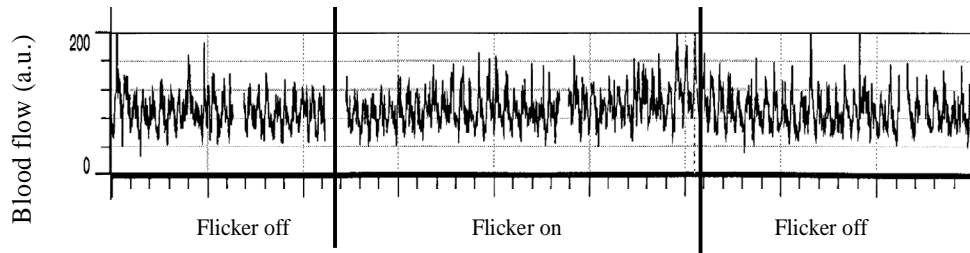


**Figure 7.5** Variation of the blood flow when the eye is stimulated according to the measurement protocol.

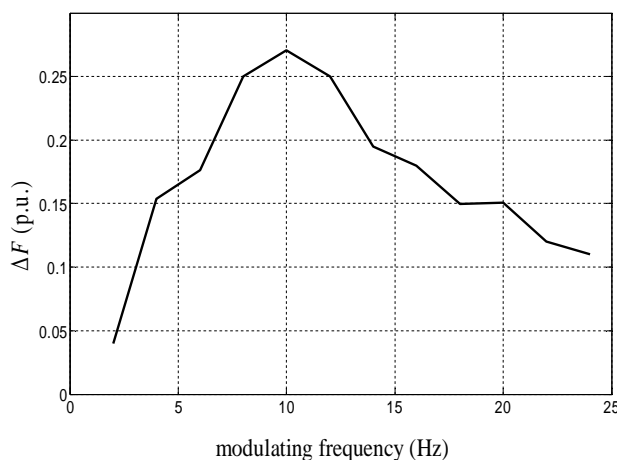
the subject under test was required to remain more motionless as possible, measurements at different frequencies were interleaved by 1 minute to allow relaxing. The time course here described is in good accordance with previous literature [8].

Figure 7.5 shows the variation of the blood flow when the eye is stimulated in accordance with the above described measurement protocol. It can be noted that, when the flicker is applied, the blood flow increases and reaches the steady state in the last part of the stimulus period. Then, when the flicker stops the blood flow decreases, arriving at a new steady-state condition at the end of the third period.

The effect of flicker on the blood flow was quantified by considering the relative variation of the blood flow with respect to the rest period. The last 10 s of each stage was processed for taking into account only the steady-state region.

The parameter  $\Delta F$  was evaluated:

$$\Delta F = \frac{F_{flicker} - F_{rest}}{F_{rest}}, \quad (7.1)$$



**Figure 7.6** Blood variation vs. modulating frequency.

where  $F_{flicker}$  is the blood flow provided by the LDF during the last 10 s of flicker and  $F_{rest}$  is the blood flow provided by the LDF in the last 10 s of the rest period.

The changing of  $\Delta F$  versus the modulating frequency is shown in figure 7.6. It refers to the mean values of three measurements performed on the

same subject in two different days and under the same nominal conditions. It can be observed that the maximum value for  $\Delta F$  (i.e. the maximum sensitivity of the human eye) occurs at 10 Hz and it corresponds to an increment of the blood flow of about 25%. Moreover, the response is not symmetrical: the values of  $\Delta F$  for frequencies greater than 10 Hz are higher than the ones related to frequencies lower than 10 Hz. These remarks are in good agreement with what is reported in scientific literature [9] (for example, it is stated that the maximum sensitivity of the human eye is located in the range 8-12 Hz) and then it seems that the obtained results are reasonable. The model proposed in [3] processes the light emitted by the lamp and allows determining the annoyance due to flicker in term of the so-called *instantaneous flicker sensation*  $p$  [10]. Therefore, such a model has been applied to the signals measured by the spectrometer during the described experimental activity. Of course, also the transmittance function depicted in figure 7.3 has been taken into account. It must be noted that the model [3] is in compliance with the standard flickermeter [1] under the same measurement conditions, as demonstrated in [3]. Figure 7.7 shows, in arbitrary unit, the obtained values of  $p$  versus the modulating frequency. At a first sight, the curves in figures. 7.6 and 7.7 seems in good agreement. By normalizing such curves to their maximum values, the plot in figure 7.8 can be drawn. It confirms that the two curves are similar even if their maximum values are located at slightly different frequencies (8 Hz and 10 Hz) and not negligible differences are shown at the lowest and highest frequencies.

As a final remark, it should be kept in mind that the measurement of the blood flow in a vessel close to the optic nerve is a complex task and hence it is affected by a significant “intrinsic” uncertainty. Moreover, it can vary from person to person. Even if

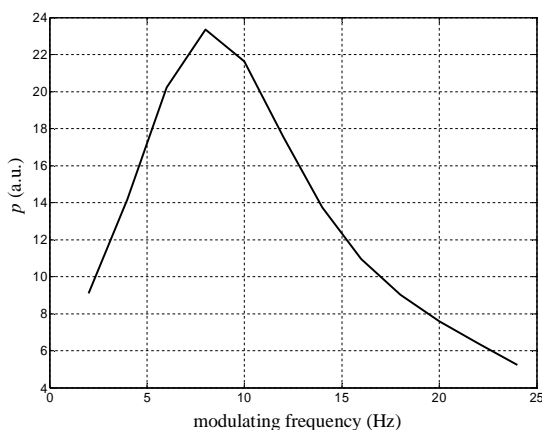


**Figure 7.7** Instantaneous flicker sensation vs. modulating frequency.

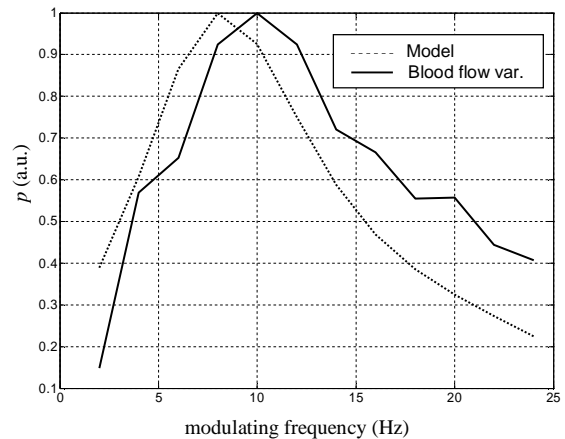


**Figure 7.8** Comparison between the model [3] and the blood flow variation

an important collection of data hasn't been analyzed, the presented results are encouraging. In fact, it seems that the blood flow variation can be a useful "objective" parameter for flicker studies and for the model validation. This method and the relative measurable index could in a future be considered as a reference for comparing and calibrating new theoretical eye-brain models which describe the annoyance effects of the light flicker on human beings.

### 7.2.2 Second activity

A second experimental activity has been conducted in collaboration with the John Glenn Research Center (NASA) in Cleveland (OH). This collaboration started because they were interested in observing new instruments and methods for performing measurement on human eye system. This area of research is important in the study of vestibular effects in aviation and space crews.

The aim has been to achieve an objective evaluation/prediction of the physiological effects induced by flicker, for this reason we compared the method based on the pupil size measurement with the blood flow analysis in the choroid.

As well known, light flickering at a rate of 4- 20 cycles per second can produce unpleasant reactions such as nausea and vertigo.

The vestibular system (inner ear canals and otoliths) in the human body controls the sense of movement, balance, and spatial orientation. When the brain receives contrasting information from the inner ear, eyes, muscles, and joints, a person may experience vertigo (causing confusion, headache, and nausea). In the specific case of pilots flying an aircraft in this condition flight safety can be seriously compromised [11,12]. Flicker vertigo occurs when eye catches light at a frequency of 4-20 Hz. Pilots flying or taxiing propeller airplanes or helicopters are frequently at risk when sunlight or strobe light is reflected off propeller or rotor blades and enter their eyes.

The experimental activity has been conducted in this way: (i) a preliminary experimental study measuring the pupil size variation under flicker green light conditions and (ii) choroidal blood flow under white strobe light stimulation, to investigate and try to supply information about the effects caused by the flicker stimuli.

Control of pupil size is governed by complex neuro-mechanisms. In normal psychophysical conditions the pupil diameter is determined by balances between sympathetic and parasympathetic innervation of the muscles of the iris. Light entering the eye is the major stimulus governing this control system. It is known that altered

conditions, induced, for example, by drugs, alcohol, nausea etc, induce distorted light pupillary response (PR). On the other hand, knowledge of the choroidal blood flow (ChBF) responses to various physiological stimuli is useful to study pathophysiology of ocular diseases involving hemodynamics [13] and neurovascular/neurometabolic coupling [14]. In particular, studies on animal and humans showed changes of hemodynamics in response to flicker stimuli with different stimulus parameters, such as modulation depth, frequency, luminance and colour [15]. The relationship existing between hemodynamics and neural activity (neurovascular/neurometabolic coupling) in the neural tissue of the eye fundus allows assessment of the neural functions by observing the blood flow [16]. Altered hemodynamical responses to flicker were observed during a number of physiological conditions, in particular, hyperoxia [17].

PR and ChBF were analyzed under different flicker stimulations in order to determine possible objective evaluation/prediction of the physiological effects induced by flicker vertigo in pilots [18].

## **Tests**

The experimental activity has been carried out in two steps. First, PR was recorded during green LED flicker stimulation at different frequencies, subjecting six people (three males and three females with an age included between 24 and 54 years old) and, second, ChBF of a subject participating in the first set of experiments was recorded during a white light stroboscopic stimulus.

- **The pupil size measurement**

The experimental procedure is described in section 6.2.2 (protocol#4) and here summarized. All the experiments were performed in a dark room where the subject was positioned in front of a camera. In order to avoid the pupil size variations because of the pupillary accommodation reflex, the subject under test was asked to focus on a target located behind and in the close proximity of the camera.

All the experiments were performed by using a green LED (540 nm) in addition to the two IR LEDs which were used to illuminate the eye during the image acquisition.

At this IR wavelength (850 nm) the human eye is not sensitive. The RGB and IR LEDs illumination optical power impinging the eye was set respectively to  $1 \text{ mW/m}^2$  and  $10 \text{ mW/m}^2$ , in accordance with the IEC 60825 [19]. The power was measured by a hand-held power meter (LaserCheck, USA).

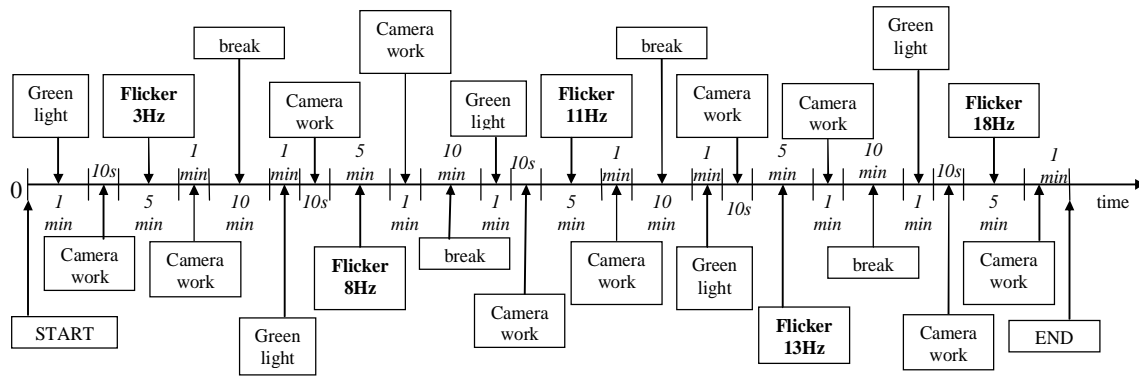


**Figure 7.9** Block diagram of pupil size measurement protocol.

The pupil diameter measurements were conducted as follows:

- 1) adaptation to the flicker stimulus;
- 2) image acquisition;
- 3) rest condition.

Five flicker frequencies have been used in the following order: 3Hz – 8Hz – 11Hz – 13Hz – 18Hz. Figure 7.9 schematically presents the measurement protocol. All subjects were exposed to a fixed light having a luminous flux equal to the mean value of that used during the flicker time. This, before to turn on all the flickering stimuli, has been executed for a period of 10-s.

This way, a necessary reference value for the pupil size was evaluated and used to normalize with the one obtained under flicker condition. After five minutes of beating light, a 1-min acquisition time has been stored.

The pupil size measurements were made on six healthy volunteer subjects under an informed consent. The characteristics of the examined subjects are summarized in Table 7.1.

**Table 7.1.** Volunteers characteristics.

Volunteer	Age	Gender	Eyes Colour	Visual Correction (R=right eye)
1	24	male	blue	Myopia R -0.5 [D]
2	26	male	brown	---
3	54	female	blue	Myopia R -6.00 [D]
4	22	female	blue	Myopia R -4.00 [D]
5	26	male	brown	---
6	26	female	brown	Myopia R -8.00 [D]

- **Laser Doppler Flowmetry**

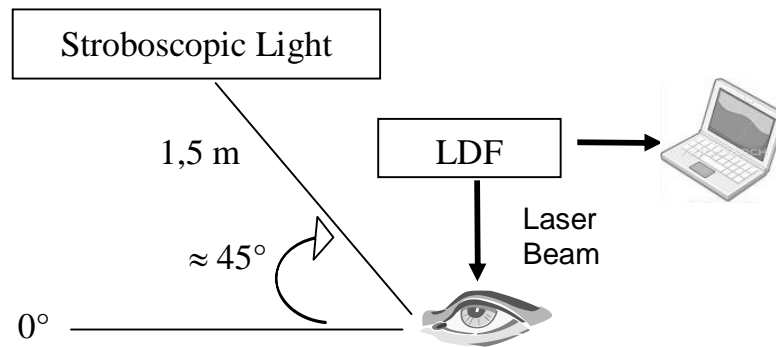


**Figure 7.10** Block diagram of LDF technique using the stroboscopic light.

The subject n. 2 of table 7.1 has been positioned from the source at a distance of about 1.5 m, as shown in figure 7.10; the ChBF in the right eye was recorded.

To obtain for the eye the maximum sensitivity to the stimuli a 30-minutes of dark condition preceded the stimulation; after that, the subject under test was exposed to 2-min fixed light for baseline (a value used as reference) data collection.

After the frequency has been set, three measurements have been taken; the first one followed by other two, every 6 minutes in a continuously, asking the subject to fix the laser beam for 10 s. Figure 7.11 shows the time sequence of the measurement protocol. The same procedure was repeated, for three frequencies: 4 Hz, 8 Hz and 13 Hz. These tests were not performed at the same day to avoid and excessive eye stress.

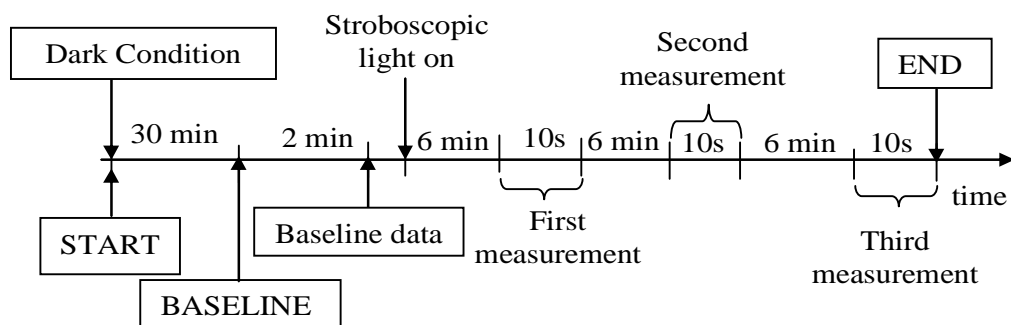


**Figure 7.11** Time sequence of the measurement protocol.

## Results and discussion

- **Pupil size measurement results**

PRs of the subjects were evaluated by monitoring the mean pupil diameter  $\bar{\Phi}_f$  defined as:

$$\bar{\Phi}_f = \frac{1}{N} \sum_{k=1}^N \frac{\bar{d}_{k,f}}{dref_{k,f}} \quad (7.1)$$

where  $f = 3\text{Hz}, 8\text{Hz}, 11\text{Hz}, 13\text{Hz}, 18\text{Hz}$  is the stimulus frequency,  $N = 6$  is the number of volunteers,  $\bar{d}_{k,f}$  is the mean diameter computed for the  $k$ -th person over the last 60 second of 6-min exposition to flicker with frequency  $f$ ,  $dref_{k,f}$  is the mean value of the diameter computed for the  $k$ -th subject over the last 10s of 70-s exposition to a fixed light just before the flicker test at frequency  $f$ . Table 7.2 shows the  $\bar{\Phi}_f$  values and the relevant standard deviation  $\sigma(\bar{\Phi}_f)$ , which ranges from about 2% to 10% of  $\bar{\Phi}_f$ . It has been demonstrated, after a characterisation procedure (section 5.6), that measurements performed by the system are affected by a standard uncertainty lower than 4 pixels which in this case turned out to be about 1.5% of  $\bar{\Phi}_f$ . Therefore the expanded uncertainty  $U(\bar{\Phi}_f)$  on  $\bar{\Phi}_f$  ranges from 3% to 10% depending on the values of  $\bar{\Phi}_f$ .

The pupil diameter was found to have a minimum value at a frequency around 10 Hz; so it seems that with those kinds of stimuli, where the eye is more sensitive to light

**Table 7.2** Normalized averages ( $\bar{\Phi}_f$ ) and standard deviations ( $\sigma(\bar{\Phi}_f)$ ) of the six normalized values.

Frequency[Hz]	$\bar{\Phi}_f$ [a.u]	$\sigma(\bar{\Phi}_f)$
3	0.991	0.19
8	0.897	0.14
11	0.884	0.09
13	0.910	0.09
18	0.978	0.06

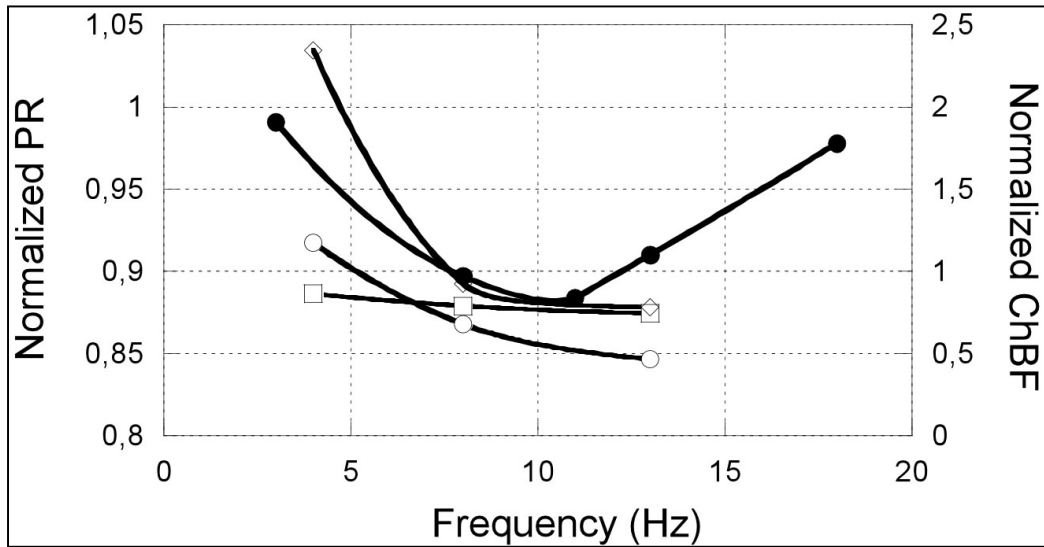


**Figure 7.12** Data collected during stroboscopic stimulation compared with the pupil size curve(●) PR, (□) ChBF Epoch 1, (○) ChBF Epoch 2, (◇) ChBF Epoch 3.

flicker (around 8.8 Hz), the pupil tends to stay contracted like it was stricken by a brighter light.

- **Flowmetry results**

The recorded values of ChBF are reported in Table 3.

**Table 7.3** ChBF recorded values.

<b>Frequency [Hz]</b>	<b>4</b>	<b>8</b>	<b>13</b>
<b><i>Time [min]</i></b>	<b>[AU]</b>	<b>[AU]</b>	<b>[AU]</b>
<i>(baseline) 0,5</i>	0.110	0.081	0.133
<i>(first try) 2,5</i>	0.095	0.064	0.099
<i>(second try) 8,5</i>	0.258	0.075	0.104
<i>(third try) 14,5</i>	0.129	0.055	0.062

Table 7.3 doesn't show a consistent difference between the baseline values and the first try, but it's evident a flow increase among the first and second measurement, especially at the lowest frequency (4 Hz), and a decrease between the second and the last collection of data.

- **Discussion**

Based on the preliminary results obtained in this activity, we offer some speculations. During the LED flicker stimulation, pupil size diameter reached its

minimum value at a frequency of around 11 Hz. Therefore, at this frequency of the stimulus, the amount of light impinging the photoreceptors is minimum since the pupil aperture is minimum; as ChBF should be minimum due to the neurovascular coupling. As shown in figure 7.12, this effect is apparently confirmed by data collected during stroboscopic stimulation on the examined subject. Here the ChBF values are normalized to their baseline levels. However, when pupil is dilated, other authors reported high choroidal blood flow at the frequency range of 8-10 Hz [20] thus observing a higher sensitivity of the photoreceptors at this flicker frequency stimulation. It is difficult to establish the cause or the effect of the observed response behavior since pupil size diameter, which could be seen as the control system response, alters the feedback signal that is, in turn, the photoreceptors neural response. In normal conditions, several factors affect the pupil size besides the level of retinal illumination, such as the accommodative state of the eye, individual's age, and various sensory and/or emotional conditions. Nevertheless, all the six subjects involved in this study showed a similar trend of the mean pupil diameter. Apparently the higher sensitivity of the photoreceptors at the flicker stimulus at 8-11 Hz induces a papillary contraction not justified by the retinal illumination thus producing stress and/or annoyance that, in turn, in some individuals could be one of the sources of nausea and vertigo induced by the light flickering.

### 7.3 The Electroretinography

The electroretinography (ERG) is a fundamental technique to learn information about the response of the retina to photopic stimulation.

This response is recorded using a small contact lens electrode that rests on the front surface of the eye, but it can also be recorded using skin electrodes placed just above and below the eye, or below the eye and next to the lateral canthus.

The retina is a collection of rod, cone, and neural cells that generate electrical signals which transmit visual information to the brain. By measuring the changes in those signals, it is possible to determine how well the different cells in the retina are working and to assess the status of the retina in eye diseases in human patients.

The basic method of recording the electrical response is by stimulating the eye with a bright light source such as a flash produced by a strobe lamp. The intense flash of light elicits a biphasic waveform recordable at the cornea similar to that illustrated below (figure 7.13). The two components that are most often measured are the a- and b-waves.

The a-wave is the first large negative component, followed by the b-wave which is corneal positive and usually larger in amplitude. Two principal measures of the ERG waveform are taken: 1) The amplitude (a) from the baseline to the negative trough of the a-wave, and the amplitude of the b-wave measured from the trough of the a-wave to the following peak of the b-wave; and 2) the time (t) from flash onset to the trough of the a-wave and the time (t) from flash onset to the peak of the b-wave (figure 7.13). These times, reflecting peak latency, are referred to as "implicit times" in the jargon of Electroretinography [21].

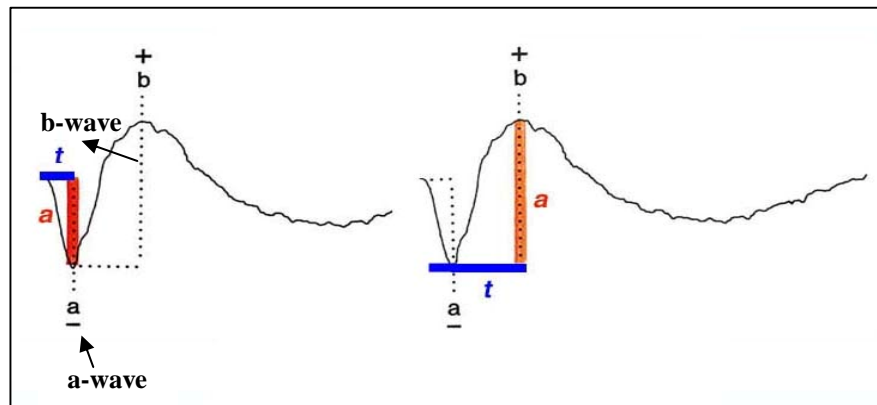


**Figure 7.13** Amplitude and implicit time measurements of the ERG biphasic waveform of a normal patient

The a-wave, sometimes called the "late receptor potential," reflects the general physiological health of the photoreceptors in the outer retina. In contrast, the b-wave reflects the health of the inner layers of the retina, including the ON bipolar cells and the Muller cells (Miller and Dowling, 1970). Two other waveforms that are sometimes

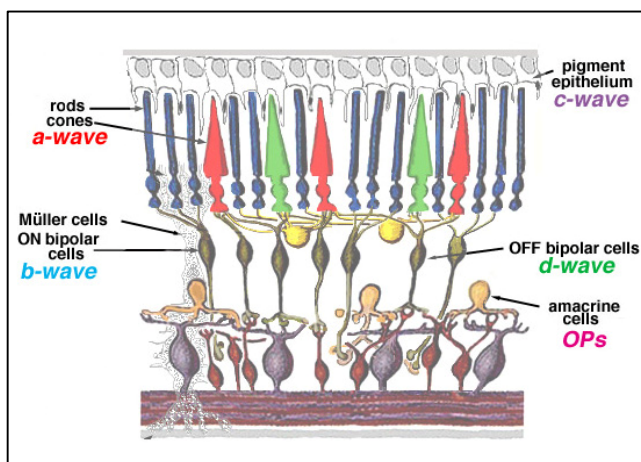


**Figure 7.14** Major components of the ERG in the retina.

recorded in the clinic, are the c-wave originating in the pigment epithelium (Marmor and Hock, 1982) and the d-wave indicating activity of the OFF bipolar cells (see Figure 7.14) [21].

This instrument, down the years, has been used for several studies [19-26] with the attempt

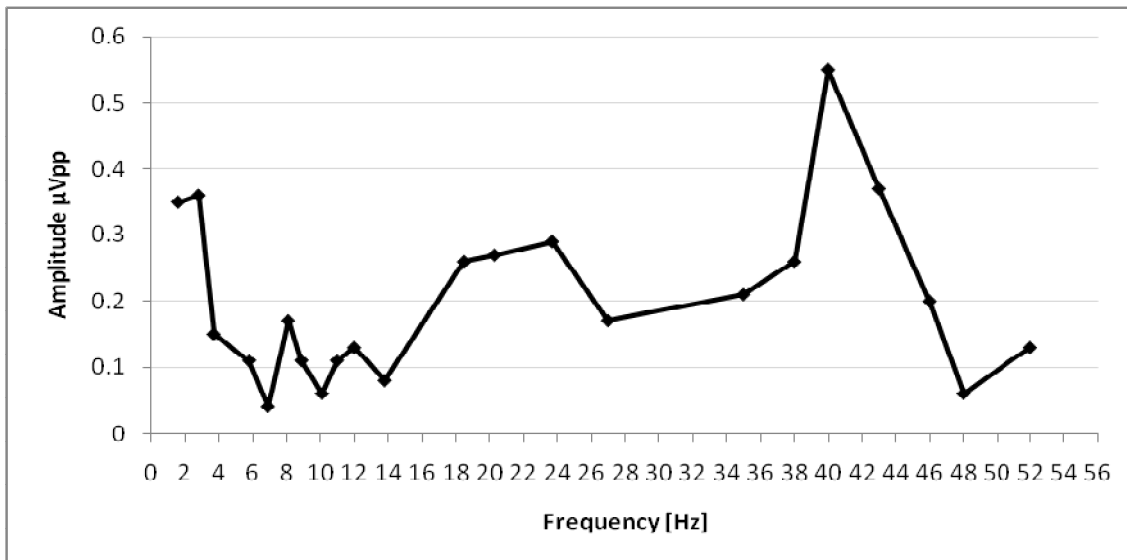


**Figure 7.15** Retinal response

to understand how the photoreceptors work in different light conditions, and what kind of information are possible to learn by analyzing the electrical signals sent to the brain.

These signals are obtained in response to a small sinusoidally modulated test light [23] superimposed on an equiluminant background [24]. The signal from the retina is acquired by eyelid electrodes, then it is amplified and averaged to improve the signal-to-noise ratio [22]. The dominating harmonics are the first and the second, with a relative ratio strongly dependant on the stimulation frequency [26].

Our interest, for the research activity, was to understand if there were significant results around frequencies considered annoying (8-10 Hz). Usually, for the ERG a LED stimulator is used and sinusoidal stimuli are considered. A typical response is shown in figure 7.15. This has been obtained subjecting a normal adult male to 22 different focal stimuli, with uniform contrast and mean luminance and frequencies ranging from 1.5 to 52 Hz. It can be observed that the amplitude trend, mainly related to photoreceptors activity, shows an initial low-pass behavior followed by a peak at about 40 Hz, and a subsequent marked decay. If we take into account that the flicker ERG decreases with increasing the luminance [27] and during the test the luminous intensity hasn't been changed, it's possible to suppose that there is an higher sensitivity of the photoreceptors for flicker stimuli at 8-11 Hz, which induces a pupillary contraction.

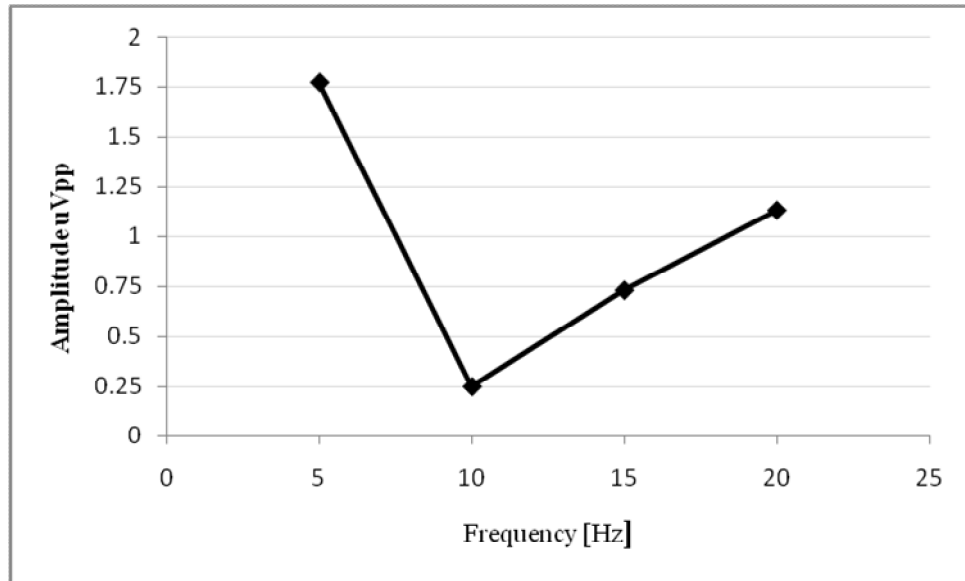


**Figure 7.16** Retinal response

Recent experimental data obtained by ERG in a normal adult women, during flicker, confirm the results of other tests conducted in the past. In this case, a mean luminance and frequencies equal to 5, 10, 15 and 20 Hz have been selected. The retinal response, shown in figure 7.16, presents a minimum value around 10 Hz. So, also in this case we can suppose that for around this frequencies, the cones are more sensitive and, consequently, the amplitude decreases. All these findings allow to conclude that the behavior of the pupil diameter under flicker conditions depends mainly on the photoreceptor behavior. This is confirmed by the very high overlapping of the curves obtained in frequencies of both the signal transmitted to brain by the photoreceptors and the pupil diameter.

For the purposes of this thesis, these are very interesting and encouraging result. The intent is to continue this activity thanks to this technique to a larger number of individuals with different ages and genders, to validate the speculative considerations and to have more data to compare.

**References**

- [1] A.E. Emanuel, and L. Peretto, "A simple lamp-eye-brain model for flicker observation," *IEEE Trans. on Power Delivery*, vol. 19, n. 3, pp. 1308-1313, 2004.
- [2] L. Peretto, E. Pivello, R. Tinarelli, and A.E. Emanuel, "Theoretical analysis of the physiologic mechanism of luminous variation in eye-brain system," *IEEE Trans. on Instrumentation and Measurement*, Vol. 56, n. 1, pp. 164-170, 2007.
- [3] L. Peretto, L. Rovati, G. Salvatori, R. Tinarelli, and A.E. Emanuel, "Investigation on the response of the human eye to light flicker produced by different lamps," accepted for the publication in *IEEE Trans. on Instrumentation and Measurement*, August 2007.
- [4] L.Peretto, C. Riva, L.Rovati, G.Salvatori, R.Tinarelli, "*Experimental Evaluation of Flicker Effects on Human Subjects*", *IEEE IMTC*, Warsaw, Poland, May 2007.
- [5] E. Logean, M. H. Geiser, and C. E. Riva, "Laser Doppler instrument to investigate retinal neural activity-induced changes in optic nerve head blood flow," *Optics and Laser in Engineering*, Vol. 43, pp. 591-602, 2005.
- [6] American National Standard Institute, American national standard for safe use of lasers: ANSI Z136. 1-2000.
- [7] R. Bonner, R. Nossal, "Model for laser Doppler measurements of blood flow in tissue," *Appl. Opt.*, Vol. 20, pp. 2097-2107, 1981.
- [8] C. E. Riva, E. Logean, and B. Falsini, "Temporal dynamics and magnitude of the blood flow response at the optic disk in normal subjects during functional retinal flicker-stimulation," *Neurosci. Lett.*, Vol. 356, pp. 75-78, 2004.
- [9] EN 61000-4-15 "Testing and measurement techniques: flickermeter – functional and design specification," Geneva, CH, 1997.
- [10] IEC 60050-161 "International Electrotechnical Vocabulary – Electromagnetic Compatibility," Geneva, Switzerland, 1997.
- [11] Brandt, T., Arnold, F., Bles, W., Kapteyn, T., S. "The mechanism of physiological height vertigo. I. Theoretical approach and psychophysics," *Acta Otolaryngol.* May-Jun, 89(5-6):513-23 (1980).
- [12] Rash C., E., "Awareness of Causes and Symptoms of Flicker Vertigo can Limit Ill Effects," *Aviation Medicine* Vol. 51 No. 2, 1-6 (2004).

- [13] Zink J., M., Grunwald J.E., Piltz-Seymour J.R., Staii A and Dupont J., "Association between lower optic nerve laser Doppler blood volume measurements and glaucomatous visual field progression". *Br J Ophthalmol* 87: 1487–1491 (2003).
- [14] Fuchsja" ger-Mayrl G., Polska E., Malec M. and Schmetterer L., "Unilateral light-dark transitions affect choroidal blood flow in both eyes". *Vision Res* 41: 2919–2924 (2001).
- [15] Riva C., E., Logean E., Falsini B., "Visually evoked hemodynamical response and assessment of neurovascular coupling in the optic nerve and retina," *Progress in retinal and eye research*, 24 (2): 183-215 (2005).
- [16] Daniel Ts'o, Jesse Schallek, Young Kwon, Randy Kardon, Michael Abramoff, and Peter Soliz, "Noninvasive Functional Imaging of the Retina Reveals Outer Retinal and Hemodynamic Intrinsic Optical Signal Origins," *Jpn J Ophthalmol*, 53: 334–344 (2009).
- [17] Kashikura, K., Kershaw, J., Kashikura, A., Matsuura, T. and Kanno, I., "Hyperoxia-enhanced activation-induced hemodynamic response in human VI: An fMRI study," *NeuroReport*, 11(5): 903-906 (2000).
- [18] United States Naval Flight Surgeon's Manual: Third Edition, Chapter 9 "Ophthalmology: Perceptual Disorders; Naval Aerospace Medical Institute" (1991).
- [19] ISO 23539, CIE S 010/E, "Photometry — The CIE system of physical photometry," *International Organization for Standardization*, Geneva, CH, (2005).
- [20] Falsini, B., Riva, C.E., and Logean, E., "Flicker-Evoked Changes in Human Optic Nerve Blood Flow: Relationship with Retinal Neural Activity," *Investigative Ophthalmology and Visual Science*: 43: 2309-2316 (2002).
- [21] <http://webvision.med.utah.edu/ClinicalERG.html#start>
- [22] A.Fadda, B.Falsini, "Precision LED-based stimulator for focal electroretinography" *Med. Biol. Eng Comput.*, 1997, **35**, 441-444.
- [23] F.A. Abraham, M. Alpern, D.B. Kirk, D.B (1985): Electroretinograms evoked by sinusoidal excitation of human cones", *J.Physiol.*, **363**, pp. 135-150.
- [24] W.R. Biersdorf (1989): "The clinical utility of the foveal electroretinogram: A review", *Doc.Ophthalmol.*, **73**, pp.313-327.
- [25] C.L. Baker, R.F. Hess (1984): "Linear and non linear components of human electroretinograms", *J. Neurophysiol.*, 51, pp.952-967.

- [26] V.Porciatti, B.Falsini, A.Fadda, R.Bolzani (1989): “Steady state analysis of the focal ERG to pattern and flicker: Relationship between ERG components and retinal pathology”, *Clin. Vis. Sci*, 4, pp. 323-332.
- [27] R.Verma, M.J. Pianta, “The contribution of human cone photoreceptors to the photopic flicker electroretinogram”, *Journal of vision* (2009), 9(3):9, 1-12.

## 8. Conclusions

Aim of this thesis has been to investigate on a methodology which allows gathering information regarding the annoyance condition of human being due to light flicker.

Due to practical and theoretical reasons, the Flickermeter described by the relevant International Standard may lead to incorrect results when used to correlate voltage variations with annoyance caused by fluctuations of light emitted by types of lamps different than those based on the incandescent-filament principle. Therefore, its replacement is under consideration by some international organizations given that these last type of lamps will be no more available on the market starting from September 2011.

This research, principally, has been focused on finding a new method for detecting the human being annoyance in presence of luminous flicker. Starting from the study of the human visual system model, we learned important information about the operating principle of the human eye. In particular, we paid attention to the actions of the photoreceptors and, consequently, how the brain manages the iris muscles movements to control the amount of light that strikes the human eye. In presence of an intense radiation, the pupil is more contracted and it has been verified that this condition is representative of a suffering state.

In this connection, a significant step in the direction of a new flickermeter may be the development of an improved visual system model starting from information obtained by measuring a physiological parameter, thus allowing to get a more “objective” representation of the human eye response to flicker.

For this reason, the use of the mean value of the pupil diameter has been proposed and investigated. In this thesis the two systems assembled for the experimental activity and their characterization have been presented along with experimental results carried out on a sample of human subjects. Such systems allow to select and generate different flickering lights, to store images thanks to the camera and compute, in an off-line processing, the mean diameters with an ad-hoc software developed under Labview environment. The numerous results show a solid correlation between the flicker frequency, the pupil size and the annoyance caused by the stimuli. So, they confirm the possibility to use this physiological parameter for the implementation of the next generation flickermeter and the updating of the current International Standard.

---

1. Introduction	p.1
2. Power Quality in Electrical Systems	
2.1 Introduction	p.4
2.2 Power quality	p.5
2.2.1 Steady State Voltage Characteristics	p.6
2.2.2 Transients	p.6
2.2.3 Harmonic Distortion	p.7
2.2.4 Short Duration Voltage Variations	p.8
2.3 Power Quality Evaluation	p.11
2.3.1 Research and Standardization Activity	p.11
2.3.2 Basic Definition of Voltage parameters	p.14
2.3.3 Overview of Power Quality Indices	p.17
2.3.4 Standard Measurement methods of PQ parameters	p.22
2.3.5 Non Conventional Parameters for PQ Parameters	p.33
2.4 European Scenario: Standards, guides and PQ level	p.35
2.4.1 Reliability regulation	p.39
2.4.2 Voltage Quality Regulation	p.42
2.4.3 Monitoring the Voltage Quality within EU	p.44
2.4.4 Minimum Standards	p.47
2.4.5 Incentive Schemes	p.48
<b>References</b>	p.50
3. The Human Visual System	
3.1 Anatomy and function	p.52
3.2 How the eye works	p.53
3.2.1 The iris and the pupil	p.53
3.2.2 The sclera and the cornea	p.56
3.2.3 The choroid, the ciliary body and the lens	p.58
3.2.4 The retina	p.58
3.2.5 The aqueous humor	p.62
3.2.6 The vitreous body	p.63
3.2.7 The crystalline lens	p.63
3.2.8 Accommodation	p.64
3.2.9 The work of the retina	p.65
3.2.10 Electrophysiology of the retina	p.74

3.2.11	Color vision	p.78
	<b>References</b>	p.85
4.	Flicker and Flickermeter	
4.1	Flicker phenomena and terminology	p.84
4.2	Flickermeter UIE	p.90
4.2.1	Blocks	p.90
4.2.2	Analysis procedure	p.94
4.2.3	Short-term flicker evaluation	p.95
4.2.4	Long-term flicker evaluation	p.95
4.2.5	Outputs	p.96
4.2.6	Performance testing	p.97
	<b>References</b>	p.99
5.	Toward an Innovative Flickermeter	p.100
5.1	Introduction	p.100
5.2	First system setup “A”	p.104
5.3	Second system setup “B”	p.107
5.4	Characterization of the system “A”	p.109
5.4.1	Test of the algorithm for pupil diameter measurement	p.109
5.4.2	Radiated power	p.111
5.4.3	System accuracy	p.113
5.5	Characterization of the system “B”	p.116
5.5.1	Accuracy of the measurement system	p.117
5.5.2	Optical power stability	p.118
5.5.3	Radiated power	p.120
	<b>References</b>	p.121
6.	Experimental activities	p.124
6.1	Introduction	p.124
6.2	System “A”: results	p.124
6.2.1	First measurement campaign	p.124
6.2.2	Second measurement campaign	p.129
6.3	System “B”: results	p.136
6.3.1	Third measurement campaign	p.136
6.3.2	Fourth measurement campaign	p.140

<b>References</b>	p.145
7. Medical studies	p.146
7.1 Introduction	p.146
7.2 Laser Doppler Flowmetry	p.146
7.2.1 First activity	p.146
7.2.2 Second activity	p.152
7.3 The Electroretinography	p.158
<b>References</b>	p.162
8. Conclusions	p.165